



Horizon 2020

---

Project acronym: **LASH FIRE**  
Project full title: **Legislative Assessment for Safety Hazard of Fire and Innovations in Ro-ro ship Environment**  
Grant Agreement No: **814975**  
Coordinator: **RISE Research Institutes of Sweden**



## **Deliverable D10.4**

# **Large-scale validation of the new fire test standard for alternative fixed fire-fighting systems**

**February 2023**

Dissemination level: **Public**

## Abstract

MSC.1/Circ.1430, that supersedes previous requirements in IMO Resolution A.123 (V) and MSC.1/Circ. 1272, contains design and installation requirements for prescriptive-based and performance-based (i.e., 'alternative') fire protection systems for vehicle spaces and ro-ro spaces not capable of being sealed and special category spaces. Prescriptive-based systems should be designed per the design tables in MSC.1/Circ.1430, whilst performance-based systems should be tested in accordance with the fire test procedures in the Appendix. Concerns related to the performance of the performance-based option have been raised as the fire test procedures set a performance level that is only similar or slightly better than the performance of systems that used to be installed in accordance with Resolution A.123(V).

The objective of the work presented in this report was to suggest new, more realistic fire test scenarios and document the fire suppression performance of the prescriptive-based system design.

A review of actual fires on ro-ro ships shows that many fires start inside vehicles due to electrical failures, that may have been avoided by the disconnection of the battery. Although starting small, fire development is often rapid and may include several vehicles prior the manual activation of the fixed installed water-based fire-fighting system. The fires are difficult to access due to the short horizontal clearance between vehicles and they are shielded from direct application of water from overhead sprinklers or nozzles by the body or by the roof and sides of a trailer. None of the fire investigation reports documented fuel spill fires from the vehicles. One case with a fire starting in an electric car was identified. The car was originally a conventional combustion engine car but had been rebuilt by the owner. A review of the characteristics of fires in battery electric vehicles (BEV) was made, indicating that the severity of fires is comparable to that of conventional internal combustion engine vehicles (ICEV). Some data indicate that the maximum heat flux from a BEV may be slightly higher compared to an ICEV, which could be due to the jet flames generated from the battery pack. However, other data indicate the opposite as a result of a fuel spill fire.

New fire test scenarios representing fires in a passenger car as well as a freight truck trailer were developed. The design of the mock-ups resembled those used in the current fire test procedures in the Appendix of MSC.1/Circ.1430, but the aim was to generate more intense fires. Thereafter, benchmark fire suppression tests were conducted with an automatic sprinkler system and a deluge water spray system designed per the prescriptive-based requirements in MSC.1/Circ.1430.

Fire suppression tests were also conducted involving two pairs of geometrically similar internal combustion engine and battery electric vehicles in test conditions that were as equivalent as possible. Fire ignition was arranged in such a way that the liquid fuel or the battery pack was involved at the initial stage of the fire. It is concluded that fires in the two types of vehicles are different but have similarities. However, a fire in a BEV does not seem to be more challenging than a fire in an ICEV for a drencher system designed in accordance with current recommendations in MSC.1/Circ.1430.

The experience and outcome documented in the report will serve as the baseline for a revision of the fire test procedures in the Appendix of MSC.1/Circ.1430. This work will be documented in D10.5.



*This project has received funding from the European Union's Horizon 2020 research and innovation programme under grant agreement No 814975*

*The information contained in this deliverable reflects only the view(s) of the author(s). The Agency (CINEA) is not responsible for any use that may be made of the information it contains.*

The information contained in this report is subject to change without notice and should not be construed as a commitment by any members of the LASH FIRE consortium. In the event of any software or algorithms being described in this report, the LASH FIRE consortium assumes no responsibility for the use or inability to use any of its software or algorithms. The information is provided without any warranty of any kind and the LASH FIRE consortium expressly disclaims all implied warranties, including but not limited to the implied warranties of merchantability and fitness for a particular use.

© COPYRIGHT 2019 The LASH FIRE Consortium

This document may not be copied, reproduced, or modified in whole or in part for any purpose without written permission from the LASH FIRE consortium. In addition, to such written permission to copy, acknowledgement of the authors of the document and all applicable portions of the copyright notice must be clearly referenced. All rights reserved.

## Document data

Document Title:	D10.4 – Large-scale validation of the new fire test standard for alternative fixed fire-fighting systems		
Work Package:	WP10 – Extinguishment		
Related Task(s):	T10.9, T10.11		
Dissemination level:	Public		
Deliverable type:	R		
Lead beneficiary:	01 – RISE		
Responsible author:	Magnus Arvidson		
Co-authors:			
Date of delivery:	2023-02-28		
References:	D10.5		
Approved by	Antti Virkajärvi on 2023-01-26	Benoît Loicq on 2023-01-19	Maria Hjohlman on 2023-02-09

## Involved partners

No.	Short name	Full name of Partner	Name and contact info of persons involved
1	RISE	RISE Research Institutes of Sweden AB	Magnus Arvidson ( <a href="mailto:magnus.arvidson@ri.se">magnus.arvidson@ri.se</a> )
5	MAR	Marioff Corporation Oy	Antti Virkajärvi ( <a href="mailto:antti.virkajarvi@carrier.com">antti.virkajarvi@carrier.com</a> ), Maarit Tuomisaari ( <a href="mailto:maarit.tuomisaari@carrier.com">maarit.tuomisaari@carrier.com</a> )
6	UNF	Unifire AB	Mattias Eggert ( <a href="mailto:mattias@unifire.se">mattias@unifire.se</a> ), Roger James ( <a href="mailto:roger@unifire.com">roger@unifire.com</a> )
25	F4M	FiFi4Marine BV	Cor Meedendorp ( <a href="mailto:c.meedendorp@fifi4marine.com">c.meedendorp@fifi4marine.com</a> ), Martijn Teela ( <a href="mailto:m.teela@fifi4marine.com">m.teela@fifi4marine.com</a> )

## Document history

Version	Date	Prepared by	Description
01	2022-08-18	Magnus Arvidson	Draft of structure
02	2023-01-15	Magnus Arvidson	Draft of final report, circulated to reviewers
03	2023-02-28	Magnus Arvidson	Final report



## Content

1	Executive summary .....	9
1.1	Problem definition.....	9
1.2	Method.....	9
1.3	Results and achievements.....	10
1.4	Contribution to LASH FIRE objectives.....	11
	Exploitation and implementation.....	11
2	List of symbols and abbreviations .....	12
3	Introduction.....	14
4	The conditions in ro-ro spaces, vehicle spaces and special category spaces.....	16
4.1	General .....	16
4.2	Cargo and distances between cargo .....	16
4.3	Design and production aspects .....	17
4.3.1	Vehicle space deck structure arrangement.....	17
4.3.2	Vehicle space equipment arrangement .....	20
4.3.3	Materials.....	20
4.4	Environmental aspects .....	20
5	Short review of actual fires on ro-ro ships .....	21
5.1	General .....	21
5.2	Courage (vehicle carrier) .....	21
5.3	Honor (vehicle carrier) .....	21
5.4	Höegh Xiamen (vehicle carrier) .....	22
5.5	Joseph and Clara Smallwood (ro-ro passenger ship) .....	24
5.6	Commodore Clipper (ro-ro ship) .....	26
5.7	Pearl of Scandinavia (ro-ro passenger ship) .....	27
5.8	Mecklenburg-Vorpommern (ro-ro passenger ship) .....	28
5.9	Victoria Seaways (ro-ro passenger ship) .....	30
5.10	URD (ro-ro passenger ship) .....	31
5.11	Stena Spirit (ro-ro passenger ship) .....	33
5.12	Britannia Seaways (ro-ro cargo ship) .....	34
5.13	Corona Seaways (ro-ro cargo ferry) .....	35
5.14	Conclusions based on the actual fires .....	36
6	The development of MSC.1/Circ.1430 .....	38
6.1	The requirements in SOLAS Chapter II-2, Part G, Regulation 20.....	38
6.2	The requirements in IMO Resolution A.123 (V) .....	38

6.3	The publication of MSC/Circ. 914.....	39
6.4	Concerns raised by Maritime and Coastguard Agency (MCA) .....	39
6.5	The development of new fire test procedures.....	40
6.6	The development of MSC.1/Circ.1430 .....	40
7	Electric vehicle (EV) fire characteristics.....	42
7.1	Fires in electric vehicles.....	42
7.1.1	Battery cell failure .....	42
7.1.2	Jet flames.....	42
7.2	Fire test review .....	43
7.2.1	Small- and intermediate-scale fire tests.....	43
7.2.2	Large-scale fire tests of battery packs.....	44
7.3	Large-scale fire tests of EVs.....	45
7.3.1	Fire tests at INERIS.....	45
7.3.2	Fire tests by Watanabe et al.....	46
7.3.3	Fire tests at National Research Council of Canada (NRC).....	46
7.3.4	Fire tests by NHTSA (without measuring the HRR) .....	47
7.3.5	Fire tests in the ETOX project .....	48
7.3.6	Summary of large-scale fire test results.....	49
7.4	Fire suppression of ICEV's vs BEV's .....	50
7.5	Conclusion .....	51
8	The design and installation guidelines in MSC.1/Circ.1430/Rev.2.....	52
8.1	Introduction.....	52
8.2	General requirements .....	52
8.3	Additional requirements for prescriptive-based systems .....	55
8.4	Additional requirements for performance-based systems .....	58
9	The fire test procedures in MSC.1/Circ.1430/Rev.2.....	60
9.1	General requirements .....	60
9.2	The fire test scenarios .....	60
9.2.1	General requirements .....	60
9.2.2	The freight truck trailer fire test scenario .....	60
9.2.3	The passenger car fire test scenario.....	61
9.3	The positioning of sprinklers or nozzles .....	62
9.4	Instrumentation and measurements .....	62
9.5	The test approaches .....	63
9.6	Fire test procedures .....	63
9.7	Acceptance criteria.....	63

9.7.1	Principle requirements and fire damage evaluation.....	63
9.7.2	Freight truck fire test scenario evaluation .....	64
9.7.3	Passenger car fire test scenario evaluation.....	64
10	Examples of certified alternative, performance based fire-fighting systems .....	65
11	The inadequacies of the fire test procedures in MSC.1/Circ.1430/Rev.2 .....	68
11.1	Primary inadequacies .....	68
11.2	Other opportunities for improvements .....	68
12	The main features of the revised test procedures .....	70
12.1	Basic requirements of the revised fire test scenarios .....	70
12.2	Suggested fire test scenarios.....	70
12.2.1	Freight truck trailer fire test scenario.....	70
12.2.2	Passenger car fire test scenario.....	71
12.3	The fire test hall and the environmental conditions.....	72
12.4	Instrumentation and measurements .....	72
12.5	The activation of the system .....	73
12.6	The ceiling construction and nozzle positioning .....	76
12.7	Simulation of a heat detection system.....	76
12.8	Fire test procedures .....	77
12.9	Acceptance criteria.....	78
13	Fire test approach during any benchmark fire suppression tests .....	79
13.1	General .....	79
13.2	Ceiling heights used in any benchmark tests .....	79
13.3	Type of systems used in any benchmark tests and system activation delay times .....	79
13.4	Water discharge densities used in any benchmark tests .....	80
13.5	Automatic sprinkler and water spray nozzles used in any benchmark tests .....	80
14	Benchmark fire suppression tests .....	82
14.1	General .....	82
14.2	The suspended ceiling .....	82
14.3	The system pipe-work, the sprinklers, and the nozzles .....	83
14.3.1	System layout .....	83
14.3.2	The automatic sprinklers and water spray nozzles .....	84
14.4	The fire test scenarios .....	85
14.4.1	Passenger car fire test scenario.....	85
14.4.2	Freight truck trailer fire test scenario.....	88
14.5	Instrumentation and measurements .....	89
14.5.1	General .....	89

14.5.2	The measurement of ceiling gas temperatures above the fire .....	89
14.5.3	The ceiling gas temperatures at the simulated heat detectors .....	89
14.5.4	Surface temperature measurements on steel sheet screens .....	89
14.5.5	Measurements of system operating pressure and water flow rates .....	93
14.6	Fire procedures .....	93
15	Observations during the benchmark fire suppression tests .....	94
15.1	The fire test program .....	94
15.2	Test 1 .....	94
15.3	Test 2 .....	95
15.4	Test 3 .....	97
15.5	Test 4 .....	98
15.6	Test 4b .....	99
15.7	Test 7 .....	100
15.8	Test 8 .....	103
15.9	Test 5 .....	105
15.10	Test 6 .....	108
16	Benchmark fire suppression test results .....	111
16.1	Passenger car scenario .....	111
16.2	Freight truck trailer scenario .....	112
16.3	The moisture content of individual wood pallets .....	115
17	Discussion .....	117
17.1	The objective of the work .....	117
17.2	The conditions in ro-ro spaces, vehicle spaces and special category spaces .....	117
17.3	Electric vehicle (EV) fire characteristics .....	117
17.4	The re-design of the fire test scenarios .....	118
17.5	The re-design of the fire test procedures .....	118
17.6	Benchmark fire suppression tests .....	118
17.7	The moisture content of the wood pallets .....	119
17.8	The next steps .....	121
18	References .....	122
19	Indexes .....	125
19.1	Index of tables .....	125
19.2	Index of figures .....	125
20	ANNEX A .....	130
20.1	The first test series .....	130
20.2	The second test series .....	133

20.2.1	Test 1 .....	134
20.2.2	Test 2 .....	135
20.2.3	Test 3 .....	136
21	ANNEX B .....	140
21.1	Introduction.....	140
21.2	The vehicles used in the tests.....	140
21.3	The positioning of the vehicles.....	141
21.4	The preparation of the vehicles .....	142
21.5	The deluge water spray system.....	143
21.6	Fire test procedures .....	144
21.7	Instrumentation and measurements .....	144
21.7.1	Heat release rate measurements.....	144
21.7.2	The gas temperature inside the vehicle .....	145
21.7.3	The gas temperature above the vehicle.....	145
21.7.4	The surface temperature on steel sheet screens to the sides of the vehicle .....	145
21.7.5	Heat radiation measurements.....	145
21.7.6	Plate Thermometer measurements .....	146
21.7.7	Measurements of the system operating pressure and water flow rate .....	146
21.7.8	Still photographs and video recordings.....	146
21.8	Fire test observations.....	146
21.9	Test results .....	154
21.10	Discussion .....	156
21.10.1	The fire scenarios .....	156
21.10.2	The performance of the water spray system .....	158
21.11	Conclusion .....	158
21.12	Acknowledgement.....	159

# 1 Executive summary

## 1.1 Problem definition

Vehicle spaces and ro-ro spaces not capable of being sealed and special category spaces shall be fitted with a fixed water-based fire-fighting system complying with the provisions of the Fire Safety Systems Code (FSS Code). Detailed design and installation requirements for prescriptive-based and performance-based (i.e., ‘alternative’) systems are given in MSC.1/Circ.1430, published in its first version in 2012. Prescriptive-based systems should be designed per the design tables in MSC.1/Circ.1430, whilst performance-based systems should be tested to the satisfaction of the Administration in accordance with the fire test procedures in its Appendix.

Concerns related to the fire suppression performance of the performance-based option have been raised as the fire test procedures set a performance level that is only similar or slightly better than the performance of systems that used to be installed in accordance with Resolution A.123(V). This is the primary question that is supposed to be re-solved in Action 10-C, denoted “Updated performance of alternative fixed fire-fighting systems”, by the establishment of a revised fire test procedure and a harmonized performance level for prescriptive-based and performance-based systems.

## 1.2 Method

The initial work in the report was based on a literature review that summarises the requirements in SOLAS Chapter II-2, the FSS Code and MSC.1/Circ.1430 (as revised) along with a description of the development work, research and previous IMO circulars that resulted in the requirements in MSC.1/Circ.1430. Input on the conditions on vehicle, special category, and ro-ro spaces in terms of the transported cargo distance between vehicles and the ceiling construction was given by WP05 of the LASH FIRE project. A short review of actual fires, compiled from accident investigation reports, was made with the objective to identify which types of vehicles are involved in fires, how the fires start, the performance of the fixed installed fire protection system and the consequences in terms of fire damage. A compilation of the design and installation criteria of performance-based systems was also made, to investigate how these systems in general are designed as compared to prescriptive-based systems.

A literature review documented the characteristics of fires in electric vehicles (EV) as compared to conventional combustion engine vehicles (ICEV).

In the second phase, the design and installation guidelines as well as the fire test procedures in MSC.1/Circ.1430/Rev.2 were summarised and commented, with the intent to identify the aspects that need to be covered in the revised fire test procedures. Thereafter, revised fire test scenario mock-ups were developed, partly based on input from free-burn fire tests.

Finally, a series of large-scale fire suppression benchmark tests were conducted. These tests were conducted with prescriptive-based systems designed per MSC.1/Circ.1430/Rev.2 in order to establish a basis for new performance acceptance criteria for the testing of performance-based systems.

The increased use of electric vehicles has raised a concern about the performance efficiency of water spray fire suppression systems typically installed on ro-ro cargo and ro-ro passenger ships. This was investigated in a test series involving testing of two pairs of geometrically similar gasoline-fueled and battery electric vehicles under as equal test conditions as possible. Fire ignition was arranged to initiate fire in such a way that the liquid fuel or the battery pack was involved at the initial stage of the fire.

### 1.3 Results and achievements

Resolution A.123 (V) was published in 1967, but concerns were raised in the 1990's whether its guidelines for the installation of fixed water spray fire-fighting systems offered sufficient protection of vehicle, special category, and ro-ro spaces in the light of modern vehicles and new types of cargo. A desire to install 'alternative' (equivalent) water-based fire protection systems led to the development of MSC/Circ. 914 and later MSC.1/Circ. 1272. The latter document permitted alternative systems to be automatically activated, a feature that (if used) was expected to improve system performance. However, an inadequacy of the fire test procedures of MSC.1/Circ. 1272, as adopted in MSC.1/Circ. 1430, is that the performance requirements of alternative, performance-based systems are only equal or slightly better than those of a system designed per Resolution A.123 (V).

The review of actual fires on ro-ro ships shows that many fires start inside vehicles due to electrical failures, that may have been avoided by the disconnection of the battery. Although starting small, fire development is often rapid and may include several vehicles prior the manual activation of the fixed installed water-based fire-fighting system or Carbon Dioxide system. For several of the fires, the shielding effect by the body of the vehicle or trailer on water distribution by overhead sprinkler or nozzles is observed. Most of the fires documented in the fire investigation reports started inside the actual vehicle, a couple of fires in the review started on top of a lorry. Another observation is that used vehicles may be filled with combustibles (furniture, electrical appliances, clothing, etc.) that increase the fire load and the severity of a fire. It is apparent that the cause of fire due to failure in the electrical system on older vehicles is not uncommon. None of the fire investigation reports documented fuel spill fires from the vehicles. One case with a fire starting in an electric car was identified. The car was originally a conventional combustion engine car but had been rebuilt by the owner.

The review of the characteristics of EV fires indicates that the severity of fires in EV's is comparable to that of ICEV's. Some data indicate that the maximum heat flux from an EV may be slightly higher compared to an ICEV, which could be due to the jet flames generated from the battery pack. However, other data indicate the opposite as a result of a fuel spill fire.

The compilation on the design and installation criteria of performance-based systems that have been tested and certified to the requirement in the Appendix of MSC.1/Circ. 1430 reveals a significant difference between these systems and prescriptive-based systems in terms of discharge densities and nozzle coverage areas. However, there are no field experience indicating that the performance-based system would not perform satisfactorily.

New fire test scenarios representing fires in a passenger car as well as a freight truck trailer were developed. The design of the mock-ups resembled those used in the fire test procedures in the Appendix of MSC.1/Circ.1430, but the aim was to generate more intense fires. Thereafter, benchmark fire suppression tests were conducted with an automatic sprinkler system and a deluge water spray system designed per the prescriptive-based requirements in MSC.1/Circ.1430. It is concluded that the fire growth rate seems very repeatable. But for some of the tests, the fire was too severe for a meaningful test, which calls for a reduction of the fire load. It was also observed that the performance of the tested systems was to a large degree influenced by the position of the point of fire ignition relative to the nozzles/sprinklers at the ceiling.

The fire tests involving ICEV's and BEV's indicates that a fire in a BEV does not seem to be more challenging than a fire in an ICEV for a system design in accordance with the prescriptive-based requirements in MSC.1/Circ.1430. The gasoline fuel spill fire in the ICEV tests developed rapidly and

the application of water was initiated after around a minute. The fire in the battery pack of the BEV's developed slower, involved other combustibles gradually and the application of water was initiated after more than twelve minutes and sixteen minutes, respectively. The total heat release rate from fire ignition and to the end of water application was slightly higher for ICEV1 as compared to BEV1 and higher for ICEV2 as compared to BEV2. The same trend is observed for the total heat release rate for the entire test, which included the burn-out of the vehicles. The overall conclusion is that a fire in a battery electric vehicle does not seem to be more challenging than a fire in a gasoline-fueled vehicle for a drencher system designed in accordance with current recommendations in MSC.1/Circ.1430.

#### 1.4 Contribution to LASH FIRE objectives

The overall objective of WP10 is to provide for efficient, effective, and safe fire extinguishment in ro-ro spaces, regardless of the type or size space and with less crew dependence. The objective of Action 10-C, denoted "Updated performance of alternative fixed fire-fighting systems", is to establish a harmonized performance level for alternative fixed water-based fire-fighting systems for ro-ro spaces and special category spaces. The following tasks are included, as given in the Description of work, with the role of partners:

**Task T10.1:** WP10 management (RISE).

**Task T10.9:** Literature study (RISE), with focus on regulations, research, fire hazards and previous test methods for alternative fixed water-based fire-fighting systems for ro-ro spaces and special category spaces.

**Task T10.10:** Development of relevant fire test procedures for alternative fixed water-based fire-fighting systems intended for ro-ro spaces and special category spaces. RISE will with the support of MAR develop a more realistic and relevant fire test standard (to replace that described in MSC.1/Circ.1430) representing the safety level provided by current prescriptive-based system requirements.

**Task T10.11:** Large-scale validation of the new fire test standard for alternative fixed water-based fire-fighting systems (RISE). Validation of fire test standard by large-scale tests (RISE) performed with fixed water-based fire-fighting system. Performance assessment delivery to WP04 and consolidation of D10.4 (RISE).

This report covers Tasks T10.9 and T10.11. Task T10.10 will be documented in the report D10.5, "Updated test standard for alternative fixed fire-fighting systems".

#### Exploitation and implementation

This report forms the basis for the further work in Action 10-C, which will ultimately be documented in D10.5.



## 2 List of symbols and abbreviations

ADR	European Agreement Concerning the International Carriage of Dangerous Goods by Road
AFFF	Aqueous Film Forming Foam
APV	Alternative Powered Vehicles (the term used by IMO in preference of the older term AFV, Alternative Fuelled Vehicles). APV is a group name for vehicles that use either pure batteries (Electrical Vehicle, EV) or some type of gas such as: Compressed Natural Gas (CNG), Liquid Petroleum Gas (LPG), Liquid Natural Gas (LNG) and Hydrogen as primarily energy source, pure or in combination with other energy storage such as batteries or diesel/gasoline.
BEV	Battery electric vehicle
CEA	The European Insurance and Reinsurance Federation
CEU	Car Equivalent Unit, a unit of measurement indicating the car carrying capacity of a vessel
CFD	Computational Fluid Dynamics
CINEA	The European Climate, Infrastructure and Environment Executive Agency
EUR	Marking on load pallets as specified by the European Pallet Association
EV	Electric vehicle
FSS	International Code for Fire Safety Systems, also known the Fire Safety Systems Code
F4M	FiFi4Marine B.V. (partner of WP10)
ICEV	Internal combustion engine vehicle
IMDG	International Maritime Dangerous Goods Code
IMO	International Maritime Organization
ISO	International Organization for Standardization
MAR	Marioff Corporation Oy (partner of WP10)
MCA	Maritime and Coastguard Agency
MSC	Maritime Safety Committee
NEF	The EU project New European Ferry
NFPA	National Fire Protection Association
NRC	National Research Council of Canada
PHEV	Plug-in hybrid electric vehicle
RISE	RISE Research Institutes of Sweden
RTI	Response Time Index

SOLAS	Safety of Life at Sea
SP	SP Technical Research Institute of Sweden and SP Swedish National Testing and Research Institute (the former names of RISE)
SSE	IMO Sub-Committee on Ship Systems and Equipment
SUV	Sport Utility Vehicle
UNF	Unifire AB (partner of WP10)
VdS	VdS Schadenverhütung GmbH, a subsidiary of the German Insurance Association
WP	Work package

### 3 Introduction

Main author of the chapter: Magnus Arvidson, RISE.

Vehicle spaces and ro-ro spaces not capable of being sealed and special category spaces shall be fitted with a fixed water-based fire-fighting system complying with the provisions of the Fire Safety Systems Code (FSS Code). Detailed design and installation guidelines for such systems are given in ([MSC.1/Circ.1430](#)). These guidelines were published in 2012 and are intended to replace both the prescriptive requirements of Resolution A.123(V) (from 1967) for conventional water spray systems (often denoted 'drencher systems') and the performance-based requirements of MSC.1/Circ.1272 (from 2008) for automatic sprinkler and deluge systems.

Two different system options can be used according to MSC.1/Circ.1430:

- **Prescriptive-based systems:** These systems are designed and installed per sections 1, 2 and 3 in MSC.1/Circ.1430. In addition, prescriptive-based systems should comply with section 4 and be designed per the design tables 4-1 to 4-3 of MSC.1/Circ.1430.
- **Performance-based (or 'alternative') systems:** These systems are designed and installed per sections 1, 2 and 3 in MSC.1/Circ.1430. In addition, performance-based systems should comply with section 5 and should be tested to the satisfaction of the Administration in accordance with the fire test procedures in the Appendix of MSC.1/Circ.1430.

Note: Performance-based (or 'alternative') systems are typically water mist fire protection systems.

Concerns related to the fire suppression effectiveness of the performance-based option have been raised as the fire test procedures set a performance level that is only similar or slightly better than the water spray systems that used to be installed in accordance with Resolution A.123(V). This is the primary question that is supposed to be re-solved in Action 10-C, denoted "Updated performance of alternative fixed fire-fighting systems", by the establishment of a harmonized performance level for prescriptive-based and performance-based systems.

Two different fire test scenarios are described in the Appendix of MSC.1/Circ.1430, a scenario simulating a passenger car fire and a scenario simulating a cargo fire of a simulated freight truck.

The two primary inadequacies of the fire test procedures are that:

1. The fire test scenarios do not reflect the severity in terms of the fire load of modern vehicles and cargo. The estimated peak heat release rate of the passenger car mock-up is around 2,5 MW and the heat release rate of the freight truck trailer mock-up is around 22,5 MW. These figures are estimated based on the assumption that all combustibles of the scenarios are burning at the same time.
2. The acceptance criteria in terms of the maximum allowed ceiling gas temperatures, fire damage and ignition of the targets were established with a water spray system designed per Resolution A.123(V).

Therefore, the concern is that the performance-based systems that have passed the tests do not provide a fire suppression performance that is comparable to that of the prescriptive-based system design in MSC.1/Circ.1430. Consequently, the design discharge densities for the currently certified performance-based systems are low or very low (from about half to almost one tenth) of the minimum discharge densities required for prescriptive-based systems. However, it should be noted

that there are currently no field experience indicating that the performance-based system would not perform satisfactorily.

The objective of the work summarized in this report is to develop revised fire test scenarios that better reflect fires in modern vehicles and cargo. Thereafter, large-scale fire suppression tests were conducted using automatic sprinkler and water spray systems that fulfil the prescriptive-system requirements in MSC.1/Circ.1430. Thereby, a basis for new acceptance criteria was established. This report describes the fundamentals of a revised fire test procedure, i.e., the fire test sources and the large-scale fire tests that were conducted to establish the acceptance criteria in terms of ceiling gas temperatures, surface temperatures of target objects and fire damage.

Based on this, revised fire test procedures will be written. This work will be documented in D10.5, “Updated test standard for alternative fixed fire-fighting systems”.

## 4 The conditions in ro-ro spaces, vehicle spaces and special category spaces

Main author of the chapter: Vito Radolovic, FLOW.

### 4.1 General

This section summarises the conditions within ro-ro spaces, including a description of the ship's structure and equipment as well as cargo type categories and stowage arrangements.

### 4.2 Cargo and distances between cargo

Indication of the cargo type categories on ro-ro passenger and ro-ro cargo are listed below:

#### Ro-ro passenger ships

- Passenger cars, vans, campers, including APVs.
- Trucks, semi-trailers, and trailers, including APVs.
- Refrigeration/heating units (Reefers), including APVs.
- Classified goods (IMDG and ADR), including APVs.
- Special cargo (non-typical vehicles or units such as roll trailers, excavators, etc.), including APVs.
- Containerized cargo.

#### Ro-ro cargo ships

- Passenger cars including APVs, vans, campers.
- Trucks, semi-trailers, and trailers, including APVs.
- Refrigeration/heating units (Reefers), including APVs.
- Classified goods (IMDG and ADR), including APVs.
- Special cargo (non-typical vehicles or units such as roll trailers, excavators, etc.), including APVs
- Containerized cargo. Note: Containers are commonly carried on deep sea ro-ro ships by forklift and on short sea ro-ro ships they are carried on roll trailers

On ro-ro passenger and ro-ro cargo ships, cargo is (mainly) stowed in lanes, including passenger cars, trucks, trailers and other. Typical cargo stowage is illustrated in Figure 1.



Figure 1. Typical cargo stowage on ro-ro passenger and ro-ro ships. Photo: FLOW.

## 4.3 Design and production aspects

### 4.3.1 Vehicle space deck structure arrangement

The most common structural arrangement within the vehicle spaces on ro-ro passenger and ro-ro cargo ships includes a grillage consisting of long span transverse girders (side to side) and longitudinal girders, with no pillars. This results in web heights [depth] of the primary supporting structure (longitudinal and transversal beams) in the range 600 mm to 1200 mm, where beams are extending from side to side.

Typical spacing of transversal beams can vary from about 2200 mm to 3600 mm. Spacing of longitudinal beams can vary from about 3000 mm to 10 000 mm. Openings in girder webs can be arranged for the passage of equipment (piping, cables, ducts, etc.) and to the reduce the weight.

Arrangement of movable (hoistable) car decks is very common on ro-ro passenger ships, usually within one vehicle space above the bulkhead deck. Structural height of movable decks can vary from 300 mm to 400 mm. Similar arrangement can be also found on ro-ro cargo ships and vehicle carriers, sometimes with more levels (two or three) of hoistable decks in the same space. Hoistable decks may or may not be equipped with open lashing holes.

For Stena Flavia (generic ro-ro passenger ship) and Magnolia Seaways (generic ro-ro cargo ship) the structural arrangement is described in Table 1 and Table 2, respectively.

Table 1. Structural heights of beams at Stena Flavia.

Deck	Primary structure height, mm	Openings in primary structure, mm	Stiffeners height, mm
2	230	-/-	80
3	625	400 × 200	220
4	950	800 × 400	220
5	875	600 × 350, 750 × 350	80

Table 2. Structural heights of beams at Magnolia seaways.

Deck	Primary structure height, mm	Openings in primary structure, mm	Stiffeners height, mm
Main Deck	1 130	1 000 × 300	280
Upper deck	1 150	1 000 × 300	240
Weather deck	980	800 × 250	240

Figure 2 through 5 illustrate a typical vehicle space on a ro-ro passenger and ro-ro cargo ships.



Figure 2. Typical vehicle space on a ro-ro passenger ship (photo from Stena Flavia). Photo: FLOW.





Figure 3. Typical vehicle space deck structure arrangement with insulation of the steel deck. Photo: FLOW.

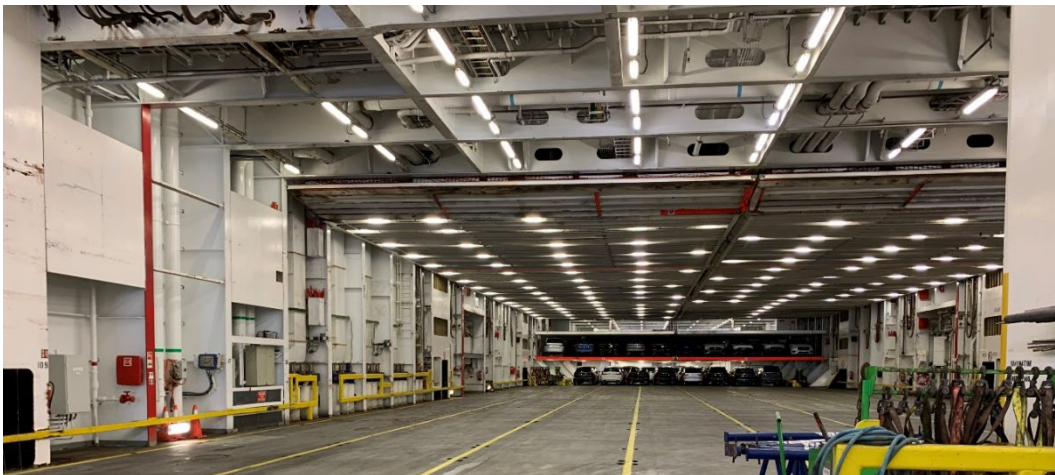


Figure 4. Typical vehicle space on a ro-ro cargo ship, with the arrangement of a movable deck. Photo: FLOW.





Figure 5. Typical vehicle space on a ro-ro passenger and ro-ro cargo ship with movable deck arrangement.  
Photo: FLOW.

#### 4.3.2 Vehicle space equipment arrangement

Typical equipment that can be found within a vehicle space includes the lightning system, cabling and piping of ship systems and the fire-fighting system that is usually arranged within the ship structure to avoid obstructions of the space available for cargo. In vehicle spaces arranged with movable decks, specific equipment is additionally arranged such as electro-hydraulic jigger winches with flexible piping connections or deck lifters.

#### 4.3.3 Materials

Typical structural material used on ro-ro ships for ro-ro decks structural application is steel. Further, aluminum alloys can be used as well as alternative materials such as plywood and composite materials.

#### 4.4 Environmental aspects

Environmental aspects can be considered related to the extinguishing media type, quantity of the released media etc. mixed with fire by-products that could be released into the environment. The medium used to extinguish fire should not be harmful to humans or marine life to the extent similar to the requirement for other parts of the ship.

## 5 Short review of actual fires on ro-ro ships

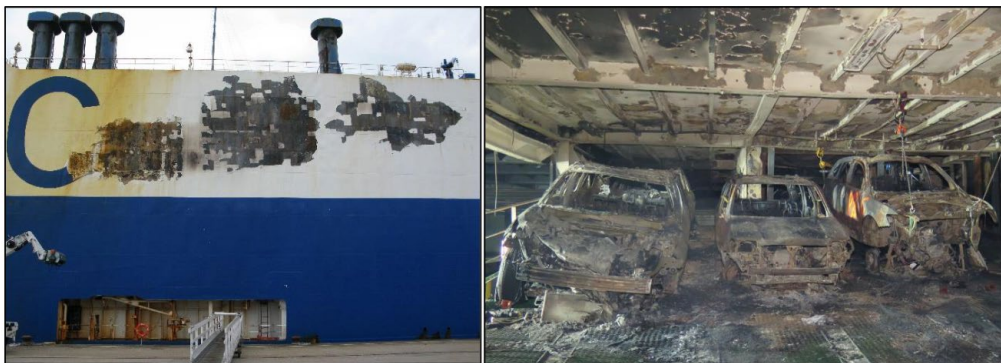
Main author of the chapter: Magnus Arvidson, RISE.

### 5.1 General

This section contains a short review of actual fires, compiled from accident investigation reports. The objective was to identify which types of vehicles that are involved in fires, how the fires start, the performance of the fixed-installed fire protection system and the consequences in terms of fire damage. The focus of the review was to provide input to the design of the development of relevant fire tests procedures.

### 5.2 Courage (vehicle carrier)

A fire started on June 2, 2015, in the cargo hold of the ro-ro vehicle carrier *Courage* (built in 1991) when on route from Bremerhaven, Germany, to Southampton, United Kingdom [1]. The likely cause of the fire was electrical arcing in the automatic braking system module of a 2002 Ford Escape sport utility vehicle (SUV). It was found that this particular make and model was the subject of recalls in 2007 and 2010 due to non-crash-related fires or thermal events in the vehicles' engine compartments. The owner had been overseas for a number of years and was not aware of the recalls. The fire was extinguished by the operation of the fixed Carbon Dioxide system. No persons were injured but based on the extent of fire damage, refer to Figure 6, the owner of the ship decided to scrap it.



Left photo shows exterior damage to *Courage* starboard side in the vicinity of the fire. Right photo shows damaged ramp and destroyed vehicles near the origin of the fire. (Photos by Coast Guard)

Figure 6. The fire damage to the vehicle carrier *Courage* [1].

**Comments:** The extensive fire damage illustrates how fast a fire that starts small (electrical arcing) could spread to an extent that results in severe damage. Note that these types of ships have not a fixed-installed water-based fire-fighting system.

### 5.3 Honor (vehicle carrier)

On February 24, 2017, a fire started in the upper vehicle deck on the ro-ro vehicle carrier *Honor* (built in 1996) when on route from Southampton, England, to Baltimore, USA [2]. The fire was extinguished by the operation of the fixed Carbon Dioxide system. One crew member was injured during the fire-fighting efforts and the fire damage was extensive to the cargo hold and the cargo of about 5,000 vehicles, refer to Figure 7.



At top, damaged cars on the garage deck. At bottom from left to right, damage to the top deck above the garage and the exterior bulkhead on the port side of the garage while looking aft.

Figure 7. The fire damage to the vehicle carrier Honor [2].

However, it was concluded that the crew's appropriate and effective use of the Carbon Dioxide system, along with boundary cooling, likely prevented the spread of the fire and reduced the damage. The likely cause of the fire was a fault in the starter motor solenoid in one of the personally owned vehicles in shipment. Preliminary testing of this scenario confirmed that a fault within the solenoid could cause ignition of the insulation and covering on the adjacent wiring.

**Comments:** Another example of an electrical cause of fire and extensive fire damage on a vehicle carrier. Note that these types of ships have not a fixed-installed water-based fire-fighting system.

#### 5.4 Höegh Xiamen (vehicle carrier)

The vehicle carrier Höegh Xiamen was built in 2010, designed for unrestricted oceangoing worldwide service with a capacity of 4,900 vehicles. The ship caught fire at about 15:30 on June 4, 2020, while in Jacksonville, Florida, USA during loading operations [3]. The fire was discovered by crew members on deck 8, which had been loaded with used vehicles. It was also observed that flaming material was dripping to deck 7 through holes used for lashing on deck 8, i.e., the fire was spreading from the deck with the initial fire to the deck below.

The crew members tried to fight the fire but had to retreat due to heavy smoke. Shoreside fire department teams from the Jacksonville Fire and Rescue Department arrived at the scene at 16:03. The captain, after consulting with the fire department, decided to discharge the Carbon Dioxide system into decks 7 and 8. These two decks covered one (Zone 3) of the five fire zones. Thereafter the crew evacuated from the ship. The fire-fighters monitored the fire using a thermal imaging camera and judged that the fire was continuing to spread despite the discharge of Carbon Dioxide. Therefore, they decided to enter decks 7 and 8 from the port aft stairwell. Nine fire-fighters were



subsequently injured, five of them seriously, in an explosion. The “explosion” occurred about the same time that the fire-fighters opened an exhaust in the aft ventilation trunks located near the port aft stairwell. Deck 9 likely contained a rich atmosphere of heated flammable vapours (thick, black smoke had been observed), which rapidly combusted when fresh air was introduced via the opening of the ventilation trunks for decks 9 and 10/11. The fire-fighters who were in the stairwell and on deck 5 near the stairwell during the over-pressurization event described a violent rush of extremely hot air.

Consequently, a defensive strategy was adopted, cooling external exposed surfaces of the ship with fire monitors and fire hoses, refer to Figure 8.



**Figure 6.** Firefighters conducting exterior boundary-cooling on June 5, 2021, the day after the fire was discovered. (Source: JFRD)

*Figure 8. Exterior boundary-cooling during the fire in the vehicle carrier Höegh Xiamen, a defensive strategy following an explosion that injured nine firefighters, five of them seriously [3].*

The investigation showed that the fire detection was delayed as there were no procedures to reduce the time that the fire detection system remained deactivated after loading. The shoreside fire department’s response was also delayed because the master of the ship did not have immediately available contact information.

The fire burned for over a week and resulted in a total loss of the vessel and its cargo of 2 420 used vehicles. Total damages are estimated at \$40 million. After salvage operations were completed, the vessel was towed to Turkey to be recycled. The investigation after the fire concluded that many of the vehicles had batteries that were not disconnected and secured in accordance with established procedures. It is likely that the fire was caused by an electrical arc or component fault in one of the used vehicles.

**Comments:** Another example of an electrical cause of fire and extensive fire damage on a vehicle carrier. The fire was not fully extinguished by the the discharge of Carbon Dioxide and an “explosion” occurred during manual fire-fighting operations that injured nine firefighters, five of them seriously. Note that these types of ships have not a fixed-installed water-based fire-fighting system.

### 5.5 Joseph and Clara Smallwood (ro-ro passenger ship)

On the afternoon of 12 May 2003, a fire started on the lower vehicle deck on the ro-ro passenger ship Joseph and Clara Smallwood (built in 1989) on route between North Sydney and Port aux Basques in Canada [4]. The deluge water spray system was manually activated, and the fire was additionally fought with fire hoses as the vessel continued on to its destination. Shortly after midnight, the vessel docked at Port aux Basques and the passengers were evacuated. Assisted by the local fire department, the crew continued to fight the fire. Two hours after arriving to port, the fire was declared under control, and 1 ½ hours later, it was extinguished.

The vehicle deck accommodates six lanes for trailers. If fully load, the horizontal clearance between vehicles in adjacent lanes may be reduced to 30 cm. The deluge system effectively contained the fire and extinguished the flames on the exterior of the vehicles. This allowed the fire-fighters to concentrate their efforts on the interiors and undersides of the vehicles. These shielded areas were not accessible by the water from the deluge system. The resulting damage to the vessel included buckling of deck plating and damage to the thermal insulation above the origin of the fire in an area of about 40 m<sup>2</sup>. Various electrical fixtures (as lighting fixtures, heat detectors, annunciators, and associated wiring) were damaged and various internal and external areas were smoke damaged.

One freight ('tractor') truck was severely damaged, and the attached trailer was heavily damaged. The cargo of orange juice was destroyed. The contents of a moving and storage company trailer had heavy damage and a drop trailer with building supplies sustained heavy damage. Several other tractor-trailer rigs suffered varying degrees of smoke and water damage and a private motor vehicle sustained heat damage to the rear bumper, left tail-light and rear tires. It was concluded that fire likely started in the freight truck. This vehicle was too badly damaged to be easily removed from the deck and was finally towed off the vessel later in the morning. Figures 9 and 10, respectively, shows the fire damage to the freight truck and trailers.



Tractor fire damage



Trailer fire damage

Figure 9. The fire damage to the freight ('tractor') truck and the attached trailer on board Joseph and Clara Smallwood. It was concluded that fire likely started in the freight truck. Note: From these photos it appears that fire have spread from the cabin of the freight truck and towards the back, thereby involving the attached trailer. The exterior of the trailer exhibit (at least the side shown in the photo) very little fire damage [4].



Moving and storage trailer fire damage



Drop trailer fire damage

Figure 10. The fire damage to the moving and storage trailer and drop trailer (containing building supplies) in the fire on board Joseph and Clara Smallwood. Note: From these photos it seems that the fire never involved the content of the moving storage trailer, which looks like a metal structure. The photo indicate that a tarpaulin has been fitted over its top, which could be an indication of efforts to protect its content after the fire. The drop trailer has been involved but to a small extent. The photos do not tell if the fire spread through the roof of the trailer [4].

**Comments:** This fire incident shows that the operation of a deluge water spray system combined with manual firefighting effort can successfully control a fire in large vehicles and trailers. In this case, the fire involved a freight truck with an attached trailer and two adjacent trailers. From the photos of the report, it is noted that the fire does not seem to have involved the tires of the vehicles, maybe with the exception of the back tires of the freight truck, the photos of the report do not tell.

The fire does not seem to have involved any significant portion of the content of the adjacent trailers, whilst the roof of the cabin of the freight truck burnt through. Fire burn-through will expose the fire to the water spray of sprinklers which results in fire suppression or fire control.

Another observation is that the trailer or the freight truck where the fire is believed to have started contained a cargo of orange juice, which must be considered as a relatively harmless cargo in terms of the fire load.

## 5.6 Commodore Clipper (ro-ro ship)

On June 16, 2010, a fire was detected on the main vehicle deck of the ro-ro ship Commodore Clipper when on passage from Jersey to Portsmouth, UK [5].

The deck was loaded with freight truck trailers and an unaccompanied refrigerated trailer unit, powered from the ship's electrical supply caught fire. The fire started due to sustained overheating, caused by an assembly error in the reefer cable plug that was connected to the trailer. The fire was contained by using the fixed water spray system and boundary cooling from above. The deck boundary between the main and upper vehicle deck had no thermal insulation. Without the boundary cooling from fire hoses, it is likely that heat would have ignited the tires of the cars parked on the upper vehicle deck. Fire-fighting efforts had to be suspended as cargo debris (mainly fresh potatoes from the trailer on fire) blocked vehicle deck drains, causing water to accumulate and reduce the vessel's stability. Four trailers, in total, were found to be damaged by fire.

The distance between trailers on the main vehicle deck of Commodore Clipper was generally in the order of 150 mm to 450 mm and in some cases, adjacent trailers were nearly touching. The report concludes that this density of trailers encourages higher rates of fire growth and reduces the effectiveness of fixed water spray systems and portable firefighting equipment. It is reported that crew and fire-fighters saw water from the water spray system bouncing off the roofs of the trailers and running down their sides. The cargo continued to burn inside, shielded but still ventilated through the damaged curtain-sides. It is reported that the potatoes were contained in plastic crates. Figure 11 illustrates the damage to one of the refrigerated trailers.



Figure 11. The damage to one of the refrigerated trailers in the fire on board Commodore Clipper [5].

**Comments:** From the photos of the one of the refrigerated trailers during and after firefighting efforts it seems that a low profile trailer was used. The shorter side wall tire on a lower profile wheel will reduce the distance from the ground to the center of the axle, translating to a lower deck height. This increase the overall height of the cargo that is hauled. It is also observed that the cargo (potatoes in plastic crates) extends virtually the full height of the cargo space of the trailer and that the cargo (except for the front part of the trailer) is supported by steel beam racks with two levels above the deck. These racks will improve the stability of the cargo, preventing or delaying a full collapse, which is generally considered as disadvantageous for the performance of a sprinkler system.

Another observation is that only part of the roof of the trailer have burnt through. It may well be that the application of water from the overhead water spray nozzles have prevent burn through.



The potatoes would likely have contributed very little, if at all to the severity of the fire. They could rather serve as ballast that reduces the fire size. But the plastic crates would contribute to a high fire load.

### 5.7 Pearl of Scandinavia (ro-ro passenger ship)

Pearl of Scandinavia (built in 1989) departed from Oslo, Norway on November 16, 2010, at 17:30 on route to Copenhagen, Denmark. At 05:58 the morning after, the fire alarm indicated fire on the car deck [6].

The fire started in an electric car, which was originally a conventional combustion engine car, but had been re-built by the owner. The car was allowed to be connected to a 220 V charging station on the port side of the car deck aft and had charged for approximately 13 hours when the fire broke out.

The car deck is divided into sections by flooding control doors. These doors do not extend all the way to the deck above, there is a vertical gap of approximately 0,5 m. The electric car was parked just behind such a flooding control door (section 5) and in the adjacent section (section 6) there was another car and a freight truck trailer.

An attempt to fight the fire by fire hoses was considered to be hazardous and was terminated. The sprinkler system in section 5 was manually operated at 06:15. At 07:00 Swedish fire-fighters arrived at the ship by a helicopter and at 07:12 the water flow from the sprinkler system on deck 3 was shut off. The Swedish fire-fighters (using breathing apparatus) then entered the space and could ascertain that there were still some small fires. One of these under the bonnet of one of the cars. These small fires were extinguished by portable fire extinguishers. At 07:51 the fire was reported extinguished, and guards were posted for monitoring deck 3. It was concluded that an explosion in the battery pack in the rear end of the electric car spread fragments of red-hot metal through the gap between the flooding control door that resulted in a fire in two trailers. One of these trailers were carrying plastic pipes. The fire damage is shown in Figure 12.



*The electric car and a trailer carrying plastic pipes*

*Figure 12. The damage to the electric car in the fire on board Pearl of Scandinavia [6].*

Although the fire was effectively extinguished, it caused damage resulting in the ship being taken out of service for some days.



**Comments:** From photos after the fire, it seems that the electric car was severely damaged by the fire and virtually all combustibles as the interior, combustible exterior parts and the tires have been consumed. It seems that the body of the car have effectively prevented distribution of water to the fire. However, the sprinkler system prevented the fire being established in the other vehicles.

## 5.8 Mecklenburg-Vorpommern (ro-ro passenger ship)

The Mecklenburg-Vorpommern is a ro-ro passenger ship built in 1996 that regularly operates between Trelleborg, Sweden and Rostock, Germany. At about 20:35 on November 19, 2010, shortly before arrival at the port of Rostock, a vehicle transported on a semi-trailer on deck 4 caught fire [7].

At 20:37, a crew member who passed this deck while proceeding to the maneuvering station discovered a fire in a trailer and alerted the bridge using the internal ship telephone. At 20:39, the fire was also detected by the fire detection system and an alarm followed. Attempts were made to start the drencher system in this area (sections 8 and 9), but this did not work immediately due to the stiffness of a control valve. At 20:45, the drencher system was working and at 20:49 the ventilation fans on deck 4 were turned on to extract the smoke and the response team proceeded to the deck to start fighting the fire. At 21:55, the on-shore fire brigade took over the entire fire-fighting operation. Deck 4 was still filled with heavy smoke and the fire flared up repeatedly. The drencher system was turned off at 22:06. From 22:23, an interconnected vehicle was driven off the vessel and two others were moved to provide a better overview and access to the remaining fire. During an initial inspection, it was found that one of the three vehicles located on a semi-trailer was severely burnt and the two others were damaged.

Three older, used vehicles were transported on the semi-trailer. A VW Transporter minibus (positioned in the front of the trailer), a Mercedes-Benz C Class saloon (in the middle) and a Volvo 240 estate wagon (positioned at the rear of the trailer). All the vehicles were destined for further transportation to Africa. The front and the rear vehicles were fully loaded with used items, such as furniture, electrical appliances, and clothing. In addition, three used car engines were stowed in the VW Transporter.

The fire started in VW Transporter, which was almost completely burnt out, refer to Figure 13, including all four tires that were completely or severely burnt. Of the two other vehicles, only the rear of the middle vehicle located in the immediate vicinity of the VW Transporter showed signs of fire damage. A battery located under the passenger seat of the VW Transporter is the probable cause of ignition.



Figure 9: Driver's side of the VW Transporter

Figure 13. The damage to the VW Transporter in the fire on board Mecklenburg-Vorpommern [7].

The investigation concluded that water from the drencher system and the manual fire-fighting operation did not or did only indirectly reach the seat of the fire due to shielding by the tarpaulin on the semi-trailer. Fire damage to the side tarpaulins and roof of the semi-trailer was most severe in the area where the VW Transporter was positioned, refer to Figure 14. The floor of the trailer was burnt, and its front wall sustained moderate fire damage. There was no fire damage on the freight truck unit.



Figure 11: Fire-damaged semi-trailer with VW Transporter



Figure 12: Fire-damaged semi-trailer with VW Transporter

Figure 14. The fire damage to the semi-trailer and the VW Transporter in the fire on board Mecklenburg-Vorpommern.

It was concluded that the early discovery the fire by a crew member, the immediate initiation of the fire-fighting operation, the favorable slot position of the semi-trailer and the proximity to the port facility, were the main reasons why it was possible to prevent a severe damage. In addition, the assistance of the shore-based fire brigade made it possible to bring the fire under control. The drencher system was activated, but there was a time delay of six minutes due to a stiff valve. The drencher system on board the ship is divided into 15 sections, but no more than three sections can be operated at the same time.

**Comments:** Another example of a fire that is fully or partly shielded from direct application of water from overhead sprinklers or nozzles. The extent of damage to the roof of the semi-trailer is unclear, as this is not documented by any photos in the report. But it is obvious that the body of the VW Transporter have prevented water from suppressing the fire, as such a large part of the combustibles of the vehicle seems to have been consumed. The fact that the car was filled with combustibles

(furniture, electrical appliances, clothing, etc.) may have increased the fire load and the severity of the fire.

### 5.9 Victoria Seaways (ro-ro passenger ship)

The Victoria Seaways, a ro-ro passenger ship (built in 1991) travelled its regular international route between Kiel, Germany and Klaipėda, Lithuania when a fire started at 01:53 on April 23, 2013, on cargo deck 3 [8]. The ship was carrying trailers with various cargo, second-hand cars (from Germany) and passengers. The ship had a crew of 37 at the time of the incident, but the report does not provide the number of passengers.

A starboard fire detector on deck 3 detected a fire, rapidly followed by additional detectors, and visible smoke was observed in a video camera located on the stern of deck 3. The ship ventilation was stopped at 01:54. A crew member on duty pressed the fire button, reported open fire and the necessity to activate the drencher system. The decision was made to activate drencher sections 7 and 8 on deck 3 and these sections activated at 02:05. At 02:10, the fire-fighting teams found a hot spot above the seat of fire on deck 4 and boundary cooling of the deck was initiated using fire hoses.

At 02:25, two additional fire pumps were started and connected to the drencher system, and sections 9 and 10 were activated on deck 3. At 03:00, sections 7 and 10 were deactivated while sections 8 and 9 remained on. At 03:25, deck 4 had completely cooled above the seat of fire and it was visually confirmed there were no open flames but a considerable amount of smoke. The drencher system was deactivated and cooling and inspections of deck 4 were performed on a regular basis. At 03:45, sections 8 and 9 were reactivated on deck 3 to ensure the fire was completely extinguished. No temperature changes were observed on deck 4 and at 04:00 the seat of fire had been extinguished.

The fire destroyed six cars and the car trailer, refer to Figure 15, but there were no casualties or personal injuries.



Figure 4: Burned down cars

Figure 15. The fire damage to the cars on the trailer after the fire on Victoria Seaways [8].

It is likely that a short circuit in the electrical system one of the second-hand cars in the cargo caused sparks that fell on a dirty surface of the engine and caused the fire. It was recommended that the crew should check if the batteries of all transported second-hand cars are disconnected before the ship leaves the port.

**Comments:** Two sections of the drencher system were activated within 10 minutes after fire detection. Additional sections were activated at a later stage and boundary cooling of the deck surface of the deck above was initiated using fire hoses. In total, the drencher system was activated (although partly or fully deactivated for certain periods) for about 2 hours. Fire spread between the cars on the trailer occurred and these cars were severely, although not completely damaged. The report does not tell if the fire started in a car at the lower or at the top level of the car trailer. However, from the photos of the report it seems that car where the fire started was positioned at the lower level.

#### 5.10 URD (ro-ro passenger ship)

On March 4, 2014, the ro-ro passenger ship URD (built in 1981) departed from Liepaja, Latvia bound for Travemünde, Germany. The car decks of the ship were fully loaded, and 110 passengers were on board. At 07:40, two crew members, randomly passing the main car deck, discovered a fire on top of a lorry [9]. The bridge was alerted, and the drencher system was rapidly activated. Ten minutes later, the drencher system was stopped in order to allow judgement of its effect. As the fire was not completely extinguished, the fire-fighting crew tried to extinguish it by means of a fire hose.

Approximately 30 minutes after the initial discovery, the fire was extinguished, and normal operation was continued. A fire watch was established on the car deck for the remainder of the voyage and the ship arrived as scheduled on March 5, 2014.

It was concluded that the early discovery of the fire contributed to the successful outcome of the accident. The crew noticed the fire approximately 6 minutes prior the automatic smoke detection system. The cause of the fire was a malfunction in a fluorescent light fixture at the ceiling that made the diffuser catch fire. At some point, the diffuser got detached from the light fixture and landed on the tarpaulin of the lorry situated underneath. The tarpaulin caught fire and flames and smoke developed. The investigation concluded that the close proximity of the burnt fixture to a sprinkler head that was regularly tested may have contributed to the existence of the excessive humid and saline atmosphere inside the light fixture. Figures 16 and 17, respectively, shows the main car deck at the day of the fire and the fire damage.





Figure 4: Main car deck on board URD, fully stowed on the day of the fire. Looking aft  
Source: Stena Line

Figure 16. The main car deck on board URD, that was fully stowed on the day of fire [9].



Figure 5: Burnt lorry. Picture taken after arrival in port  
Source: Stena Line

Figure 17. The fire damage to the lorry on board URD [9].

**Comments:** The fire started due to an electrical failure of light fixture at the ceiling that involved the tarpaulin of a trailer positioned below. The fire never grew large due to prompt action by the crew. It seems that both the roof and the sides of the lorry were covered by a tarpaulin.

### 5.11 Stena Spirit (ro-ro passenger ship)

On August 31, 2016, the ro-ro passenger ship Stena Spirit (built in 1988), was underway on the regular voyage from Karlskrona, Sweden to Gdynia, Poland. At 06:47, shortly prior reaching the port, a fire alarm was activated as a result of a smoke being detected on car deck 3 [10]. It was visually observed that the smoke was originating from the V-belts of the refrigerator unit's drive on a truck.

Several minutes thereafter, fire was noticed on the roof of a truck next to the refrigerator unit. Attempts were made by a watchman to manually extinguish the fire using a 50 kg transportable dry-chemical fire extinguisher, but this failed. Due to thick smoke, he had to evacuate the space and the drencher system was activated. At 07:35, the fire had been suppressed. The ship anchored at the pier, but without the mooring winches that were inoperative due to damage caused by fire. At 07:57, the passengers were allowed to leave the ship and 20 minutes thereafter, the stern ramps were opened to allow on-shore firemen to board the ship and to fully extinguish the fire of the refrigerator truck. At 08:20 the last passengers got ashore, and the fire-fighting operation was completed within 20 minutes.

The report concludes that the drencher system was activated too late and in an incorrect manner according to ship's procedures. At around 07:12, drencher system sections 1 and 13 were manually activated. At 07:19, sections 2 and 3 on deck 3 was also activated and after several minutes, sections 14 and 15 on deck 5. The simultaneous activation of several (in this case as many as six) sections result in a reduced operating pressure at the nozzles located directly above or close to the vehicles in fire, thus resulting in ineffective performance. However, the system managed to suppress the fire and prevented the fire from spreading to adjacent vehicles.

In its first phase, the fire was relatively small and was developing slowly for more than a dozen minutes. At this stage, it could have been easily extinguished (which failed due to the difficulties of accessing the elevated source of the fire). In its second phase the fire developed rapidly, which resulted in breakage of a hydraulic oil pipeline above the fire location. Leaking oil therefore fed the fire that spanned the entire width of the vehicle's roof. The fire temperature was high enough to cause the paint to burn and the deck steel plate to deform directly above the fire source. Probably, additional hydraulic oil pipelines cracked and leaked oil that, in turn, maintained the fire in another spot on the vehicle roof which is confirmed by the second spot of burnt paint on deck 5 (the deck above the fire).

Figures 18 and 19, respectively, shows the fire damage to the refrigerator truck and the freight truck positioned adjacent.



*Photograph No. 13. Burnt vehicle roof with damaged refrigeration unit*

Figure 18. The fire damage to roof of the refrigerator truck on board Stena Spirit [10].



*Photograph No. 16. Burnt tarpaulin of the truck parked next to the refrigerator truck and its cargo*

Figure 19. The fire damage to the freight parked next to the refrigerator truck on board Stena Spirit [10].

### 5.12 Britannia Seaways (ro-ro cargo ship)

On November 14, 2013, at 18:10 hours, the ro-ro cargo ships Britannia Seaways (built in 2000) departed from Sørreisa, Norway, on a voyage to Bergen, Norway. The ship carried military equipment, vehicles, a number of tank containers and open cargo units with jerrycans (i.e., about 20 liter flat-sided metal containers for storing or transporting liquids) containing petrol and aviation/jet fuel [11].



There were 12 passengers, all military personnel on board. The weather forecast for the planned journey predicted storm, which required satisfactory lashing of the cargo. However, during severe rolling a tank container on the forepart of the weather deck loosened from its lashings and caused damage to some jerrycans. Ultimately, leaked petrol was ignited by sparks generated by one or more tank containers that slid across the deck, steel against steel.

The heat from the fire caused the web lashings on all other cargo units on the weather deck to burn or melt, and all units could slide across the deck and create damage and leakage to fuel containers and jerrycans, thereby enhancing the fire. The fire-fighting effort involved three to four fire hoses from each walkway and from the weather deck, behind the cargo units. At the initial stage, the crew fought the fire, at a later stage assisted by volunteers from the military personnel.

No person was injured and there was no pollution of the environment. The fire resulted in burned fuel cargo and damaged military equipment, including military vehicles, but moderate damage to ship's construction.

**Comments:** This fire started on the weather deck in fuel leaking petrol from small transportation containers ('jerrycans') but involved fuel from tank containers. The fire started on the weather deck and the experience from the fire is therefore not directly relevant for closed or open ro-ro spaces. The primary observation of importance is that fire started in leaking fuel.

### 5.13 Corona Seaways (ro-ro cargo ferry)

At 02:15 on December 4, 2013, a fire was discovered on the main deck of the ro-ro cargo ferry Corona Seaways (built in 2006), on route from Fredericia to Copenhagen, Denmark [12].

The cargo included used driveable and non-driveable vehicles, loaded low heavy-duty trailers, trailers, car transporters, and agricultural and heavy plant machinery. At 21:00 on December 3, 2013, the cargo loading operations were finished in Fredericia and a total of 170 units were tightly stowed in the lower hold, on the main, upper, and weather decks.

At 02:15, on December 4, 2013, the fire detection system indicated a fire in Zone 12 (starboard side) on the main deck. The ventilation louvres to the space were closed at 02:25, boundary cooling started, and the fixed-installed Carbon Dioxide fire-extinguishing system was operated at about 02:30. At 03:10, it was determined that likely only 9 tons of the 21,3 tons of Carbon Dioxide stored in the tank had been released into the main deck space instead of the required 19,8 tons. Therefore, the system was operated once more. Following this second release, it was determined that the fire appeared to be under control. At 04:00, it was indicated that over 10 tons of Carbon Dioxide was still remaining in the storage tank. The master authorized the chief engineer to manually operate the system from the storage tank compartment.

At 06:40, the vessel entered the Swedish port of Helsingborg, where assistance was provided by the local Fire and Rescue Service. At 12:08, cargo unloading started and the fire was declared out at 13:25.

The ship suffered light structural damage and the loss of some minor electrical supplies. The majority of the structural damage was located above the fire on the underside of the upper deck. Approximately 15 m<sup>2</sup> of the steel deck was required to be replaced, including seven slightly distorted longitudinal deck head stiffeners. The pipe-work and nozzles of the Carbon Dioxide system was not damaged.

Three vehicles and six trailers were severely damaged and other vehicles suffered minor radiant heat damage, refer to Figure 20.





**Figure 4:** Damaged vehicles and trailers on the main deck

Figure 20. The fire damaged vehicles and trailers on the main deck on board Corona Seaways [12].

It was concluded that the fire was caused by an electrical defect of the engine starting system on one of the vehicles.

**Comments:** The delay time from fire detection to operation of the Carbon Dioxide system was in the order of 15 minutes. It appears that the discharge was effective, although the desired amount was not discharged immediately. Although the structural fire damage was judged to be minor, it is likely that the boundary cooling of the deck steel plating could have important for the prevention of fire spread to the space above. The space (closed ro-ro space) had no fixed-installed water-based fire-fighting system, the main observation of importance is how quickly several vehicles can be involved in a fire.

#### 5.14 Conclusions based on the actual fires

Several of the cases summarised here included include fires on board vehicle carriers (Courage, Honor and Höegh Xiamen) and a ro-ro cargo ferry (Corona Seaways). The ro-ro spaces of these ships are protected by a fixed-installed Carbon Dioxide system and not a fixed-installed water-based fire-fighting systems. Still, the cases are interesting to refer to as they illustrate the fire growth rate and severity of fires in vehicles. The fires on board Courage, Honor and Höegh Xiamen resulted in extensive fire damage, that in two of the cases resulted in an extent of damage that called for scrapping of the ships.

The horizontal distance between vehicles is generally much shorter than that used in the fire test procedures in MSC.1/Circ.1430. A shorter horizontal distance may increase the exposure from a fire to adjacent vehicles and increase the degree of obstruction for the water spray from overhead sprinklers or nozzles. For several of the fires, it was also proved to be difficult for the fire-fighters to successfully approach the fire due to densely stowed vehicles. Although it should be recognized that

manual fire-fighting is not scope of Action 10-C, it underlies the importance of an efficient fixed-installed fire-fighting system, whether it be a water-based or a gaseous agent system.

For several of the fires, the shielding effect by the body of the vehicle or trailer on water distribution by overhead sprinkler or nozzles is observed. It is also noted that the body of a passenger car is surprisingly intact, even after a very severe fire. This means that water from overhead sprinkler or nozzles will be shielded for the full duration of a fire, which need to be reflected in the fire test procedures.

Most of the fires described here started inside the actual vehicle, but the fire on board URD started on top of a lorry. The cause of the fire was a malfunction in a fluorescent light fixture at the ceiling that made the diffuser catch fire. At some point, the diffuser got detached from the light fixture and landed on the tarpaulin of the lorry situated underneath. The tarpaulin caught fire and flames and smoke developed. Another example of a fire that started on top of a freight truck is the fire on board Stena Spirit that originating from the V-belts of the refrigerator unit. The fire spread to the truck roof. A fire that starts on an elevated position is extraordinary difficult to fight by manual means, which was illustrated here. Even though the drencher system was started at a late stage and in an incorrect manner, the fire was, however, effectively suppressed.

Another observation is that used vehicles, as in the fire onboard Mecklenburg-Vorpommern may be filled with combustibles (furniture, electrical appliances, clothing, etc.) that increase the fire load and the severity of a fire. This fire started in a VW Transporter that was carried on a car trailer, along with other passenger vehicles, intended for sale on the open market in a developing country. The fires on board Victoria Seaways and Corona Seaways did also include car trailers with second-hand cars. It is obvious that a fire ignition scenario that involves the electrical system on older vehicles is common. Other examples include the fires on board the vehicle carriers Courage, Honor and Höegh Xiamen.

None of the fire investigations reports about fuel spill fires from the vehicles. However, in the fire on board Stena Spirit, hydraulic oil pipes were damaged with resulted in spills of hydraulic oil and the fire on the weather deck of Britannia Seaways started when petrol from leaking from jerrycans was ignited by sparks generated by one or more tank containers that slid across the weather deck, steel against steel.

One case with a fire starting in an electric car was identified, the fire on board Pearl of Scandinavia. The car was originally a conventional combustion engine car but had been re-built by the owner. The fire started during charging on board the ship.

## 6 The development of MSC.1/Circ.1430

Main author of the chapter: Magnus Arvidson, RISE.

### 6.1 The requirements in SOLAS Chapter II-2, Part G, Regulation 20

SOLAS Chapter II-2, Part G, Regulation 20, "Protection of vehicle, special category and ro-ro spaces" states:

*"6.1.2 Vehicle spaces and ro-ro spaces not capable of being sealed and special category spaces shall be fitted with a fixed water-based fire-fighting system for ro-ro spaces and special category spaces complying with the provisions of the Fire Safety Systems Code which shall protect all parts of any deck and vehicle platform in such spaces. Such a water-based fire-fighting system shall have:*

- .1 a pressure gauge on the valve manifold;*
- .2 clear marking on each manifold valve indicating the spaces served;*
- .3 instructions for maintenance and operation located in the valve room; and*
- .4 a sufficient number of drainage valves to ensure complete drainage of the system.*

*6.1.3 The Administration may permit the use of any other fixed fire-extinguishing system \*\* that has been shown that it is not less effective by a full-scale test in conditions simulating a flowing petrol fire in a vehicle space or a ro-ro space in controlling fires likely to occur in such a space.*

*\*\* ) Refer to Guidelines for the approval of fixed water-based fire-fighting systems for ro-ro spaces and special category spaces equivalent to that referred to in resolution A.123(V) (MSC.1/Circ.1272) and Revised Guidelines for the design and approval of fixed water-based fire-fighting systems for ro-ro spaces and special category spaces (MSC.1/Circ.1430)."*

When fixed pressure water-spraying systems are fitted, means should be taken to prevent serious loss of stability which could arise due to large quantities of water accumulating on the deck or decks due to the discharge of water. These requirements are given in sections 6.1.4. and 6.1.5 and are not discussed in detail here. The overall requirement is that the drainage system shall be sized to remove no less than 125% of the combined capacity of both the water-spraying system pumps and the required number of fire hose nozzles. Additionally, means shall be provided to prevent the blockage of drainage arrangements, based on the guidelines in MSC.1/Circ.1320.

Chapter 7, "Fixed pressure water spraying and water-mist fire-extinguishing systems" of the International Code for Fire Safety Systems (FSS Code) provides specifications for "fixed pressure water-spraying and water-mist fire-extinguishing systems" as required by SOLAS Chapter II-2. Section 2.4 states that "Fixed water-based fire-fighting systems for ro-ro spaces, vehicle spaces and special category spaces shall be approved by the Administration based on guidelines developed by the Organization\*.

*\*) Refer to the Revised guidelines for approval of fixed water-based fire-fighting systems for ro-ro spaces and special category spaces (MSC.1/Circ.1430)."*

### 6.2 The requirements in IMO Resolution A.123 (V)

Detailed requirements for the design and installation of water spray systems for vehicle and ro-ro cargo spaces are given in IMO Resolution A.123 (V) from 1967 [13]. Some requirements that can be mentioned in particular are that:

- The system shall be designed for a water discharge density of at least 3,5 mm/min for decks with a maximum height of 2,5 m height and at least 5 mm/min for decks with higher height.
- The system is allowed to be divided into sections where each section should cover the entire width of the ship. Exemptions from this requirement may be allowed if the deck is separated longitudinally by 'A' class divisions.
- Each section must be at least 20 m long, and the system's pumps must have a capacity sufficient for either the entire deck or at least two sections.
- Section valves must be located outside the protected space.

The technical background to the requirements is possibly a series of fire trials carried out in Denmark in 1961 [14].

In the 1990's, concerns were raised as to whether a water spray system in accordance with Resolution A.123 (V) is able to control or suppress a fire in modern cars, coaches, freight trucks and trailers, see SP Report 1997:03 [15] and SP Report 1997:15 [16]. The latter report describes a large-scale fire test with a layout representing two trucks, side by side, on a ro-ro deck. The test is documented on video [17].

### 6.3 The publication of MSC/Circ. 914

In 1999, IMO published MSC/Circ. 914 [18] containing principal design and installation requirements and fire test procedures for alternative - to Resolution A.123 (V) - systems for special category spaces. The fire test set-up mimics a freight truck trailer fire and was based on that used in the large-scale fire tests described in SP Report 1997:15. A pool fire tray scenario was used to represent a fuel spill fire, with the intent to determine the area of operation of wet-, dry- or pre-action systems.

In retrospect, it seems that no systems were tested in accordance with these fire tests procedures, at least no systems were certified and reached the market.

In 2002, a feasibility study was carried out by RISE (then SP) where the requirements and alternative fire-fighting systems for cargo were discussed [19].

### 6.4 Concerns raised by Maritime and Coastguard Agency (MCA)

In 2006, the Maritime and Coastguard Agency (MCA) examined the issue of fire protection in ro-ro spaces, including the high fire load and the effectiveness of existing sprinkler systems [20]. The report draws two interesting conclusions: 1) the international shipping industry should coordinate their efforts and their knowledge in this area and 2) a program with large-scale fire tests should be carried out to increase the understanding regarding fires and fire scenarios in ro-ro spaces. In such a program, factors such as the type of combustible materials, ignition sources, vehicle size, vehicle breakdown on the deck, the position of sprinklers, water discharge densities ventilation flow rates, fire detection, additives to the water, drainage, etc., should be studied. Additionally, it was proposed that the ability to use "water mist" systems or other types of fire-fighting systems should be studied. The report and its conclusion were presented in a submission to IMO FP51 in February 2007 [21].

In addition to the research described above, the EU project New European Ferry (NEF), whose outcome was presented in 2005, conducted an analysis of existing fire detection and water spray systems in ro-ro spaces. Within the NEF project, improved solutions were investigated with the help of Computational Fluid Dynamics (CFD) simulations [22]. The analysis shows that a spill fire consisting of diesel combined with fire in a freight truck reaches around 200 MW when the water spray system is not activated. A sprinkler designed under current requirements would only reduce the fire to between 40 to 60 MW, mainly because the vehicles prevent the water from reaching the seat of the fire. Higher water discharge densities do not seem to be more effective because of the shielding

effect. An alternative system with low-mounted foam Aqueous Film Forming Foam (AFFF) nozzles and water mist nozzles at the ceiling limited the spill fire such that the fire was reduced to around 20 MW.

### 6.5 The development of new fire test procedures

During 2005 and 2006, RISE (then SP) worked together with Marioff Corporation Oy, Det Norske Veritas and VTT Technical Research Centre of Finland to develop an alternative fire test procedure to that in MSC/Circ.914, see references [23] and [24]. A draft [25] was presented at IMO FP51 in February 2007. It is important to point out that the test method was adapted to the effectiveness of a system designed and installed in accordance with Resolution A.123 (V), with a certain safety factor. In other words, an alternative system meeting the requirements of the fire test method would not be expected to exhibit any significantly improved performance than a system per Resolution A.123 (V). The installation guidelines and fire test procedures were adopted by the Maritime Safety Committee (MSC) in 2008 and published as MSC.1/Circ.1272 [26] which superseded MSC/Circ.914.

It was clearly stated in the working group at IMO acting with these issues that the long-term goal should be to replace the requirements of Resolution A.123 (V).

### 6.6 The development of MSC.1/Circ.1430

With the introduction of MSC.1/Circ.1272 in 2008, alternative systems were allowed to be automatically activated. The guidelines provided a performance-based fire test method for the approval of “fixed water-based fire-fighting systems for ro-ro spaces and special category spaces equivalent to that referred to in Resolution A.123(V)”. As discussed above, the benchmark fire suppression tests were conducted with a water spray system designed in accordance with Resolution A.123(V). The acceptance criteria were chosen such that they were somewhat higher than reflected by the performance of a relevant water spray system.

The installation guidelines and fire test procedures were intended for the design and approval of fixed water-based fire-fighting systems for open and closed ro-ro spaces and special category spaces. Deluge systems could be applied in open ro-ro spaces when the actual wind condition is taken into consideration, for example through the use of high velocity nozzles. Systems using automatic sprinklers or nozzles [i.e., wet, dry- or pre-action systems] were only permitted for closed ro-ro and special category spaces or other spaces where wind conditions are not likely to affect system performance.

Research conducted by RISE in the IMPRO-project [27, 28, 29, 30], along with several serious ro-ro fires in the early 2000’s, showed that a water spray system design based on Resolution A.123(V) needed improvement. Proposed design and installation guidelines for automatic sprinkler and deluge water spray systems were submitted to the relevant IMO Correspondence Group by Sweden.

The relevant working group at FP55, meeting in July 2011, concluded that the suggested guidelines should be combined with the performance-based guidelines in MSC.1/Circ.1272 for alternative systems, to provide for a prescriptive-based as well as a performance-based option. The working group considered that existing fixed fire-fighting systems for special category spaces, approved and installed based on Resolution A.123(V), should be permitted to remain in service if they are serviceable. In May 2012, MSC 90 adopted the revised guidelines as MSC.1/Circ.1430 [31].

MSC.1/Circ.1430 replaced both the prescriptive requirements of Resolution A.123(V) for conventional water spray systems and the performance-based requirements in MSC.1/Circ.1272 for alternative systems. All systems should comply with sections 1, 2 and 3 of MSC.1/Circ.1430. Prescriptive-based systems should additionally comply with section 4, and performance-based,

alternative systems should additionally comply with section 5. This section gives some basic requirements, where the most important ones probably are that the system should be capable of fire suppression and control and be tested to the satisfaction of the Administration in accordance with the appended fire test procedures.

However, concerns related to the performance-based option have been raised [32] as the fire test procedures in MSC.1/Circ.1430 set a performance level of alternative systems that is only similar or slightly better than the performance of systems that used to be installed in accordance with Resolution A.123(V).



## 7 Electric vehicle (EV) fire characteristics

Main author of the chapter: Magnus Arvidson and Roeland Bisschop, RISE.

### 7.1 Fires in electric vehicles

#### 7.1.1 Battery cell failure

When a battery cell is abused, it may follow two stages until its final failure point is reached. The term “abuse” includes (but is not limited to) overcharge, short circuit, external heating, and mechanical impact [33]. First, temperature increase result in internal decomposition processes which lead to the build-up of pressure in the cell. Critical temperature varies with the type of lithium-ion battery but is primarily related to its internal chemistry and material composition, i.e., the anodes, cathodes, the separator material, and the electrolyte [34]. To make a general assumption is very difficult, but it may occur when the battery itself has temperatures above 80 °C, typically this results in venting of gas and temperature increase [34]. Note that it may not be a fire at this point, if there is no external ignition source, the cell may stabilise but may not be functional.

To initiate thermal runaway, higher temperatures are normally needed, in the range of 150 °C to 250 °C. When this happens, pressure and temperature inside the battery build up much more rapidly. The battery can then eject a lot of gas, which may be ignited either due to high temperature surfaces, autoignition or sparks originating from the failing battery. Ignition of the pressurized gasses can result in a powerful jet flame.

#### 7.1.2 Jet flames

Jet flames from battery modules originate from individual cells releasing flammable gas that burns. The more cells that release gas and the greater their capacity, the more powerful the jet flame as the pressure increases within the battery module/pack. For electric vehicles, dedicated gas release openings such as safety valves or weak spots may be aimed towards the sides, front or rear of the vehicle but there may be no ventilation openings at all. Most battery packs will have cable feedthroughs and once those are open, jet flames may also originate from there. Figure 21 shows an example.



Figure 21. The jet flame from a cable feedthrough in a battery back [35]. Photo: RISE.

Tesla Motors has, from the beginning, chosen to use 18650 (18 mm in diameter and 65 mm in length) cylindrical cells, whilst other manufacturers often is using the prismatic or pouch type. Some battery cells (common for cylindrical and prismatic cells) have protection embedded in the cell casing for overpressure and high currents that breaks or limits the electronic circuit and protects the cell from overcharge, heat, over current and short circuit. This makes the cell less likely to overheat and start a fire compared to unprotected cells. Tesla Model 3 has larger 21700 (21 mm in diameter and 70 mm in length) cylindrical cells. The release openings from the battery pack are aimed towards the side of the vehicle, which may increase the risk for fire spread to adjacent (parked) vehicles. When small cylindrical cells go into thermal runaway, they do not normally result in very long jet flames, several cells will need to be involved simultaneously.

Figure 22 shows 21700 cylindrical cells in a module failing due to external heat. The jet flames can be quite long even, especially with multiple cells failing. Other vehicle manufacturers are using larger cells of the prismatic or pouch type. The pressure build-up in pouch cells is less, that may result in smaller jet flames. However, the magnitude of the jet flames is also dependent on the pressure build-up inside the enclosure, for example the battery pack.



Figure 22. Jet flames from 21700 cylindrical cells. Photo: RISE. Note that the image is distorted as it is proprietary. The flame length is approximately 1.5 m. The system shown had several hundreds of 21700 cells.

## 7.2 Fire test review

### 7.2.1 Small- and intermediate-scale fire tests

Larsson, et al. [36] have exposed commercial lithium-ion battery cells to a controlled propane fire in order to evaluate the heat release rate (HRR), the total heat release (THR), emission of toxic gases as well as cell temperature and voltage under this type of abuse. Six tests on cells having lithium-iron phosphate (LFP) cathodes and one test on a conventional laptop battery pack with cobalt based cathode were conducted. The influence of different state of charge (SOC) was investigated. It was found that cells having a higher SOC resulted in a higher HRR. The THR had a lower correlation with SOC. The THR was determined to be 28-75 kJ per Wh battery energy capacity and the maximum HRR values were 110-490 W per Wh battery energy capacity. This work focused mainly on carbon-LFP cells, which according to the article currently is seen as state of the art on the market for Li-ion batteries when it comes to safety from a fire and heat release perspective. Although many battery systems for automotive applications use less stable chemistries in order to achieve, for example, higher energy density.

Baird [37] investigated the fire hazard and fuel loads of Lithium cobalt oxide (LCO) pouch cells in small-scale tests (ISO 5560 Cone calorimeter). As these types of cells produce oxygen during thermal runaway, fire testing was conducted using dried (from the electrolyte) cells and cells at 0 % state of charge. They concluded that the total heat released by the dried cell is about 30 % to 40 % less than the non-dried cells, but the heat of combustion per mass is larger as the electrolyte had a lower heat of combustion than the plastics constructing the cell. Taking the data from the lithium-ion cells, it was determined that placing them between a Class III and a mixed group A exposed commodity per NFPA 13 definitions can be used for sprinkler designs.

### 7.2.2 Large-scale fire tests of battery packs

In a project for the National Fire Protection Research Foundation, Long Jr et al. [38] conducted a large-scale fire test with a stand-alone battery pack used for an EV. The battery pack (denoted Battery B) was a 16 kWh battery (used in the Chevrolet Volt) that is installed under the vehicle floor pan and spans nearly the length of the vehicle from the rear axle to the front axle. It contained lithium-ion pouch cells and was enclosed in a T-shaped fibreglass case. The battery pack was fully charged before the test. An external heat source consisting of four propane gas burners symmetrically positioned under the battery pack was used to initiate thermal runaway and a fire. The gas burners provided a constant heat release rate of 400 kW. The maximum heat release rate measured during testing was approximately 700 kW, at a test time of 17 minutes and 30 seconds (about 3 minutes prior to the burners being turned off). Figure 23 shows the heat release rate history. The peak heat release attributed by the battery pack to the fire was therefore only approximately 300 kW. During the most intense period, visible flames were observed venting out of the top fuse of the battery, a cable connection port and the three battery vents. Once the burners were turned off at about 20 minutes, the heat release rate slowly decayed from time 20 minutes to 36 minutes, when it essentially had burnt out. The total heat released was 720 MJ, which included the period when the gas burners were on.

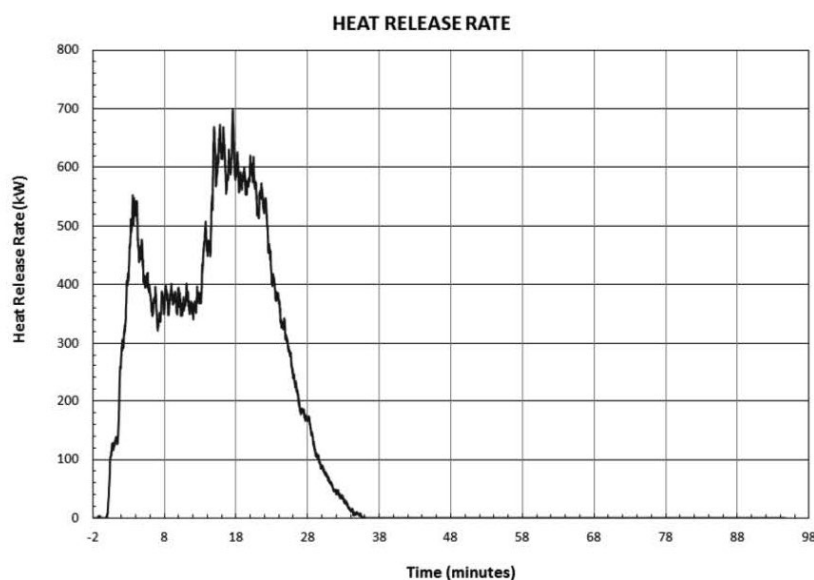


Figure 23. The measured heat release rate from a stand-alone battery pack used for an electric vehicle. The gas burners used to initiate the fire provided a constant heat release rate of 400 kW (turned off at about 20 minutes) that is included in the graph [38].

## 7.3 Large-scale fire tests of EVs

### 7.3.1 Fire tests at INERIS

Lecocq et al. [39] at the French National Institute for Industrial Environment and Risks (INERIS) have conducted free-burn comparison fire tests using internal combustion engine vehicles (ICEVs) and EVs from two French car manufacturers, in total four tests. The fuel tanks of the ICE vehicles were fully filled with diesel. All fires were started inside the passenger compartment of the vehicles, with the windows fully open. Fire development was similar for all vehicles; the fire spread inside the passenger compartment before propagating to the rear and then to the front of the vehicle. No explosion or projectiles related to the battery was observed during the EV fire tests. The peak heat release rate was close for both analogous vehicles; 4,2 MW (EV) and 4,8 MW (ICEV) as well as 4,7 MW (EV) and 6,1 MW (ICEV). Figure 24 and 25, respectively, show the heat release rate histories from the tests. The battery pack of the EV from manufacturer 1 had an energy capacity of 16,5 kWh and that from manufacturer 2 had an energy capacity of 23,5 kWh. Peaks attributed to the burning of the battery pack appeared at approximately 35 minutes after ignition. Based on the data, it is not possible to determine the specific contribution of the battery fire to the overall heat release rate. There is no information in the paper whether the diesel fuel tanks of the ICEVs were involved in the fire or not.

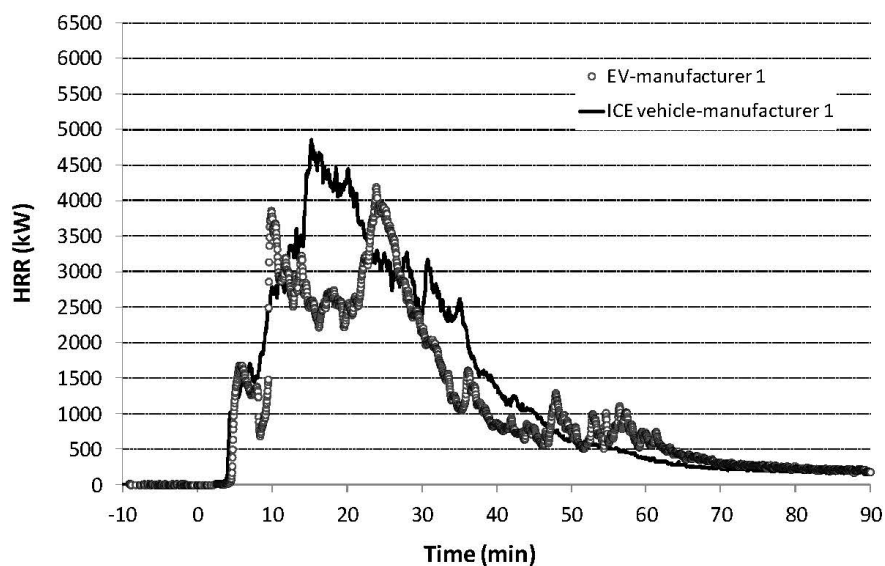


Figure 24. The heat release rate histories for an EV and an analogous ICE vehicle from car manufacturer 1 in the tests at INERIS reported by Lecocq et al. [39].

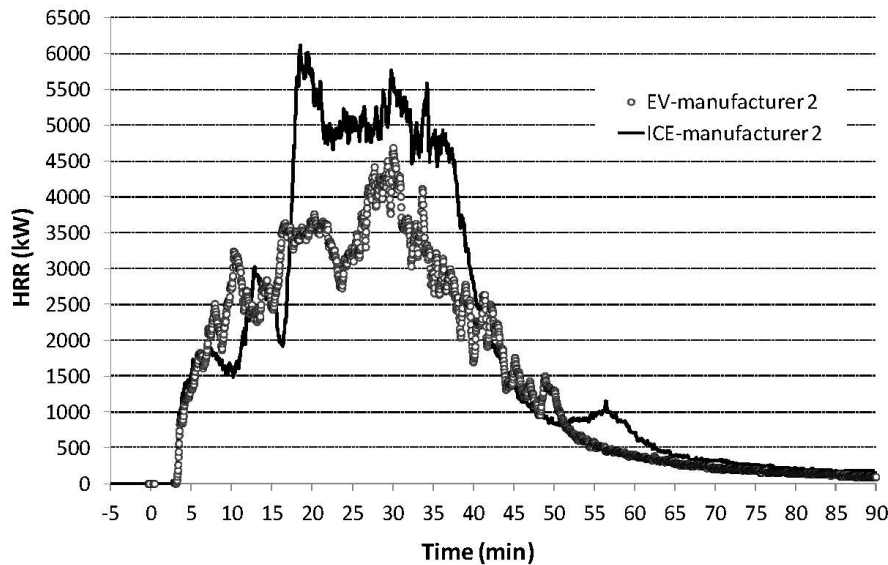


Figure 25. The heat release rate histories for an EV and an analogous ICE vehicle from car manufacturer 2 in the tests at INERIS reported by Lecocq et al. [39].

### 7.3.2 Fire tests by Watanabe et al.

Watanabe et al. [40], have conducted large-scale tests comparing the severity of a fire in an EV (Nissan Leaf) with a gasoline powered vehicle (Honda Fit). It should be noted that the ICEV is significantly smaller than the EV. When tested, the actual vehicle was placed on a weighing platform to determine the rate of mass loss (10 g accuracy). The heat release rate and total heat release were estimated by multiplying the combustion heat of a burning vehicle per unit weight by the mass loss rate and total mass loss. Fire ignition was achieved with a small fuel pan filled with 80 g of alcohol gel fuel positioned at the left-hand side rear end of the vehicle.

The heat flux from the fire was measured at different positions. The vehicles were allowed to burn until they are self-extinguished and both types of vehicles self-extinguished after around 120 minutes.

The lithium-ion battery pack of the EV released gas 40 minutes after the test started, which coincides with the peak heat release and with the peak heat fluxes towards the side of 61 kW/m<sup>2</sup>. Fire in and near the right rear tire at about 22 minutes generated a peak heat flux of 51 kW/m<sup>2</sup>. The upper and lower parts of the battery pack are made of steel. No explosions occurred during the test nor did the pack burst. A comment is made in the reference that the EV contained less combustible material than the ICEV. For the ICEV test, the gasoline tank did not burst or leak fuel during the tests, likely it evaporated through the fuel filling pipe. A maximum heat flux of the ICEV was measured at its side, 40 kW/m<sup>2</sup>. A correction is used for soot production meaning that the total heat release is in the higher range compared to that from other tests.

The reference does also include information from testing of the following ICEV's, Toyota luxury sedan, Toyota minivan, Nissan minivan, Subaru station and Toyota sedan. Table 3 summarizes all test results.

### 7.3.3 Fire tests at National Research Council of Canada (NRC)

Lam et al. [41] have conducted large-scale fire tests on three EVs, two plug-in hybrid electric vehicles (PHEV) and two ICEVs in a fire test facility at the National Research Council of Canada (NRC). The tests were conducted under a 6 m by 6 m oxygen consumption calorimeter. The actual vehicle was positioned on a propane sand burner sized 2,4 m by 1,2 m that generated 2 MW and a flame temperature of about 800 °C. The intent of using the burner was to simulate a fuel spill fire under the

vehicle. The clearance between the burner and undercarriage of the vehicle was 203 mm. All windows and doors of the vehicle under test were kept fully closed and all parts were original. The engine was not running during the test. The weight of the vehicle was measured before and after the test.

For Vehicle A, the ICEV was not identical to the EV, but was of similar size (slightly smaller) and from the same manufacturer. For Vehicle B, the ICEV and EV were of the same model, but with different propulsion systems. The EV models of Vehicles A and B contained similar battery energy storage capacities, but Vehicle B contained two separate battery packs in different locations instead of a single pack, as in Vehicle A. Vehicles C and D were PHEVs from different manufacturers, with Vehicle C having a smaller battery than Vehicle D. The fuel tanks (where applicable) were completely filled.

Heat fluxes were measured at either sides and in the front of the vehicle. Additionally, gas temperatures were measured underneath the vehicle, inside the passenger compartment, inside the engine compartment and inside the battery pack (where applicable). Surface temperatures were measured on the chassis, the metal flooring and on the outside of the battery pack (where applicable). Concentrations of species as CO, CO<sub>2</sub>, HF and HCl were measured inside the passenger compartment at the drivers' head height.

It was observed that the peak heat release rate and heat flux values were higher for the ICEVs for the cases when the fuel tank burst compared to when the battery pack of an EV became involved. Burning of the battery pack did not seem to result in any significant spike in heat release rate or heat flux.

Vehicle type D was the only vehicle that had a metal fuel tank. The flames from the fire damaged the heat flux gauge facing the rear of the vehicle, just after 7 minutes. This event was most likely caused by the release of the fuel. After the gasoline burned off, the heat release rate and heat flux remained relatively constant until shortly after 10 minutes, when they started to decrease gradually until the end of the test.

Higher SOC resulted in faster involvement of the battery. For Vehicle type A, the maximum heat flux at the rear was 40 kW/m<sup>2</sup> (EV) and 35 kW/m<sup>2</sup> (ICEV). The maximum heat flux at the passenger side was 25 kW/m<sup>2</sup> (EV) and 35 kW/m<sup>2</sup> (ICEV).

For Vehicle type B the maximum radiation at the rear was 40 kW/m<sup>2</sup> for the EV and 20 kW/m<sup>2</sup> for the ICEV. The maximum radiation levels at the sides were 20 kW/m<sup>2</sup> (EV) and 25 kW/m<sup>2</sup> (ICEV).

The heat flux rear of Vehicle D caused instrument failure, but the maximum recorded value was 55 kW/m<sup>2</sup>. The heat flux rear of Vehicle C was 30 kW/m<sup>2</sup>. The measured heat flux at the sides of both vehicles was 30-35 kW/m<sup>2</sup>.

The peak heat release rates for the ICEV models were higher than those for their EV counterparts and the times of the peak heat release rates were similar to or earlier than those for the EVs. Given that the peak HRR for the ICEVs corresponded to the burning of gasoline, it seems that a vehicle with a full fuel tank produces a greater hazard in terms of HRR than one with a battery pack.

Correspondence with the authors of the paper have revealed that the 'small' lithium-ion battery pack relates to an energy capacity of < 10 kWh, the 'medium' battery pack to an energy capacity of < 20 kWh and the 'large' battery pack to an energy capacity in excess of 20 kWh.

#### 7.3.4 Fire tests by NHTSA (without measuring the HRR)

The National Highway Traffic Safety Administration (NHTSA) have conducted large-scale vehicle tests where they initiated thermal runaway in a single cell within an EV battery pack [42]. The battery pack was installed in the vehicle and initial thermal propagation within the battery pack was measured



and observed. Three different commercial vehicles having three types of lithium-ion form factors were tested:

- Manufacturer A (seems from the photos to be a Tesla Model S): Battery pack was built with small cylindrical cells and mounted to the floor of the vehicle. The cells were arranged into 14 modules. A small film heater single cell initiation method was used to initiate the event.
- Manufacturer B (not identified): Battery pack built with eight large, hard case prismatic cells connected in series and mounted to the floor. A large film heater single cell initiation method was used.
- Manufacturer C (seems from the photos to be a Nissan Leaf 2013-2017): Battery pack built with large pouch cells that was mounted to the floor of the vehicle. Within the battery pack, pouch cells were arranged in groups of four within modules. A large film heater single cell initiation method was used, and the heater was positioned between two cells.

Prior to all tests, the battery packs were fully charged following the manufacturer's specifications. The initiation location was selected to be the most likely to result in thermal runaway propagation within the battery pack. The tests were conducted outdoors, and no heat release rate measurements were made.

For the manufacturer A tests, a single cell runaway was initiated after approximately 26 minutes of heating. A clear pop noise was heard, and some grey smoke was observed exiting the battery pack. However, the smoke faded after a few seconds and no additional thermal runaway events were noticed. The battery pack was allowed to sit for approximately one month without any additional thermal runaway reaction.

For the manufacturer B tests, a single cell runaway was initiated after approximately 11 minutes of heating. There was an audible popping followed by emission of a large amount of smoke from underneath the vehicle. Approximately 10 minutes later the next cell underwent thermal runaway and subsequent cells underwent thermal runaway in 4 to 5 minute intervals. The total of eight cells underwent thermal runaway during the test, the final cell after approximately 53 minutes. There was no ignition of flammable gases.

For the manufacturer C tests, a single cell runaway was initiated after approximately 7 minutes of heating. There was an audible noise followed by emission of a large amount of smoke from the underside of the vehicle. Three additional thermal runaway events occurred within the next 90 seconds. About 7 minutes later, a similar event involving four thermal runaway events occurred in rapid sequence followed by more events at increments between 2 minutes and 5 seconds. This resulted in a steady smoke stream exiting the rear of the vehicle and at 23 minutes fire ignition of the ventilated gases occurred. These burning gases ignited the rear bumper of the vehicle. The cell runaways and vehicle fire continued, and flames were observed inside the cabin at approximately 28 minutes. The fire continued until approximately 50 to 55 minutes after the heat was initiated.

### 7.3.5 Fire tests in the ETOX project

In the ETOX project [43], three large-scale free-burn fire tests were conducted, involving one conventional internal combustion engine vehicle (ICEV) and two battery electric vehicles (BEVs). The ICEV and one of the BEVs were of the same vehicle model from the same manufacturer which allows a good comparison of the influence on the fire by the powertrains.

The ICEV A was a full-size van (model year 2011), and the fire was initiated by a diesel spill fire in a 500 mm by 500 mm fire tray fire located directly underneath the fuel tank. The total amount of

diesel (44 l) used in the test, which corresponded to 80 % of full tank, was split between the fuel tank and the fire tray.

The BEVs were charged to approximately 80 % SOC and a propane gas burner with a defined output of 30 kW was used to ignite the vehicles. The gas burner was positioned underneath the battery pack and was operating for the entire test duration. The vehicle BEV A was a full-size van (model year 2019) and had battery capacity of 40 kWh, the vehicle BEV B was a small family car (model year 2016) with a battery capacity of 24 kWh.

The heat release rate from the fire was measured by oxygen consumption calorimetry. Figure 26 shows the heat release rate histories. As the fuel tank ruptured for the ICEV used in Test 1 there was a much more rapid fire development compared to the BEVs. The subsequent diesel pool fire burned out before the fire that involved the engine bay and passenger compartment and reached its maximum. Therefore, a higher peak heat release rate was achieved for BEV A (BEV similar to the ICE) where the battery ventilation and the fire involvement of the rest of the vehicle occurred at approximately the same time. In addition, the heat release rate from the diesel pool fire might as well have been higher in case no barriers had limited the outflow on the ground potentially resulting in a larger pool area.

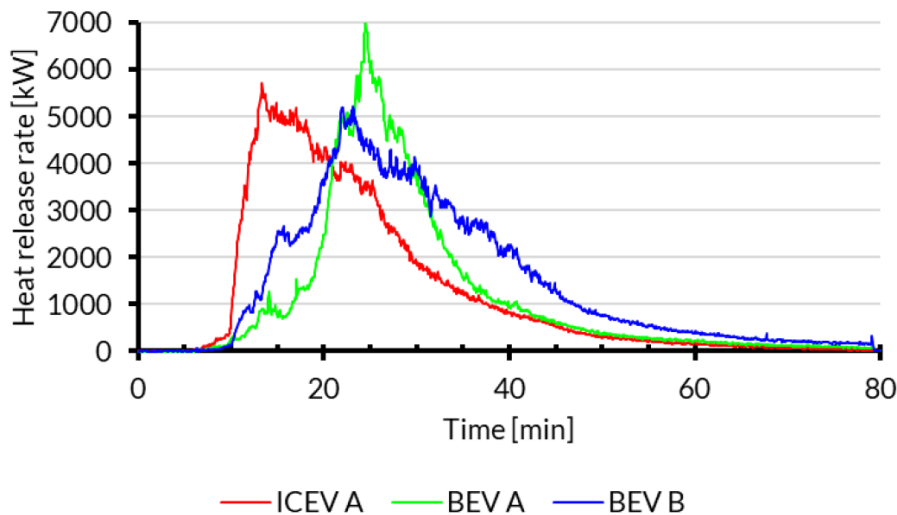


Figure 26. The heat release rate histories in the ETOX-project that involved an ICE and two BEVs. The ICEV A and BEV A vehicles were similar except for the powertrain [34].

### 7.3.6 Summary of large-scale fire test results

Main author: Roeland Bisschop.

Table 3 provides a summary of the test conditions and results associated with the heat release rate and total heat release for the three references discussed above. The HRR data from Lam et al. [41] is shown without the contribution of the propane gas burner.

Table 3 Summary of the test conditions and results associated with the heat release results from the references discussed above.

Type	Vehicle [Reference]	Mass [kg]	Energy stored	Peak HRR [MW]	Time to peak HRR [min]	Total heat release [GJ]
BEV	2011 Nissan Leaf [Watanabe]	1520	24 kWh	6,3	40	6,4
	Unknown [Lecocg]	1122	16,5 kWh	4,2	~25	6,3
	Unknown [Lecocg]	1501	23,5 kWh	4,7	~20	8,5
	2014 Vehicle A [Lam]	1448	'Large' LIB 100 % SOC	6,0	7	-
	2013 Vehicle A [Lam]	1475	'Large' LIB 85 % SOC	5,9	5,8	4,9
	2013 Vehicle B [Lam]	1659	'Large' LIB 100 % SOC	6,9	10,2	4,7
	2019 BEV A [Willstrand]	-	40 kWh	~7	~27	5,2
	2016 BEV A [Willstrand]	-	24 kWh	~5,2	~21	6,7
PHEV	2013 Vehicle C [Lam]	1466	'Small' LIB 85 % SOC and full tank of gasoline	6,0	7,5	4,6
	2014 Vehicle D [Lam]	1711	'Medium' LIB. 100 % SOC and full tank of gasoline	7,9	8,3	5,9
ICEV	Unknown [Lecocg]	1128	Full tank of diesel	4,8	~20	6,9
	2003 Honda Fit [Watanabe]	1275	10 l of gasoline	2,1	35	4,3
	Unknown [Lecocg]	1404	Full tank of diesel	6,1	~30	10,0
	2015 Vehicle A [Lam]	1096	Full tank of gasoline	7,1	6	3,3
	2013 Vehicle B [Lam]	1344	Full tank of gasoline	10,8	8	5,0
	Toyota luxury sedan [Watanabe]	-	10 l of gasoline	-	-	7,4
	Toyota minivan [Watanabe]	-	10 l of gasoline	-	-	5,9
	Toyota minivan [Watanabe]	-	10 l of gasoline	-	-	5,3
	Subaru stationwagon [Watanabe]	-	10 l of gasoline	-	-	5,6
	Toyota sedan [Watanabe]	-	10 l of gasoline	-	-	5,1
	2011 ICEV A [Willstrand]	-	44 l of diesel	~5,6	~14	5,9

The peak heat release rates for the BEVs range from 4,2 MW to 7,0 MW, between 6,0 MW and 7,9 MW for the PHEV and between 2,1 MW and 10,8 MW for the ICEV. The total heat released by the BEVs ranges from 4,7 GJ to 8,5 GJ, between 4,6 GJ and 5,9 GJ for the PHEV and between 4,3 GJ and 10,0 GJ for the ICEV.

Based on the data, it seems that the severity of a fire in a BEV is comparable to that of a PHEV or ICEV. Some data indicate that the maximum heat flux from a BEV may be slightly higher compared to ICEV, which could be due to the jet flames generated from the battery pack. However, other data indicate the opposite as a result of a fuel spill fire.

#### 7.4 Fire suppression of ICEV's vs BEV's

The literature review did not identify any fire tests comparing the fire suppression performance of sprinkler or water spray systems using ICEV's as compared to BEV's. Therefore, such tests were conducted, refer to Annex B. A test series involving testing of two pairs of geometrically similar

internal combustion engine and battery electric vehicles under as equivalent test conditions as possible was conducted. During testing, key parameters as the heat release rate, the gas temperature above the vehicle and the surface temperature of target steel sheet screens at the sides of the vehicle were measured. Fire ignition was arranged to initiate fire in such a way that the liquid fuel (gasoline) or the battery pack was involved at the initial stage of the fire. It is concluded that a fire in the two types of vehicles is different but share similarities. However, a fire in a BEV does not seem to be more challenging than a fire in an ICEV for a drencher system designed in accordance with current recommendations in MSC.1/Circ.1430/Rev.2.

## 7.5 Conclusion

Electric car deployment has been growing rapidly over the past ten years and will likely continue to grow. Basically, all car manufacturers in the world are introducing new fully electric or hybrid vehicles over the next few years, partially in response to increasing efficiency and emissions standards. Fires in electric vehicles have gained a lot of space in the media and an indication of the severity of such fires on ro-ro spaces on board ships are desired.

This report summarizes small-, intermediate- and large-scale fire tests with lithium-ion batteries and/or electric vehicles and discuss the associated fire characteristics and severity. The literature study of this report indicates that the peak heat release of an electric vehicle fire is comparable to that of a vehicle with an internal combustion engine, given similar sized vehicles. However, the number of large-scale fire tests involving electric vehicles are relatively limited and no fire test data for vehicles having a large energy capacity (in the order of 100 kWh or larger) battery pack is available.

A key question is the contribution of energy from the fire in a battery pack. This question cannot be answered with certainty, due to limited amount of test data. An estimation of the total heat release of a large energy capacity battery pack indicate that it is similar with that of the liquid fuel of a fuel tank. But a modern passenger contains a lot of combustible material. The calculated fire load of ordinary combustibles as plastics, rubber, and textiles of large sized (SUV or similar) modern car is in the order of 10 GJ. Fluids and lubricants add an estimated additional fire load of 3 GJ and the liquid fuel about 2 GJ. These rough estimations reveal that; 1) the calculated, theoretical total energy of the combustibles of a vehicle is in the order of 15 GJ and 2) that the fire load of the liquid fuel of the fuel tank represents about 15 % of the overall energy content. These theoretical values correlates well with measured values obtained during fire tests, justified by the fact that all material may not be consumed in an actual fire, that the combustion efficiency probably is in the order of 0,8 and a certain calorimeter measurement underestimation for some of the tests.

## 8 The design and installation guidelines in MSC.1/Circ.1430/Rev.2

Main author of the chapter: Magnus Arvidson, RISE.

### 8.1 Introduction

The guidelines in MSC.1/Circ.1430 was published on 31 May 2012 and has undergone two revisions, MSC.1/Circ.1430/Rev.1 on 7 December 2018 and MSC.1/Circ.1430/Rev.2 on 8 December 2020.

Member Governments are invited to apply these revised guidelines when approving fixed water-based fire-fighting systems for ro-ro spaces and special category spaces installed on or after 1 January 2021 and bring them to the attention of ship designers, shipowners, equipment manufacturers, test laboratories and other parties concerned. Existing systems for special category spaces approved and installed based on Resolution A.123(V), MSC.1/Circ.1272, MSC.1/Circ.1430 and MSC.1/Circ.1430/Rev.1 installed before 1 January 2021 should be permitted to remain in service as long as they are serviceable.

The content is summarised below, followed by a discussion about the differences between prescriptive-based and performance-based systems.

### 8.2 General requirements

The guidelines in MSC.1/Circ.1430 were intended to replace both the prescriptive requirements of Resolution A.123(V) for conventional water spray systems and the performance-based requirements of Circular MSC.1/Circ.1272 for automatic sprinkler and deluge systems. All systems should comply with sections 1, 2 and 3. In addition, prescriptive-based systems should comply with section 4, and performance-based systems should comply with section 5.

Section 1 contains the basics described above, section 2 contains definitions and section 3 principal requirements for all systems. The requirements in section 3, "Principal requirements for all systems" of MSC.1/Circ.1430/Rev.2 are cited below. The requirements that influence the design and procedures of fire test procedures are commented.

**3.1** *The system may be automatically activated, automatically activated with provisions for manual activation or manually activated. Comment: Wet-pipe and dry-pipe have automatic sprinklers or nozzles (i.e., nozzles featuring a thermal element like a glass bulb or thermal link) that are individually activated by the heat from a fire. These systems could hypothetically have provisions for manual operation, by using electronically activated sprinklers, although this is relatively uncommon. Those sprinklers incorporate an electrically activated actuator. An electrical signal from a fire detection device ignites a small quantity of explosive that forces a piston to extend into and break the glass bulb. Thereby, a single, or a number of sprinklers in the area of detection can be activated, either automatically (by fire detection or by the heat from the fire) but also manually if desired. Deluge systems can be automatically activated by a fire detection system in protected area or by manual means, by remote or physical operation of a deluge section valve. Pre-action systems use automatic sprinklers or nozzles with a supplemental fire detection system installed in the same area as the sprinklers or nozzles.*

**3.2** *All systems should be divided into sections. Each section should be capable of being isolated by one section control valve. The section control valves should be located outside the protected space, be readily accessible without entering the protected spaces and their locations should be clearly and*



*permanently indicated. It should be possible to manually open and close the section control valves either directly on the valve or via a control system routed outside of the protected spaces.*

**3.2.1** *It should be possible to manually open and close the section control valves either directly on the valve or via a control system routed outside of the protected spaces. Means should be provided to prevent the operation of the section control valves by an unauthorized person. Control valve locations should be adequately ventilated to minimize the build-up of smoke.*

**3.2.2** *A continuously manned control station and release station(s) for deluge systems should have remote indication of pump running and pressure in valve manifold. For deluge systems, release stations with controls for start and stop of pump(s) and operation (opening and closing) of section control valves should be provided in the valve room and in a continuously manned control station or the safety centre, if fitted. Remote indication of position of valves (open/closed) should be provided in the continuously manned control station or the safety centre, if fitted.*

**3.3** *The piping system should be sized in accordance with a hydraulic calculation technique<sup>1</sup> such as the Hazen-Williams hydraulic calculation technique or the Darcy-Weisbach hydraulic calculation technique, to ensure the availability of the flows and pressures required for correct performance of the system. The design of the system should ensure that full system pressure is available at the most remote sprinkler or nozzle in each section within 60 s of activation. **Comment: The delay time (due to water filling of the pipe-work) need to be reflected in the fire test procedures.***

**3.4** *The system supply equipment should be located outside the protected spaces and all power supply components (including cables) should be installed outside of the protected space. The electrical components of the pressure source for the system should have a minimum rating of IP 54.*

**3.5** *Activation of an automatic system should give a visual and audible alarm at a continuously manned station. The alarm in the continuously manned station should indicate the specific section of the system that is activated. The system alarm requirements described within this paragraph are in addition to, and not a substitute for, the detection and fire alarm system required by SOLAS regulation II-2/20.4.*

**3.6** *Wet pipe systems on board vessels that can operate in areas where temperatures below 0°C can be expected, should be protected from freezing either by having temperature control of the space, heating coils on pipes, antifreeze agents or other equivalent measures.*

**3.7** *The capacity of the system water supply should be sufficient for the total simultaneous coverage of the minimum coverage area of tables 4-1 to 4-3 and 5-1 and the vertically applicable area as defined in paragraph 3.22.*

**3.8** *The system should be provided with a redundant means of pumping or otherwise supplying a water-based extinguishing medium to the system. The capacity of the redundant means should be sufficient to compensate for the loss of any single supply pump or alternative source. Failure of any one component in the power and control system should not result in a reduction of required pump capacity of deluge systems. In the case of wet pipe, dry pipe and pre-action systems, failure of any one component in the power and control system should not result in a reduction of the automatic release capability or reduction of required pump capacity by more than 50%. However, systems*

*requiring an external power source need only be supplied by the main power source. Hydraulic calculations should be conducted to assure that sufficient flow and pressure are delivered to the hydraulically most demanding section both in normal operation and in the event of the failure of any one component.*

**3.9** *The system should be fitted with a permanent sea inlet and be capable of continuous operation during a fire using sea water.*

**3.10** *The system and its components should be designed to withstand ambient temperatures, vibration, humidity, shock, impact, clogging and corrosion normally encountered. Piping, pipe fittings and related components except gaskets inside the protected spaces should be designed to withstand 925°C. Distribution piping should be constructed of galvanized steel, stainless steel, or equivalent. Sprinklers and nozzles should comply with paragraph 3.11.*

**3.11** *The system and its components should be designed and installed based on international standards acceptable to the Organization<sup>2</sup>. The nozzles should be manufactured and tested based on the relevant sections of appendix A to circular MSC/Circ.1165 (Revised Guidelines for the approval of equivalent water-based fire-extinguishing systems for machinery spaces and cargo pump-rooms).*

**3.12** *A means for testing the automatic operation of the system and, in addition, assuring the required pressure and flow should be provided.*

**3.13** *If the system is pre-primed with water containing a fire suppression enhancing additive and/or an antifreeze agent, periodic inspection and testing, as specified by the manufacturer, should be undertaken to assure that their effectiveness is being maintained. Fire suppression enhancing additives should be approved for fire protection service by an independent authority. The approval should consider possible adverse health effects to exposed personnel, including inhalation toxicity.*

**Comment:** This section mentions the use of fire suppression enhancing additives, which calls for inclusion of such tests in the fire test procedures, reference to any other relevant standards or that such tests are specifically excluded from the scope of the revised fire test procedures (which would indirectly mean that the performance is only tested with water and that any improved performance due to an additive is an additional advantage).

**3.14** *Operating instructions for the system should be displayed at each operating position.*

**3.15** *Installation plans and operating manuals should be supplied to the ship and be readily available on board. A list or plan should be displayed showing spaces covered and the location of the zone in respect of each section. Instructions for testing and maintenance should be available on board.*

**3.16** *Spare parts should be provided as recommended by the manufacturer. In the case of automatic sprinkler systems, the total number of spare sprinkler heads for each type of sprinklers shall be six for the first 300, 12 for the first 1,000.*

**3.17** *Where automatic systems are installed, a warning notice should be displayed outside each entry point stating the type of medium used (i.e. water) and the possibility of automatic release.*

**3.18** All installation, operation and maintenance instruction/plans for the system should be in the working language of the ship. If the working language of the ship is not English, French or Spanish, a translation into one of these languages should be included.

**3.19** Any foam concentrates used as system additives should comply with the Revised Guidelines for the performance and testing criteria and surveys of foam concentrates for fixed fire-extinguishing systems (MSC.1/Circ.1312). **Comment: Refer to the comment for section 3.13. If the fire suppression additive is a foam concentrate, it should as a minimum fulfill the requirements of section 3.19. Whether it should also be included or excluded in the scope of the revised fire test procedures need to be determined.**

**3.20** Means for flushing of systems with fresh water should be provided.

**3.21** The presence of obstructions and the potential for shielding of the water spray should be evaluated to ensure that the system performance is not affected. Supplementary sprinklers or nozzles should be installed beneath obstructions. In addition, nozzles should be located to protect spaces above and below intermediate decks, hoistable decks and ramps. Nozzles below hoistable decks should be capable of protecting all applicable heights.

**3.22** Vertically the applicable area of all decks, including hoistable decks or other intermediate decks, between reasonably gastight steel decks (or equivalent materials), should be included for simultaneous coverage (example: with one hoistable deck, both the layer above and below this deck with a dimensioning area complying with tables 4-1 to 4-3 or 5-1 should be included in the water supply calculations). Decks with ramps are accepted as reasonably gastight decks assuming that the ramps are always in their closed position at sea and the ramps and the decks which these ramps are part of are reasonably gastight.

**3.23** The length of a deluge section (along the lanes) should not be less than 20 m and the width of the section should not be less than 14 m. Further, the sections need not be longer or wider than the distance between reasonably gastight steel bulkheads (or equivalent materials). The maximum size of a section on any single deck should be 48 m multiplied by the width of cargo space (measured as distance between tight steel divisions). Vertically one section can cover up to three decks.

---

<sup>1</sup>Where the Hazen-Williams Method is used, the following values of the friction factor *C* for different pipe types which may be considered should apply:

Pipe type	<i>C</i>
Black or galvanized mild steel	100
Copper and copper alloys	150
Stainless steel	150

<sup>2</sup>Pending the development of international standards acceptable to the Organization, national standards as prescribed by the Administration should be applied.

### 8.3 Additional requirements for prescriptive-based systems

In addition to the requirements in section 3, prescriptive-based systems should comply with section 4, "Additional prescriptive-based system design requirements". This section is cited below.

The requirements that influence the design of the revised fire test procedures and the benchmark fire tests are commented.

**4.1** Wet pipe, dry pipe and pre-action systems should be designed for simultaneous coverage of the hydraulically most demanding area at the minimum water discharge density given in tables 4-1 to 4-3. The minimum operating pressure of any sprinkler should be 0.05 MPa. **Comment: 0.05 MPa equals 0.5 bar. This requirement influences the choice of K-factor of sprinklers and thereby the choice of automatic sprinkler for the benchmark performance fire testing.**

**4.2** Deluge systems should be designed for the simultaneous activation of the two adjacent deluge sections with the greatest hydraulic demand at the minimum water discharge density given in tables 4-1 to 4-3. The minimum operating pressure of any sprinkler should be 0.12 MPa. **Comment: 0.12 MPa equals 1.2 bar. This requirement influences the choice of K-factor of open nozzles and thereby the choice of nozzles for the benchmark performance fire testing.**

Table 4-1 Minimum required water discharge density and area of coverage for decks having a free height equal to or less than 2.5 m.

Type of system	Minimum water discharge density (mm/min)	Minimum coverage area
Wet pipe system	6.5	280 m <sup>2</sup>
Dry pipe or pre-action system	6.5	280 m <sup>2</sup>
Deluge system	5	2 × 20m x B <sup>1</sup>

Table 4-2 Minimum required water discharge density and area of coverage for decks having a free height in excess of 2.5 m but equal to or less than 6.5 m.

Type of system	Minimum water discharge density (mm/min)	Minimum coverage area
Wet pipe system	15	280 m <sup>2</sup>
Dry pipe or pre-action system	15	365 m <sup>2</sup>
Deluge system	10	2 × 20 m x B <sup>1</sup>

Table 4-3 Minimum required water discharge density and area of coverage for decks having a free height in excess of 6.5 m but less than 10.0 m.

Type of system	Minimum water discharge density (mm/min)	Minimum coverage area
Wet pipe system	20	280 m <sup>2</sup>
Dry pipe or pre-action system	20	365 m <sup>2</sup>
Deluge system	15	2 × 20 m x B <sup>1</sup>

<sup>1</sup> B = full breadth of the protected space.

**4.3** Automatic sprinklers or nozzles intended for decks with a free height equal to or less than 2.5 m should have a nominal operating temperature range between 57°C and 79°C and standard response characteristics. If required by ambient conditions, higher temperature ratings may be acceptable.

**Comment:** These requirements influence the choice of sprinklers for the benchmark performance fire testing.

**4.4** Automatic sprinklers or nozzles intended for decks with a free height in excess of 2.5 m and hoistable decks that can be raised above 2.5 m should have a nominal operating temperature range between 121°C and 149°C and standard response characteristics. **Comment:** These requirements influence the choice of sprinklers for the benchmark performance fire testing.

**4.5** Sprinklers or nozzles should be positioned in such a way that:

- .1 they are not exposed to damage by cargo;
- .2 undisturbed spray is ensured; and
- .3 water is distributed over and between all vehicles or cargo in the area being protected.

Automatic sprinklers or nozzles should be positioned and located so as to provide satisfactory performance with respect to both activation time and water distribution. **Comment:** The first version of MSC.1/Circ.1430 stipulated that “The maximum horizontal spacing between nozzles or sprinklers should not exceed 3.2 m”. For the benchmark performance fire tests, a nozzle and sprinkler spacing need to be chosen and this particular figure should be considered.

**4.6** Only upright sprinklers or nozzles are allowed for dry pipe or pre-action systems. **Comment:** This requirement suggests that that benchmark performance fire testing is conducted with upright sprinklers, as dry-pipe systems are likely used in ro-ro spaces and special category spacing due to the risk for freezing.

**4.7** For wet pipe and dry pipe sprinkler systems, fire detection systems should be installed in accordance with the requirements of SOLAS regulation II-2/20.4.

**4.8** For manual deluge systems, automatic deluge systems and pre-action systems, fire detection systems should be provided complying with the International Code for Fire Safety Systems (FSS Code) and the following additional requirements:

1. the detection system should consist of flame, smoke or heat detectors of approved types, arranged as described below. The flame detectors should be installed under fixed continuous decks according to the limitation and application defined by the maker and the approval certificate. The smoke and heat detector arrangement shall comply with the FSS Code. Smoke detectors with a spacing not exceeding 11 m or heat detectors with a spacing not exceeding 9 m should be installed under hoistable ramps;
2. the detection system should ensure rapid operation while consideration should also be given to preventing accidental release. The area of coverage of the detection system sections should correspond to the area of coverage of the extinguishing system sections. The following arrangements are acceptable:
  1. set-up of approved flame detectors and approved smoke detectors or heat detectors; or
  2. set-up of approved smoke detectors and approved heat detectors; other arrangements can be accepted by the Administration;



3. *for automatic deluge systems and pre-action systems, the discharge of water should be controlled by the detection system. The detection system should provide an alarm upon activation of any single detector and discharge if two or more detectors activate. The Administration may accept other arrangements; and*
4. *automatically released systems should also be capable of manual operation (both opening and closing) of the section valves. Means should be provided to prevent the simultaneous release of multiple sections that result in water-flow demand in excess of the pumping system design capacity. The automatic release may be disconnected during on- and off-loading operations, provided that this function is automatically reconnected after a pre-set time being appropriate for the operations in question.*

**Comment:** The primary observation is that the use of automatic deluge systems probably is very unlikely, despite the means (activation after signal from at least two fire detectors) to avoid unintentional discharge of water. The requirement for any type of system indicate that early fire detection and alarm is likely, suggesting that even a manually operated system may be discharged when a fire is relatively small.

**4.9** *Where beams project more than 100 mm below the deck, the spacing of spot-type heat detectors at right angles to the direction of the beam travel should not be more than two thirds of the spacing permitted under chapter 9 of the FSS Code. **Comment:** This requirement will reduce the time to fire detection for spot-type heat detectors for relatively obstructed ceiling constructions.*

**4.10** *Where beams project more than 460 mm below the deck and are more than 2.4 m on centre, detectors should be installed in each bay formed by the beams. **Comment:** This requirement will reduce the time to detection for spot-type heat detectors for very obstructed ceiling constructions.*

#### 8.4 Additional requirements for performance-based systems

In addition to the requirements in section 3, performance-based systems should comply with section 5, "Additional performance-based system design requirements". This section is cited below. The requirements that influence the design of the revised fire test procedures and the benchmark fire tests are commented.

**5.1** *The system should be capable of fire suppression and control and be tested to the satisfaction of the Administration in accordance with the appendix to these Guidelines.*

**5.2** *The nozzle location, type of nozzle and nozzle characteristics should be within the limits tested to provide fire suppression and control as referred to in paragraph 5.1.*

**5.3** *System designs should be limited to the use of the maximum and minimum temperature ratings of the thermally sensitive fire detection devices tested to provide fire suppression and control as referred to in paragraph 5.1. **Comment:** This indicates that the fire detection system should be included in the fire tests, but it may also refer to the nominal operating temperature of automatic sprinklers or nozzles.*

**5.4** *The capacity of the system water supply should be sufficient for the total simultaneous coverage of the minimum coverage area of table 5-1 and the vertically applicable area as defined in paragraph 3.22, and the requirements of paragraph 5.5.*

Table 5-1 Minimum coverage area per type of system

<b>Type of system (Definition number)</b>	<b>Minimum coverage area</b>
A. Wet pipe, automatic sprinkler heads (2.18)	280 m <sup>2</sup> or area of operation as defined in the fire tests – whichever is larger
B. Deluge system, automatic <sup>1</sup> and manual release (2.4)	280 m <sup>2</sup> and the overlapping or adjacent section as defined by paragraph 5.5 <sup>2</sup>
C. Deluge system, manual release (2.5)	2 sections each of min 20 m x B <sup>2,3</sup>
D. Other systems (2.6, 2.15)	Equivalent to the above systems and to the satisfaction of the Administration

<sup>1</sup> The automatic release should comply with the requirements of paragraph 5.6.

<sup>2</sup> The pump should be sized to cover the largest section for type B systems and the two largest horizontally adjacent sections for type C systems.

<sup>3</sup> B = full breadth of the protected space.

**5.5** The section arrangement for a deluge system with automatic and manual release (system B) should be such that a fire in any location of the border zone between two or more sections would be completely surrounded by activated spray heads, either by activating more than one section or by overlapping sections (whereby two or more sections cover the same area in the vicinity of the border between sections). In case of overlapping sections, such overlap should be a minimum of two times the required spray head spacing of the section in question or five metres, whichever is larger. These overlapping sections need not comply with the minimum width and length requirements of paragraph 3.23.

**5.6** For systems of type B (see table 5-1) an efficient fire detection and fire confirmation system covering all parts of the ro-ro or special category spaces should be provided as follows:

1. the fire detection system shall consist of flame detectors and smoke detectors of approved types. The flame detectors shall be installed under fixed continuous decks according to the limitation and application defined by the maker and the approval certificate. The smoke detector arrangement shall comply with the FSS Code. Additional smoke detectors with a spacing not exceeding 11 m shall be installed under hoistable ramps;
2. a colour TV monitoring system should cover all parts of the ro-ro or special category spaces. Cameras need not be installed below hoistable decks if the camera arrangement can identify smoke (confirm fire) based on positions under a fixed continuous deck. The monitors for the colour TV monitoring system should be located in the continuously manned control station having the controls for section control valves and start/stop control of pumps addressed under 3.2.2; and
3. the relevant section of the deluge system should be automatically released when two detectors covering this area activate. Systems being released when only one detector activates may also be accepted. Automatically released systems should also be capable of manual operation (both opening and closing) of the section valves. The automatic release may be disconnected during on- and off-loading operations, provided that this function is automatically reconnected after a preset time being appropriate for the operations in question.

## 9 The fire test procedures in MSC.1/Circ.1430/Rev.2

Main author of the chapter: Magnus Arvidson, RISE.

### 9.1 General requirements

None of the two revisions discussed above include any changes to the fire test procedures in the Appendix of MSC.1/Circ.1430. The fire test procedures are intended for testing of performance-based systems installed in ro-ro spaces and special category spaces with ceiling heights up to and including 2,5 m and/or up to and including 5 m. Two different fire test scenarios are described, a fire test scenario simulating a cargo fire of a simulated freight truck and a test scenario simulating a passenger car fire. The combustibles of both fire test scenarios consist of stacks of idle wood pallets.

The test hall where the tests are conducted should have a minimum floor area of 300 m<sup>2</sup> and a ceiling height in excess of 8 m. The test hall may be equipped with a forced ventilation system, or be naturally ventilated, in order to ensure that there is no restriction in air supply to the test fires. The test hall should have an ambient temperature of between 10 °C and 25 °C at the start of each test. The tests should be conducted under a flat, smooth, non-combustible ceiling at least 100 m<sup>2</sup> in size. There should be at least a 1 m horizontal distance between the perimeters of the ceiling and any wall of the test hall.

The tests should simulate the conditions of an actual installed system regarding parameters such as time delays between the activation of the system and minimum system water pressure or water delivery. In addition, the use of a pre-primed fire suppression enhancing additive, if applicable, should be considered.

### 9.2 The fire test scenarios

#### 9.2.1 General requirements

The primary fire source for both scenarios consists of stacks of EUR standard wood pallets (ISO 6780:2003), stored indoors with a moisture content of 14±2 %.

Plywood panels made of pine or spruce are used as targets. The panels should be approximately 12 mm thick. The ignition time of a panel should not be more than 35 s and the flame spread time at 350 mm position should not be more than 100 s as measured in accordance with IMO Resolution A.653(16).

For fire ignition of the wood pallets, commercial heptane in fire trays is used.

#### 9.2.2 The freight truck trailer fire test scenario

The primary fuel package of the freight truck trailer mock-up consists of 112 standard EUR wood pallets arranged in an array of 2 pallets (wide) × 7 pallets (high) × 8 pallets (long). In the longitudinal and transversal direction, the individual stacks are to be horizontally separated a distance of 100 mm to 200 mm. It is likely that this tolerance reflects the practical difficulties of adjusting the position of the stacks.

The array is raised to a level of 2,8 m using a rack so that the top level of the array is at a vertical distance of 3,8 m to 3,9 m above the floor. The wood pallet array should be half-shielded by a 4,5 m long and 2,6 m wide steel plate (thickness at least 2 mm) at a 4 m height. The plate should be properly fixed so that it provides an obstruction of water onto this part of the wood pallet array from overhead nozzles. Plywood panel targets, acting also as obstructions, of dimensions 3,6 m (W) × 2,4 m (H) should be arranged symmetrically on both long sides of the mock-up at a horizontal

distance of 1 m. The top edge of the target panels should be at the same level as the top level of the wood pallet array. Refer to Figure 27.



*Figure 27. The freight truck trailer mock-up. A total of 112 wood pallets are arranged in two parallel stacks, each containing seven wood pallets. The overall length is eight stacks. Half of the array is shielded from direct application of water from overhead nozzles by a horizontal steel sheet plate. The other half is fully exposed to the water spray. Fire trays with commercial heptane are positioned underneath the stacks for fire ignition. Photos: RISE Fire Research AS.*

The fire should be ignited by two fire trays centrally located under the wood pallets, refer to Figure 28. The square trays are 250 mm high and 0,1 m<sup>2</sup> (316 mm by 316 mm) in size. The trays should be filled with water and 1 l of heptane so that the free rim height above the liquid surface is 40 mm. The distance between the bottom of the wood pallets and liquid surface is 290 mm.



*Figure 28. The two fire trays centrally located under the wood pallets that is used to initiate the fire. Photos: RISE Fire Research AS.*

### 9.2.3 The passenger car fire test scenario

The passenger car mock-up consists of a total of 12 EUR wood pallets arranged in an array of 1 pallet (wide) × 6 pallets (high) × 2 pallets (long) that is stacked inside a shield made from steel sheets, simulating the body of a car. The roof of the simulated car body, that is sized 2 m (long) by 1,2 m (wide) shields the stacks of wood pallets from direct application of water from overhead nozzles.



Plywood panel targets, acting also as obstructions, of dimensions 1,2 m (wide) × 1,75 m (high) should be arranged symmetrically on both long sides of the mock-up at a horizontal distance of 0,6 m. The top edge of the target panels should be at the same level as the top level of the mock-up car. Refer to Figure 29.



Figure 29. The passenger car mock-up. It includes a total of 12 EUR wood pallets arranged in two stacks, each containing six pallets. Photos: RISE Fire Research AS.

The fire should be ignited by a square 100 mm by 100 mm fire tray centrally located under the wood pallets. The fire tray should be filled with water and 1 l of heptane so that the free rim height above the liquid (fuel) surface is 40 mm.

### 9.3 The positioning of sprinklers or nozzles

Sprinklers or nozzles should be installed in an array at the ceiling level in accordance with the manufacturer's design and installation criteria. Tests should be repeated with three different relative locations between the nozzle array and the fire ignition position:

- Centre of ignition under one nozzle.
- Centre of ignition between two nozzles.
- Centre of ignition between four nozzles.

### 9.4 Instrumentation and measurements

At least the following measurements should be made:

- Gas temperature at a vertical distance of 75 mm below the ceiling at different locations. For the freight truck fire test scenario, the three locations at both ends are used for acceptance evaluation, the three locations at and around the centre of fire ignition are for safety purposes to determine during the test whether the ceiling is at danger. For the passenger car fuel package all four locations (at a circular distance of 2 m from the fire ignition position) are used for performance acceptance evaluation.
- Gas temperature at the targets to indicate ignition of targets.
- System water pressure near the centre of the piping array.

Temperatures should be measured using plain type K thermocouple wires not exceeding 0,5 mm in diameter. The thermocouple head should be protected against direct water impingement, for example by tin cans. The system water pressure should be measured by using suitable equipment or be determined by a direct measurement or indirectly by based on the system pressure and the K-factor of the nozzles or sprinklers.



## 9.5 The test approaches

The nozzles and other components to be tested should be supplied by the manufacturer together with design and installation criteria, operational instructions, drawings, and technical data sufficient for the identification of the components.

The tests should be conducted at the minimum system water pressure at the minimum distance between the lowest part of the sprinklers or nozzles and the ceiling, as specified by the manufacturer. Three tests should be conducted at the ceiling heights of 5 m and/or 2,5 m, with different nozzle grid locations relative point of fire ignition as discussed above.

The fire tests should establish both nozzle installation criteria such as spacing between the nozzles, nozzle characteristics and minimum nozzle pressure and the minimum area of operation for the hydraulic design of wet, dry- or pre-action systems. However, the text in the Appendix remarks that the minimum ceiling area of 100 m<sup>2</sup> most likely is not sufficient for defining the area of operation of a system. In order to do so, the ceiling should be large enough to allow installation of a sufficient number of nozzles so that it is clear that the number of operating nozzles actually represent the maximum number. The area of operation is determined by multiplying the largest number of operating nozzles in the tests by a safety factor of 2 and defining the corresponding nozzle coverage area.

## 9.6 Fire test procedures

Prior to starting a test, the moisture of the wood pallets should be measured at several locations along the stacks with a probe-type moisture meter and the results should be reported. As discussed above, the moisture content should be 14±2 % in accordance with the current fire test procedures.

The fire tests should be conducted as follows:

1. The water pressure used at the start of the test should be set at the minimum value for the system specified by the manufacturer, flowing six open nozzles. If more than six nozzles operate during the test, the water supply pressure should be adjusted accordingly, to keep the required minimum system water pressure.
2. The tray should be filled with 1 l of heptane on the water base.
3. The measurements are started.
4. The fire tray(s) should be lit by means of a torch or a match.
5. The fire should be allowed to burn freely for a period of 2,5 minutes. If automatic sprinklers activate already during the 2,5-minute pre-burn period, feeding water to the system should be delayed until after the 2,5 minutes.
6. The test is continued for 30 minutes after system activation.
7. Any remaining fire should be manually extinguished.
8. The test is terminated.

## 9.7 Acceptance criteria

### 9.7.1 Principle requirements and fire damage evaluation

The principal acceptance criteria are based on the following factors:

1. Gas temperatures measured at locations not directly affected by impinging flames.
2. Damage to the fuel package; and/or,
3. Fire ignition of plywood targets.

Fire damage to the wood pallets of fuel package is defined by the fraction of charring of the full array. The damage to each individual wood pallet should be evaluated separately and the total

fraction calculated based on the detailed results. Totally black, i.e., totally charred pallet is denoted as 100 % damage of the pallet (even though the pallet may have maintained its shape) and totally intact pallet is denoted as 0 % damage. Partially charred pallets should be visually evaluated. Proper and adequate photographs of the damaged fuel package should be included in the test report.

If the visibility during the test is such that ignition of targets cannot be visually observed, it is recorded as follows: A thin (about 1 mm) metal sheet is bent on top of the plywood panels. Plain charring of panels is seen as a sharp edge between the black charring on the exposed surface and intact surface under the metal sheet. When ignited in flames, charring is seen also under the sheet and verified by significant increase in the gas temperature under the metal sheet.

#### 9.7.2 Freight truck fire test scenario evaluation

For the freight truck fire test scenario, the following four criteria should be met:

1. After system activation, the maximum 5-minute average at any of the three measurement locations at the exposed end of the array of wood pallets should not exceed 300 °C.
2. After system activation the maximum 5-minute average at any of the three measurement locations at the concealed end of the array of wood pallets should not exceed 350 °C.
3. The total damage to the wood pallet array should not exceed 45 % as defined after the test.
4. The plywood targets should not ignite during the test.

#### 9.7.3 Passenger car fire test scenario evaluation

For the passenger car fire test scenario, the following two criteria should be met:

1. After system activation the maximum 5-minute average at any of the four measurement locations should not exceed 350 °C.
2. The plywood targets should not ignite during the test.

## 10 Examples of certified alternative, performance based fire-fighting systems

Main author of the chapter: Magnus Arvidson, RISE.

There are several certified alternative, performance-based fire-fighting systems in the marketplace. Tables 4 through 7 exemplifies the design and installation criteria in terms of type of system (deluge system, system with automatic nozzles and whether the system is a low-pressure or high-pressure system), the maximum ceiling height, nozzle K-factor, minimum water pressure and the associated minimum water flow rate per nozzle, nozzle spacing and the associated nozzle coverage area as well as the calculated minimum discharge density.

For comparison reasons, the tables indicate the minimum required water discharge density of a prescriptive-based system of the same type.

Table 4. The design and installation criteria of three certified deluge systems for ro-ro spaces having a ceiling height up to and including 2,5 m.

Type of system	Deluge systems		
	Low-pressure system	High-pressure system	High-pressure system
Maximum ceiling height	2,5 m	2,5 m	2,5 m
Nozzle K-factor	23,0	1,8	2,7
Minimum water pressure	6 bar	80 bar	60 bar
Minimum flow rate per nozzle	56,3 l/min	16,6 l/min	20,9 l/min
Nozzle spacing	4,0 m by 4,0 m	3,8 m by 3,8 m	4,5 m by 4,5 m
Nozzle coverage area	16,0 m <sup>2</sup>	14,4 m <sup>2</sup>	20,2 m <sup>2</sup>
Corresponding discharge density*	3,5 mm/min	1,2 mm/min	1,0 mm/min

\*) The minimum required water discharge density of a prescriptive-based deluge system is 5 mm/min.

Table 5. The design and installation criteria of two certified systems using automatic nozzles for ro-ro spaces having a ceiling height up to and including 2,5 m.

Type of system	Systems using automatic nozzles	
	High-pressure system	High-pressure system
Maximum ceiling height	2,5 m	2,5 m
Nozzle K-factor	1,9	3,4
Minimum water pressure	80 bar	60 bar
Minimum flow rate per nozzle	17,0 l/min	26,3 l/min
Nozzle spacing	3,8 m by 3,8 m	4,0 m by 4,0 m
Nozzle coverage area	14,4 m <sup>2</sup>	16,0 m <sup>2</sup>
Corresponding discharge density*	1,2 mm/min	1,6 mm/min
Design area	280 m <sup>2</sup>	280 m <sup>2</sup>

\*) The minimum required water discharge density of a prescriptive-based wet-pipe, dry-pipe or pre-action system is 6,5 mm/min over a design area of 280 m<sup>2</sup>.

Table 6. The design and installation criteria of three certified deluge systems for ro-ro spaces having a ceiling height up to and including 5 m.

Type of system	Deluge systems		
	Low-pressure system	High-pressure system	High-pressure system
Maximum ceiling height	5 m	5 m	5 m
Nozzle K-factor	23,0	3,3	2,8
Minimum water pressure	6 bar	80 bar	60 bar
Minimum flow rate per nozzle	56,3 l/min	29,5 l/min	21,7 l/min
Nozzle spacing	3,5 m by 3,5 m	3,8 m by 3,8 m	3,8 m by 3,8 m
Nozzle coverage area	12,25 m <sup>2</sup>	14,4 m <sup>2</sup>	14,4 m <sup>2</sup>
Corresponding discharge density*	4,6 mm/min	2,0 mm/min	1,5 mm/min

\*) The minimum required water discharge density of a prescriptive-based deluge system is 10 mm/min, but it can be used to maximum free height of 6,5 m.

Table 7. The design and installation criteria of three certified systems using automatic nozzles for ro-ro spaces having a ceiling height up to and including 5 m.

Type of system	Systems using automatic nozzles		
	High-pressure system	High-pressure system	High-pressure system
Maximum ceiling height	5 m	5 m	5 m
Nozzle K-factor	3,1	4,2	4,2
Minimum water pressure	80 bar	100 bar	60 bar
Minimum flow rate per nozzle	27,7 l/min	42,0 l/min	32,5 l/min
Nozzle spacing	3,8 m by 3,8 m	4,0 m by 4,0 m	3,8 m by 3,8 m
Nozzle coverage area	14,4 m <sup>2</sup>	16,0 m <sup>2</sup>	14,4 m <sup>2</sup>
Corresponding discharge density	1,9 mm/min	2,6 mm/min	2,3 mm/min
Design area	280 m <sup>2</sup>	280 m <sup>2</sup>	280 m <sup>2</sup>

\*) The minimum required water discharge density of a prescriptive-based wet-pipe system is 15 mm/min over a design area of 280 m<sup>2</sup>. For a dry-pipe or pre-action, the design area is increased to 365 m<sup>2</sup>, but it can be used to maximum free height of 6,5 m.

All systems had a valid certificate in accordance with the Marine Equipment Directive 2014/90/EU in December 2021. The manufacturers of the systems are purposely not provided, but this is open information in the certificates. The intent here is to discuss the design and installation of alternative, performance-based fire-fighting systems versus prescriptive-based systems in general terms.

A prescriptive-based deluge system utilizing open water spray nozzles would typically have a K-factor around 60 to 80 (l/min)/√bar dependent on the desired flow rate. A wet-, dry- or pre-action system, that utilize automatic sprinklers, would have a K-factor of either 80 or 115 (l/min)/√bar. The operating pressure would be in the order of 1 to 2 bars. It is thereby concluded that the K-factor is significantly higher and the operating pressure significantly lower than those for alternative, performance-based systems.

It is observed that the discharge densities for the currently certified alternative, performance-based systems are low or very low (from about half to almost one tenth) of the minimum discharge densities required for prescriptive-based systems. It should be noted that the some of the examples given above compares a prescriptive-based design acceptable up to a maximum clear height of 6,5 m, whilst the performance-based alternative only is acceptable up to 5 m. It is likely that a performance-based system tested using a 6,5 m ceiling height would require a higher discharge density, which would make the relative difference in discharge density smaller.

For all the certified systems exemplified here, it is also observed that the nozzle spacing, and the corresponding maximum nozzle coverage area is in excess of that stipulated in MSC.1/Circ.1430 for prescriptive-based systems. The maximum horizontal spacing between nozzles or sprinklers for prescriptive-based systems should not exceed 3,2 m, which corresponds to a coverage area of 10,2 m<sup>2</sup>. For one of the certified systems, the nozzle coverage area is in excess of 20 m<sup>2</sup>.

For wet-pipe, dry-pipe or pre-action, which utilize automatic nozzles, there is a potential that a large, shielded fire could overtax the capacity of the water pump if too many nozzles activate. This is because a shielded fire will not be suppressed by direct application of water and the extensive heat from the fire will operate more and more automatic nozzles as the fire grows in size and the flow rate per nozzle is reduced.

There is a noticeable design difference between the certified low-pressure and the high-pressure systems. This may be due to a difference in performance, but it is not inconceivable that it is due to poor test reproducibility, in other words that the results are influenced where and when the tests are conducted. One uncertainty could be the humidity of the idle wood pallets, which can have an impact on the fire growth rate and peak heat release rate.



## 11 The inadequacies of the fire test procedures in MSC.1/Circ.1430/Rev.2

Main author of the chapter: Magnus Arvidson, RISE.

### 11.1 Primary inadequacies

The two primary inadequacies of the fire tests procedures are that:

1. The fire test scenarios do not reflect the severity in terms of fire load and peak heat release rate of modern vehicles and cargo.
2. The acceptance criteria in terms of the maximum allowed ceiling gas temperatures, fire damage and ignition of the targets were established with a water spray system designed per the out-dated recommendations in Resolution A.123(V).

Therefore, the concern is that the performance-based systems that have passed the tests do not provide a fire suppression performance that is comparable to that of the current prescriptive-based system design in MSC.1/Circ.1430/Rev.2.

### 11.2 Other opportunities for improvements

Some other differences between prescriptive-based and performance-based systems that are related to the fire test procedures are commented below.

#### **The ceiling height limitations**

The maximum ceiling height limitation in the fire test procedures is 5,0 m. A prescriptive-based system may be designed and installed in spaces up to 10,0 m in height per Table 4-3 of MSC.1/Circ.1430/Rev.2.

#### **Ceiling height definitions**

For prescriptive-based systems, the applicable ceiling height is defined as the “free height”. Although this measure is not defined, it should be understood as the height of the space that is usable for cargo. This vertical distance is measured from the deck flooring to the underside of any obstructions such as structural ceiling members, lights, ducts, piping or similar. For ships, the synonym “clear height” is often used. For performance-based systems, the ceiling height is measured from the floor to the underside of the ceiling surface, as no beams are used in the fire tests.

#### **Ceiling construction**

Section 3.21 of MSC.1/Circ.1430/Rev.2, that is valid for both prescriptive-based and performance-based systems states that the presence of obstructions and the potential for shielding of the water spray should be evaluated to ensure that the system performance is not affected. Supplementary sprinklers or nozzles should be installed beneath obstructions.

Section 4.5 of MSC.1/Circ.1430/Rev.2, that is valid for prescriptive-based systems states that sprinklers or nozzles should be positioned such that 1) they are not exposed to damage by cargo, 2) undisturbed spray is ensured and 3) water is distributed over and between all vehicles or cargo in the area being protected. Automatic sprinklers or nozzles should be positioned and located so as to provide satisfactory performance with respect to both activation time and water distribution.

The current fire test procedure does not include any ceiling beams. In a test, nozzles should be installed in an array at the ceiling level in accordance with the manufacturer's design and installation criteria. The vertical distance from an automatic sprinkler to the ceiling surface will influence the

activation time. Therefore, it is essential that the benchmark fire tests are conducted using a specific vertical distance that should be used for fire testing of performance-based systems.

## 12 The main features of the revised test procedures

Main author of the chapter: Magnus Arvidson, RISE.

### 12.1 Basic requirements of the revised fire test scenarios

A fire test source representing fires in either a passenger car or the cargo of a freight truck trailer should:

- Simulate the geometrical dimensions.
- Provide as repeatable a fire scenario as possible
- Have a reasonably slow initial fire growth.
- Provide a realistic peak heat release rate.
- Produce as few toxic gases as possible.
- Be easily available.
- Be reasonably inexpensive.

A discussion of a fire test source that meets these requirements and appropriate fire test procedures is given below.

### 12.2 Suggested fire test scenarios

#### 12.2.1 Freight truck trailer fire test scenario

The current freight truck trailer fire test scenario involves 112 standard EUR wood pallets arranged in an array that is 2 pallets (wide) × 7 pallets (high) × 8 pallets (long). Half of the array is shielded from direct application of water from overhead nozzles by a horizontal steel sheet plate. The other half is fully exposed to the water spray.

In theory, the amount of wood pallets in the array could result in a peak heat release rate in the order of 20 MW if all pallets are burning simultaneously. However, due to the overall length of the array, it is unlikely that all pallets will be involved at the same time. As the fire progresses from the mid-point and in both directions, the stacks closest to the point of fire ignition will to some extent be consumed once the flame fronts, respectively, reach the ends of the array. Model-scale (1:4) fire tests [44] were conducted at RISE (then SP) in the IMPRO-project using stacks of idle wood pallets, simulating the fire in the cargo of a freight truck trailer. For the tests, 14 pallets were stacked on top of each other. This equalled an overall height of 504 mm (2016 mm in full scale). The number of rows of stacks in the longitudinal direction were varied, from 2 to 10 rows of stacks and tests were conducted without and with a roof over the entire array.

For the tests without a roof over the array, it was observed that flames were established in the flue space formed by the pallets facing each other after fire ignition. Thereafter, fire started to spread horizontally between the individual pallets. During this increase of the fire size, flames ignited the top surface of the first four stacks of pallets. Gradually, fire progressed in a horizontal direction, involving one stack of pallets after the other. The fire spread was fairly slow and the fire in the central four stacks decreased at about the same rate as fire was spreading towards the short ends of the array. When the combustibles of the four central stacks were consumed, they burnt out and collapsed. The one-minute peak heat release rate was the highest (1080 kW) when using six rows of stacks. The use of four rows of stacks resulted in a one-minute peak heat release rate of 951 kW (12 % lower) and the use of eight rows of stacks in 1065 kW (1 % lower). The maximum ten rows of stacks resulted in a one-minute peak heat release rate of 979 kW (9 % lower). When the point of ignition was moved to the centre point of the far right flue space, which would result in fire spread in virtually in one direction only, the one-minute peak heat release rate was 645 kW, which is 34 % lower than the peak

observed with a central fire ignition involving ten rows of stacks. Figure 30 shows a photo sequence showing the fire development with eight rows of stacks of idle wooden pallet stacks.

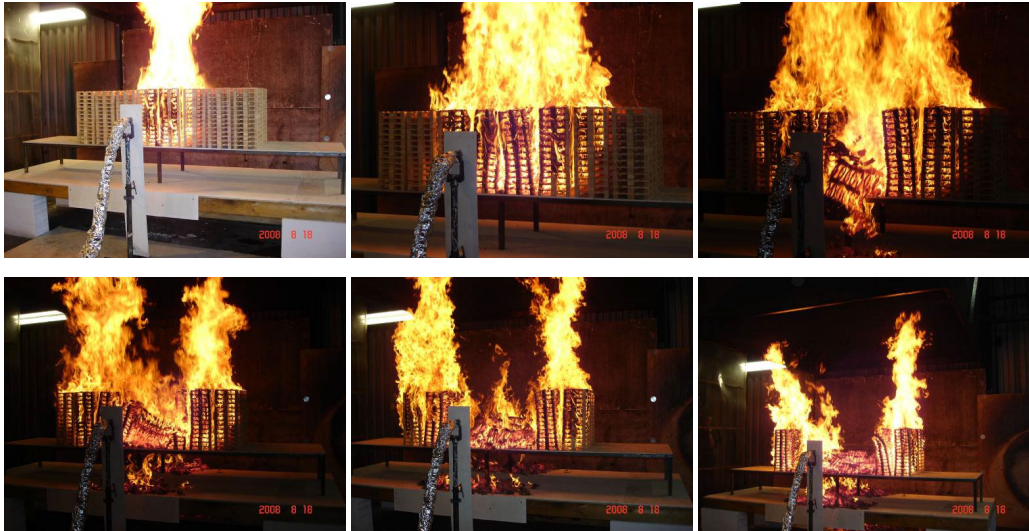


Figure 30. A photo sequence showing the fire development with eight rows of stacks of idle wooden pallet stacks during 1:4 model-scale tests. Photos: RISE.

For the tests with a roof over the array, it was observed the initial fire development was similar to the behaviour described above. However, as the fire size increased, the roof directed the flames over the tops of the adjacent stacks of pallets. This changed the fire spread such that the top layer of pallets became involved in the fire faster than without the roof. However, it seemed that the roof reduced the peak heat release rate. The one-minute peak heat release rate was the highest (932 kW) when using ten rows of stacks. The use of four rows of stacks resulted in a one-minute peak heat release rate of 735 kW (21 % lower), the use of six rows of stacks in 900 kW (3 % lower) and the use of eight rows of stacks in 856 kW (8 % lower). When the point of ignition was moved to the centre point of the far right flue space, the one-minute peak heat release rate was 744 kW, which is 20 % lower than the peak observed with a central fire ignition involving ten rows of stacks.

It is suggested that the revised fire test procedure should involve stacks that are twice as high as in the current fire test procedures, i.e., 14 pallets. This height would reflect a realistic storage height (2016 mm) on a trailer, although it is assumed that higher storage heights may be possible. By increasing the number of pallets in each stack from 7 to 14, the peak heat release rate will be higher as more pallets will be involved in the fire at the same time.

By limiting the overall array to four rows of stacks, the total amount of 112 standard EUR wood pallets could be kept. This will result in an array that is 2 pallets (wide) × 14 pallets (high) × 4 pallets (long). Half of the array is shielded from direct application of water from overhead nozzles by a horizontal steel sheet plate. The other half is fully exposed to the water spray. The data from the model-scale tests discussed above indicates that a longer array would not result in a significantly higher peak heat release rate. But is believed that the rearrangement of the 112 pallets will result in a more severe and more realistic fire test scenario than that of the current fire test procedures.

### 12.2.2 Passenger car fire test scenario

The current passenger car fire test scenario involves 12 standard EUR wood pallets arranged in an array that is 1 pallet (wide) × 6 pallets (high) × 2 pallets (long). The roof of the simulated car body shields the stacks of wood pallets from direct application of water from overhead nozzles.

Two series of free-burn fire tests, refer to the Annex A, were conducted to establish a realistic fire growth rate and peak heat release rate using different arrays of wood pallet stacks. Given that all, or virtually all wood pallets in the array are involved in the fire, it can be concluded that each wood pallet contributes with approximately 175 kW to the peak heat release rate.

The net calorific value of wood is typically assumed to be 17,5 MJ/kg, for example in Eurocode 1 [45]. The theoretical energy content of a wood pallet is thereby approximately  $22 \text{ kg} \times 17,5 \text{ MJ/kg} = 385 \text{ MJ}$ . If assuming a burning efficiency of 0,8, the characteristic fire load is approximately 300 MJ per pallet. This value corresponded well with the results documented in the Annex A.

Based on the free-burn fire tests, it is estimated that the current passenger car fire test scenario provides a fire load of about 3,6 GJ and a peak heat release rate in the order of 2 MW.

The fire growth rate and the peak heat release rate is also influenced by the position of the fire ignition source. If the fire is ignited at the mid-point of the array and allowed to spread symmetrically in both directions the fire growth rate and the peak heat release rate will be higher than if it is positioned close to the end of the array. The size of the fire ignition source will additionally influence the initial fire growth rate. The larger the fire ignition source, the faster the initial fire growth rate.

Based on the on the free-burn fire tests, it is suggested the revised passenger car fire test scenario should involve 36 standard EUR wood pallets arranged in an array that is 2 pallet (wide)  $\times$  6 pallets (high)  $\times$  3 pallets (long). This would result in a theoretical fire load of 10,8 GJ and fire that is in the order of 5 MW to 6 MW. Part of the array should be exposed to the application of overhead sprinklers or nozzles and part of it should be shielded. The suggested array is slightly different than those used in the free-burn fire tests. The reason for lowering the height of the stacks is twofold, it will improve the stability of the stack without the use of cross bars on the side faces of the stacks and it is also mimic the width of a car better.

### 12.3 The fire test hall and the environmental conditions

Tests should be conducted in principle in accordance with the current fire test procedures, i.e., inside a well-ventilated fire test hall with a sufficient area and volume and under a suspended ceiling of sufficient size (at least 100 m<sup>2</sup>).

The ceiling height should be set at 2,5 m in order to represent a typical low clear height and at a ceiling height representing spaces where large vehicles are transported. It is suggested that two fixed ceiling heights are used in the revised fire test procedures, 2,5 m and 6,5 m. Any specific test height above 6,5 m should be chosen by the manufacturer. Based on input from the partners of the project, ceiling heights in excess of 6,5 m are rare on ro-ro ships.

### 12.4 Instrumentation and measurements

It is suggested that instrumentation and measurements are similar to that of the current fire test procedures:

- Gas temperature at a vertical distance of 75 mm below the ceiling at the following different locations; directly above the point of fire ignition and a four different positions on a 1,5 m radius from the centremost thermocouple.
- Surface temperature of the target steel sheet screens.
- System water pressure near the centre of the piping array.

Temperatures should be measured using sheathed type K thermocouple having a 1 mm in diameter. Contrary the current fire test procedures, the thermocouple heads were protected against direct water impingement, for example by tin cans. The system water pressure should be measured by



using suitable equipment or be determined by a direct measurement or indirectly by based on the system pressure and the K-factor of the nozzles or sprinklers.

## 12.5 The activation of the system

Five different system types are described in MSC.1/Circ.1430/Rev.2:

**Wet-pipe system:** A system with automatic sprinklers or nozzles attached to a piping system containing water and connected to a water supply so that water discharges immediately from sprinklers or nozzles opened by heat from a fire. The system piping may contain an antifreeze liquid solution to prevent freezing of the system. The solution is discharged upon sprinkler operation, followed immediately by water from a water supply.

**Dry-pipe system:** A system with automatic sprinklers or nozzles attached to a piping system containing air or nitrogen under pressure, the release of which (as from the activation of a sprinkler or nozzle by heat from a fire) permits the water pressure to open a valve known as a dry pipe valve. The water then flows into the piping and discharges from the open nozzles or sprinklers.

**Pre-action system:** A dry-pipe system with a supplemental fire detection system installed in the same area as the sprinklers or nozzles. Two separate events must happen to initiate sprinkler discharge. Firstly, the detection system must identify a developing fire and then open the pre-action valve. This allows water to flow into system piping. Secondly, individual sprinkler heads must release to permit water flow onto the fire.

**Deluge system (manual release):** A system employing open nozzles attached to a piping system connected to a water supply through a deluges section valve that is opened by manual operation. When this valve is opened, water flows into the piping system and discharges from all nozzles attached thereto.

**Deluge system (automatic and manual):** This type of system is similar to the one described above but the deluge section valve is opened by signals from a fire detection system and by manual operation.

For all systems, there is a delay time from the start of a fire until water is discharged that need to be captured in the fire test procedures, refer to Table 8.

Table 8. The approximate delay time from the start of a fire until water is discharged.

Type of system	Fire detection time	Time delay to water discharge ('water travel time') upon system activation*
Wet-pipe	Time to activate the automatic sprinklers by the heat from a fire.	None**
Dry-pipe		60 s
Pre-action	Time for fire alarm that opens the pre-action valve and time to operate the automatic sprinklers by the heat from a fire.	60 s
Deluge (manual)	Time for fire alarm, alarm notification, decision making and operation of the correct deluge valve.	60 s
Deluge (automatic)	Time for fire detection by at least two fire detectors.	60 s

\*) Section 3.3 of MSC.1/Circ.1430/Rev.2 states that "The design of the system should ensure that full system pressure is available at the most remote sprinkler or nozzle in each section within 60 s of activation". This time is often referred to as the water travel time.

\*\*) Although a wet-pipe system is pressurized with water, there may be short delay time from the detection of the water pressure drop in the system piping until full system pressure is reached.

The activation time of automatic sprinklers (given the same fire growth rate) is dependent on many factors, including but not limited to the ceiling height, the horizontal spacing between sprinklers, the

vertical distance from the ceiling surface to the sprinkler, the operating temperature, and the thermal sensitivity (Response Time Index, RTI) of the sprinkler as well as the design of the ceiling construction. During fire testing, it is common practice that the tests are conducted at the maximum ceiling height and the maximum sprinkler spacing, as specified by the manufacturer. Some fire test procedures require that the tested sprinklers shall be installed at the maximum intended vertical distance from the ceiling surface.

The maximum allowed water travel time is 60 s per section 3.3 of MSC.1/Circ.1430/Rev.2. This time should be considered as the maximum time in an actual system as it refers to the hydraulically most remote sprinkler or nozzle. For individual sprinklers hydraulically closer to the alarm valve or deluge sections hydraulically closer to the deluge section valve, this time delay is shorter.

As discussed above, the current fire test procedures in MSC.1/Circ.1430/Rev.2 require that the fire test scenario should be allowed to burn freely for a period of 2,5 minutes. If automatic sprinklers activate during the 2,5-minute pre-burn period, feeding water to the system should be delayed until after the 2,5 minutes.

For the revised fire test procedures, an approach in accordance with Table 9 would cover the characteristics of all five types of systems. The water travel times are shorter than the maximum allowed in order to reflect actual conditions rather than the maximum allowed water travel times.

Table 9. The principal fire test approach in the revised fire test procedures.

Type of system	System activation approach	Time delay to water discharge upon system activation
Wet-pipe	<ul style="list-style-type: none"> <li>The system pipe-work is pressurized with water to the minimum stand-by pressure specified by the manufacturer.</li> <li>Automatic sprinklers or nozzles are allowed to operate by the heat from the fire.</li> </ul>	A 15 s delay time is applied from the recording of the pressure drop in the system piping until the water pump is started.
Dry-pipe	<ul style="list-style-type: none"> <li>The system pipe-work is pressurized with compressed air to the minimum stand-by pressure specified by the manufacturer.</li> <li>The flow of water to the pipe-work is controlled by a manually operated system control valve.</li> <li>Automatic sprinklers or nozzles are allowed to operate by the heat from the fire.</li> </ul>	A 45 s delay is applied from the recording of the pressure drop in the system piping until the system control valve is manually opened.
Pre-action	<ul style="list-style-type: none"> <li>The system pipe-work is pressurized with compressed air to the minimum stand-by pressure specified by the manufacturer.</li> <li>The flow of water to the pipe-work is controlled by two manually operated system control valves.</li> <li>Ceiling gas temperatures are measured at a specific radius from the point of fire ignition, mimicking spot-type heat detectors.</li> <li>When at least two of the thermocouples have reached a realistic fire detection temperature threshold, system control valve no. 1 is opened.</li> <li>Automatic sprinklers or nozzles are allowed to operate by the heat from the fire.</li> </ul>	A 45 s delay is applied from the recording of the pressure drop in the system piping until system control valve no. 2 is manually opened. System control valve no. 1 may be opened before, during or after the 45 s delay time.
Deluge (manual)	<ul style="list-style-type: none"> <li>The system pipe-work is connected to a system control valve.</li> <li>Ceiling gas temperatures are measured at a specific radius from the point of fire ignition, mimicking spot-type heat detectors.</li> <li>When at least two of the thermocouples have reached a realistic fire detection temperature threshold, the system control valve is opened after the delay time specified in the next column.</li> </ul>	A delay time is applied to account for alarm notification, decision making and operation of the correct deluge valve plus 45 s to account for the water travel time.

Type of system	System activation approach	Time delay to water discharge upon system activation
Deluge (automatic)	<ul style="list-style-type: none"> <li>The system pipe-work is connected to a system control valve.</li> <li>Ceiling gas temperatures are measured at a specific radius from the point of fire ignition, mimicking spot-type heat detectors.</li> <li>When at least two of the thermocouples have reached a realistic fire detection temperature threshold, the system control valve is opened after the delay time specified in the next column.</li> </ul>	A 45 s to account for the water travel time.

However, from a practical perspective is desired that the number of test alternatives is reduced. This will reduce the testing and certification costs for a manufacturer. It is therefore suggested that:

- Wet-pipe systems are tested as per the description described above. These systems typically use pendent sprinklers or nozzles.
- Dry- and pre-action systems are tested using a similar approach. These systems typically use upright sprinklers or nozzles.
- Deluge (manual) and deluge (automatic) systems are tested using a similar approach. These systems typically use pendent nozzles. It is noted that automatic deluge systems should be capable of manual operation and that the automatic release function may be disconnected during on- and off-loading operations, provided that this function is automatically reconnected after an appropriate pre-set time. Fire testing of manual and automatic deluge system in a similar fashion therefore makes sense.

The suggested fire test approach is shown in Table 10.

Table 10. The suggested fire test approach in the revised fire test procedures.

Type of system	System activation approach	Time delay to water discharge upon system activation
Wet-pipe	<ul style="list-style-type: none"> <li>The system pipe-work is pressurized with water to the minimum stand-by pressure specified by the manufacturer.</li> <li>Automatic sprinklers or nozzles are allowed to operate by the heat from the fire.</li> </ul>	A 15 s delay time is applied from the recording of the pressure drop in the system piping until the water pump is started.
Dry-pipe and pre-action	<ul style="list-style-type: none"> <li>The system pipe-work is pressurized with compressed air to the minimum stand-by pressure specified by the manufacturer.</li> <li>The flow of water to the pipe-work is controlled by a manually operated system control valve.</li> <li>Automatic sprinklers or nozzles are allowed to operate by the heat from the fire.</li> </ul>	A 45 s delay is applied from the recording of the pressure drop in the system piping until the system control valve is manually opened.
Deluge (manual and automatic)	<ul style="list-style-type: none"> <li>The system pipe-work is connected to a system control valve.</li> <li>Ceiling gas temperatures are measured at a specific radius from the point of fire ignition, mimicking spot-type heat detectors.</li> <li>When at least two of the thermocouples have reached a realistic fire detection temperature threshold, the system control valve is opened after the delay time specified in the next column.</li> </ul>	A 45 s to account for the water travel time. The delay time for alarm notification, decision making, and operation of the correct deluge valve associated with manual systems is not included as it is difficult to determine.

## 12.6 The ceiling construction and nozzle positioning

For automatic sprinklers or nozzles (i.e., sprinklers or nozzles that are activated by the heat from a fire), it is essential that the vertical distance from the underside of the deck to the thermal element is within certain limits to provide as fast activation as possible. Sprinklers or nozzles at the underside of 'obstructed ceiling constructions' need to also be positioned such that the ceiling construction in terms of beams, trusses, or other members do not affect the water distribution. On the other hand, a vertical distance too far from the deckhead will influence the activation time.

The January 2018 edition of FM DS 2-0 [46] defines an "Unobstructed Ceiling Construction" as a "A ceiling structural assembly that allows the flow of hot gases to spread out under the ceiling uniformly from the point of fire origin to the nearest four sprinklers in a timely fashion". Ceiling structural assemblies that meet this definition include:

- Ceiling systems that have construction materials that do not protrude downward from the ceiling more than 100 mm, or,
- Ceiling systems that have construction materials that protrude downward from the ceiling more than 100 mm, but their cross-sectional area is 70 % or more open, or,
- Ceiling systems that have construction materials that protrude downward from the ceiling more than 100 mm and are less than 70 % open in their cross-sectional area, but the volume created by the ceiling structural assembly does not exceed 2,8 m<sup>3</sup>, or
- The horizontal distance between the construction material protrusions exceeds the maximum allowable spacing for the sprinkler being installed.

FM DS 2-0 defines an "Obstructed Ceiling Construction" as a "A ceiling structural assembly that prevents the flow of hot gases from spreading out under the ceiling uniformly from the point of fire origin to the nearest four sprinklers. This would apply to ceiling structural assemblies that do not meet the definition of unobstructed ceiling construction."

It is suggested that the fire tests in the revised test procedures are conducted using a flat, smooth non-combustible ceiling of at least 100 m<sup>2</sup> in size, as per the current fire test procedures. But unlike the current fire test procedures it is suggested that sprinklers or nozzles should be installed at a given vertical distance below the ceiling of 150 mm. This vertical distance should be measured from the underside of the ceiling to the deflector or tip of the sprinkler or nozzle.

By specifying the ceiling-to-sprinkler/nozzle distance the test conditions will be similar for any system. This vertical distance will influence the activation time of automatic sprinklers and the cooling of hot combustion gases at the ceiling.

## 12.7 Simulation of a heat detection system

Section 4.8 of MSC.1/Circ.1430/Rev.2 require that manual deluge systems, automatic deluge systems and pre-action systems should be provided by a fire detection system complying with the FSS Code. The detailed requirements are discussed previously in this report.

The fire detection system should consist of flame, smoke, or heat detectors of approved types. For automatic deluge and pre-action systems, the discharge of water should be controlled by the fire detection system and coverage area of the detection system sections should correspond to the area of deluge sections. The detection system should provide an alarm upon activation of any single detector and discharge if two or more detectors activate. Automatically released systems should also be capable of manual operation (both opening and closing) of the section valves. Means should be provided to prevent the simultaneous release of multiple sections. The automatic release may be

disconnected during on- and off-loading operations, provided that this function is automatically reconnected after a pre-set time being appropriate for the operations in question.

It is considered that a heat detection system probably is the most suitable system for activation of an automatic system. A heat detection system is robust, relatively inexpensive and the probability for detection of a fire outside of a coverage area is small. A smoke or flame detection system may, however, be able to detect a smoldering (smoke) or a flaming (flame) fire, respectively, earlier than would a heat detection system. It is suggested that the focus of the revised fire test procedures is on testing performance of manual or automatic deluge systems that are controlled by a heat detection system.

Section 2.3.1.3 of the FSS Code requires that heat detectors shall be certified to operate before the temperature exceeds 78 °C, but not until the temperature exceeds 54 °C, when the temperature is raised to those limits at a rate less than 1 °C per minute. At higher rates of temperature rise, the heat detector shall operate within temperature limits to the satisfaction of the Administration having regard to the avoidance of detector insensitivity or oversensitivity.

Detectors shall be located for optimal performance. Positions near beams and ventilation ducts or other positions where patterns of air flow could adversely affect performance and positions where impact or physical damage is likely shall be avoided. Table 11 shows the maximum spacing of detectors given in the FSS Code.

Table 11. The maximum spacing of fire detectors given in the FSS Code.

Type of detector	Maximum floor area per detector	Maximum distance apart between centres	Maximum distance away from bulkheads
Heat	37 m <sup>2</sup>	9 m	4,5 m
Smoke	74 m <sup>2</sup>	11 m	5,5 m

There are two specific installation requirements for spot-type heat detectors in MSC.1/Circ.1430/Rev.2:

- Section 4.9: Where beams project more than 100 mm below the deck, the spacing of spot-type heat detectors at right angles to the direction of the beam travel should not be more than two thirds [i.e., no more than 6,0 m] of the spacing permitted under Chapter 9 of the FSS Code.
- Section 4.10: Where beams project more than 460 mm below the deck and are more than 2,4 m on centre, detectors should be installed in each bay formed by the beams.

As it is suggested (per the discussion in the previous section of the report) that a flat, smooth non-combustible ceiling should be used, the detector spacing should be at most 9 m.

It is suggested that two  $\varnothing=0,5$  mm wire thermocouples are installed at the ceiling, at radius of 4,5 m from the point of fire ignition. The thermocouples should be positioned 75 mm below the ceiling surface to reflect a likely position in practice. When the temperature of both thermocouples exceeds 78 °C, the time delay associated with the water travel time is applied and the system control valve is opened.

## 12.8 Fire test procedures

The revised fire test procedures are suggested to be similar to that of the current fire test procedures. Prior to starting a test, the moisture of the wood pallets should be measured at several locations along the stacks with a probe-type moisture meter and the results should be reported. As discussed above, the moisture content should be 14±2 %.

The fire tests should be conducted as follows:



1. The water pressure used at the start of the test should be set at the minimum value for the system specified by the manufacturer, flowing six open automatic sprinklers or nozzles or all installed open nozzles. If more than six automatic sprinklers or nozzles operate during the test, the water supply pressure should be adjusted accordingly, to keep the required minimum system water pressure.
2. The tray should be filled with 3,6 l (20 mm) of heptane on the 9 l (50 mm) water base.
3. The measurements are started.
4. The fire tray(s) should be lit by means of a torch or a match.
5. The tested system is allowed to operate as per the description in Table 2.
6. The test is continued for 30 minutes after system activation.
7. Any remaining fire should be manually extinguished.
8. The test is terminated.

### 12.9 Acceptance criteria

The principal acceptance criteria are suggested to be based on the following:

1. The peak ceiling gas temperature, based on the average temperature of the five thermocouples at the ceiling.
2. The peak surface temperature based on the average temperature of the thermocouples at the target steel sheet screens.
3. No fire damage criteria are used.

## 13 Fire test approach during any benchmark fire suppression tests

Main author of the chapter: Magnus Arvidson, RISE.

### 13.1 General

In the previous section, relevant fire test scenarios that better reflect fires in modern vehicles and cargo are discussed. In the second step, large-scale benchmark fire suppression tests are discussed. Such tests should be conducted using automatic sprinkler and water spray systems that fulfil the prescriptive-based system requirements in MSC.1/Circ.1430/Rev.2. Thereby, new acceptance criteria can be established, but the tests will also be used to establish the principal requirements of the revised fire test procedures.

The details of these tests are discussed below.

### 13.2 Ceiling heights used in any benchmark tests

The design tables 4-1 to 4-3 in section 4 of MSC.1/Circ.1430/Rev.2 provides three ceiling height limits for the design of prescriptive-based systems:

- Equal and less than 2,5 m.
- In excess of 2,5 m and up to and including 6,5 m.
- In excess of 6,5 m and up to and including 10,0 m.

As discussed, the ceiling height limits refers to the free height of the space, i.e., the vertical distance measured from the deck flooring to the underside of any obstructions such as structural ceiling members, lights, ducts, piping or similar. However, during the 8<sup>th</sup> session of the IMO Sub-Committee on Ship Systems and Equipment (SSE), held between February 28 and March 4, 2022, it was proposed that the ceiling height should instead be measured from the deck flooring to the underside of the ceiling. This ceiling height definition would then correlate with that used in the current fire test procedures in the Appendix of MSC.1/Circ.1430/Rev.2.

It is suggested that the fire suppression performance of the associated prescriptive-based system designs is established at the following three ceiling heights:

- At a ceiling height of 2,5 m, using the new passenger car mock-up.
- At a ceiling height of 6,5 m, using the new freight truck trailer mock-up.
- At a ceiling height in excess of 6,5 m, to the discretion of the manufacturer of the tested system.

For the benchmark fire tests conducted in this project, ceiling height of 2,5 m and 5,0 m were used. These are the ceiling heights used in the current fire test procedures. It is likely that the use of 5,0 m instead of 6,5 m generates higher ceiling gas temperatures.

As ceiling heights in excess of 6,5 m appear to be uncommon, no specific benchmark tests were conducted using higher ceiling heights.

### 13.3 Type of systems used in any benchmark tests and system activation delay times

It is suggested that any benchmark fire suppression tests focus on the two types of systems that are the most relevant:

- A dry-pipe system using automatic, upright sprinklers.
- A manually operated deluge system, using pendent, open water spray nozzles.

Paragraph 3.3 of MSC.1/Circ.1430/Rev.2 require that the design of the system should ensure that full system pressure is available at the most remote sprinkler or nozzle in each section within 60 s of activation. For a dry-pipe system, this time is calculated from the activation of the first automatic sprinkler. The activation of one or several sprinklers will dispel compressed air, open the dry-pipe valve, and will allow water entering the pipe-work. As per the discussion in section 8 of the report, this time was set to at least 45 s, to reflect the most realistic cases where several sprinklers activates more or less simultaneously which results in a dispel time and water travel time that is faster than the maximum allowed.

For a manually operated deluge system, the water travel time is calculated from the operation of the deluge section valve. An additional time delay is associated with the time for fire detection and the time required for the decision to operate the system and the time to start the pump and open the (correct) deluge section valve. The total time measured from fire start until water is discharged over the fire can therefore be several minutes. For the benchmark fire suppression tests described here, a 60 s delay time is suggested to be used.

### 13.4 Water discharge densities used in any benchmark tests

The system designs provided in tables 4-1 to 4-3 in section 4 of MSC.1/Circ.1430/Rev.2, as amended, are summarised in Table 12.

Table 12. The water discharge densities provided in tables 4-1 to 4-3 in section 4 of MSC.1/Circ.1430.

Ceiling height	Type of system	Minimum water discharge density (mm/min)	Minimum operating area
≤ 2,5 m	Wet-, dry- or pre-action	6,5	280 m <sup>2</sup>
	Deluge	5	2 × 20 m x B
> 2,5 m - ≤ 6,5 m	Wet-pipe	15	280 m <sup>2</sup>
	Dry- or pre-action		365 m <sup>2</sup>
	Deluge	10	2 × 20 m x B
> 6,5 m - ≤ 10 m	Wet-pipe	20	280 m <sup>2</sup>
	Dry- or pre-action		365 m <sup>2</sup>
	Deluge	15	2 × 20 m x B

The table list the minimum required water discharge densities and minimum operating areas. For an actual system, higher water discharge densities are provided when the first sprinklers of a wet-, dry- or pre-action system operates. For a deluge system, higher discharge densities are provided when one deluge section only is operated or when the deluge sections are positioned hydraulically more favourable than the sections used in the hydraulic design of the system.

For the benchmark fire suppression tests described here, it is proposed that testing is undertaken at the operating pressure corresponding to the minimum discharge densities of the table. The upcoming fire test procedures should stipulate that testing of alternative systems is also conducted at the minimum operating pressure.

### 13.5 Automatic sprinkler and water spray nozzles used in any benchmark tests

For wet-, dry- or pre-action systems, the minimum operating pressure of any sprinkler should be 0,05 MPa, which equals 0,5 bar, according to section 4.1 of MSC.1/Circ.1430/Rev.2. This requirement will affect the choice of K-factor of the automatic sprinklers used for the benchmark fire suppression tests. For dry- or pre-action systems, upright sprinklers should be used.

For deluge systems, section 4.2 of MSC.1/Circ.1430/Rev.2 states that the minimum operating pressure of any sprinkler should be 0,12 MPa, which equals 1,2 bar. This requirement affects the choice of K-factor of open nozzles and thereby the choice of nozzles for the benchmark fire

suppression tests. A system designer would typically choose a sprinkler or nozzle with a high K-factor to reduce the system operating pressure for a given water discharge density and actual sprinkler or nozzle spacing.

The current version, MSC.1/Circ.1430/Rev.2, does not provide a maximum spacing between sprinklers or nozzles, whilst the first version specified 3,2 m as the maximum. This spacing is suggested to be used in the benchmark fire suppression tests described here.

Based on the discussion above, Table 13 shows the suggested choice of automatic sprinklers and nozzles for the benchmark fire suppression tests, based on the ceiling height, the minimum discharge density for that ceiling height and a sprinkler and nozzles spacing of 3,2 m.

Table 13. The suggested choice of automatic sprinklers and nozzles for the benchmark fire suppression tests.

Ceiling height (m)	Type of system	Water discharge density (mm/min)	Spacing (m × m)	Coverage area (m <sup>2</sup> )	Water flow rate per sprinkler or nozzle (l/min)	Selected K-factor ((l/min)/√bar)	Operating pressure (bar)	Temp. rating (°C)	RTI-rating
≤ 2,5 m	Dry-pipe	6,5	3,2 × 3,2	10,24	66,6	80,6	0,68	68	Standard response
	Deluge	5			51,2	43,2	1,40	Open	Open
> 2,5 m - ≤ 6,5 m	Dry-pipe	15			153,6	161,4	0,91	141	Standard response
	Deluge	10			102,4	80,6	1,61	Open	Open
> 6,5 m - ≤ 10 m	Dry-pipe	20			204,8	242	0,72	141	Standard response
	Deluge	15			143,6	103,7	2,19	Open	Open

For the benchmark fire suppression tests described here, automatic sprinklers and nozzles per the fire two rows of the table was chosen. As previously mentioned, no benchmark tests were conducted at ceilings heights in excess of 5,0 m.

## 14 Benchmark fire suppression tests

Main author of the chapter: Magnus Arvidson, RISE.

### 14.1 General

This section describes the large-scale benchmark fire suppression tests that were conducted in May 2022 at RISE in Borås, Sweden. The tests focused on the two system types, as per the discussion in the previous section of the report:

- An automatic dry-pipe sprinkler system.
- A manual / automatic deluge water spray system.

The tests were conducted inside the large fire test hall at RISE. The test hall has a floor area of 400 m<sup>2</sup> and a corresponding volume of 6 000 m<sup>3</sup>. The facility is equipped with a ventilation system with air inlets through gratings at the floor, along the sides of the long side walls. The outlets are positioned at the top of the ceiling of the test hall.

The tests were conducted at two ceiling heights:

- A 2,5 m ceiling height.
- A 3,7 m ceiling height. However, as the overall height of the freight truck was reduced, the height simulated an actual 5,0 m high ceiling. Refer to the discussion below.

### 14.2 The suspended ceiling

The tests were conducted under a flat, smooth, suspended ceiling measuring 10,2 m (L) by 10,4 m (W), i.e., 106 m<sup>2</sup>, installed to provide the desired ceiling heights. The ceiling is constructed from non-combustible 12 mm thick PromatectT<sup>®</sup> boards in a metal frame construction. The whole area of the underside of ceiling was protected by nominally 20 mm fire insulation and the area of the ceiling directly above the fire was protected with an additional layer or nominally 20 mm fire insulation. Figures 31 and 32, respectively, shows the suspended ceiling during the preparation work prior the tests. For the tests using the passenger car mock-up, the ceiling height as measured from the floor was 2,5 m.



Figure 31. The suspended ceiling during the preparation work for the tests using the passenger car mock-up. The ceiling height was 2,5 m. The pipe-work has been prepared for the deluge system tests (pendent nozzles). Photo: RISE.



For the tests using the freight truck trailer mock-up, the ceiling height as measured from the floor was 3,7 m. The overall height of the freight truck trailer mock-up was 2,7 m and not 4 m typical for a freight truck trailer. These measures did thereby result in a clearance as measured from the top of the mock-up to the ceiling of 1,0 m, which would be realistic for a 5 m high ceiling with full-height trailers. The reason for reducing the overall height of the mock-up and the associated ceiling height was for practicability.



Figure 32. The suspended ceiling when installed for the tests using the freight truck trailer mock-up. The ceiling height was 3,7 m. With the reduced height of the mock-up, this resulted in a realistic clearance corresponding to a full-height freight truck trailer and a ceiling height of 5 m. The pipe-work has been prepared for the automatic sprinkler system tests (upright sprinklers). Photo: RISE.

## 14.3 The system pipe-work, the sprinklers, and the nozzles

### 14.3.1 System layout

The pipe-work consisted of DN40 (1 ½") branch lines connected to a DN50 (2") distribution pipe that was connected via a water flow meter to the water pump of the fire test hall. The water pump is equipped with a frequency control such that the flow rate and pressure can be adjusted during a test.

The branch lines and the associated connections for the sprinklers and the nozzles were arranged such that no modifications to the pipework were required whether the fire test source was positioned between four sprinklers or nozzles or directly below one sprinkler or nozzle. Each of the branch lines had a ball valve to include or exclude it in a test. Thereby, the position of the fire test scenario mock-up was allowed to be directly under the midpoint of the suspended ceiling in all tests.

For the tests where the fire test scenario was between four sprinklers or nozzles, a total of eight sprinklers or nozzles were included in the test. For the tests where the fire test scenario was directly below a sprinkler or nozzle, a total of nine sprinklers or nozzles were included in the test. Irrespective

of the position of the fire test scenario, a sprinkler or nozzle spacing of 3,2 m by 3,2 m was utilized. The reason for limiting the number of nozzles in the tests was due to the water flow rate capacity of the water pump and the capacity of the water treatment equipment.

#### 14.3.2 The automatic sprinklers and water spray nozzles

The tests using automatic sprinklers were conducted with upright, standard coverage sprinklers having glass bulbs with standard response characteristics, i.e., the glass bulbs had a 5 mm diameter. For the tests utilizing the passenger car mock-up, the sprinklers had a nominal operating temperature of 68 °C and a K-factor of 80,6 (l/min)/√bar.

For the tests utilizing the freight truck trailer mock-up, the sprinklers had a nominal operating temperature of 141 °C and a K-factor of 161,4 (l/min)/√bar. Figure 33 shows the two types of sprinklers.

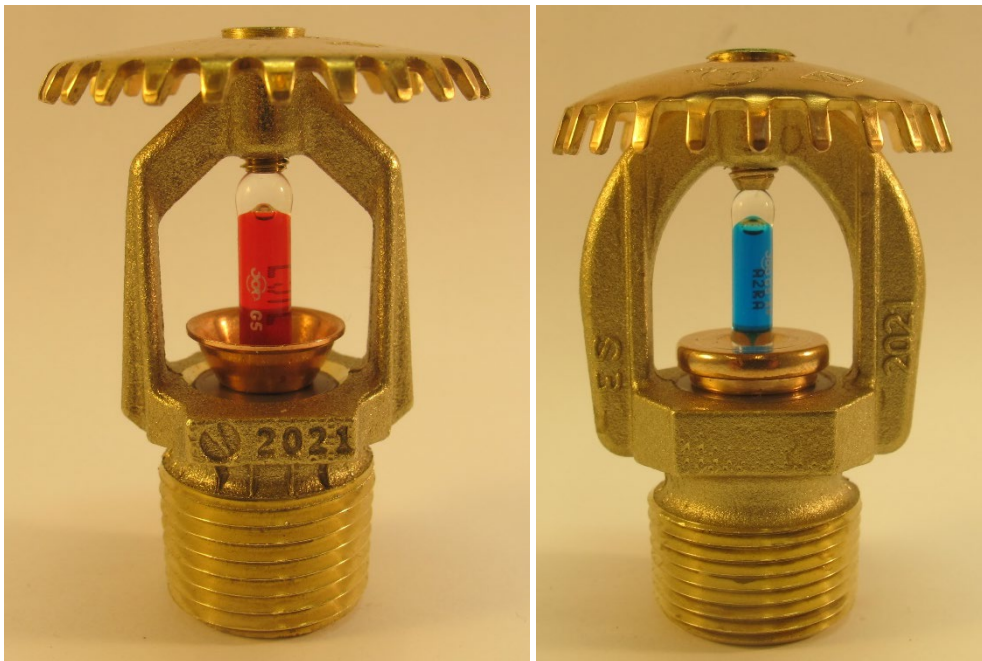


Figure 33. The automatic sprinklers used in the tests: Upright, standard coverage, standard response sprinklers with a nominal operating temperature of 68 °C and a K-factor of 80,6 (l/min)/√bar (left) and a nominal operating temperature of 141 °C and a K-factor of 161,4 (l/min)/√bar (right). The sprinklers had 5 mm diameter glass bulbs. Photos: RISE.

When installed, the plane of the sprinkler frame arms was parallel to the branch lines of the pipe-work. The vertical distance from the deflector of the individual sprinklers and the ceiling was 150 mm, as measured at the ceiling area directly above the fire (with a total of 40 mm fire insulation). Figure 34 shows the installation of an automatic sprinkler relative to the ceiling and the discharge pattern.



Figure 34. An automatic sprinklers as depicted prior Test 5 (left) and a close-up of its discharge pattern (right).  
Photos: RISE.

The nozzles used in the deluge system tests were open (non-automatic), pendent directional discharge water spray nozzles and the K-factor and operating pressure was adopted for the ceiling height.

For the tests utilizing the passenger car mock-up, the nozzles had a K-factor of 43,2 (l/min)/√bar. For the tests utilizing the freight truck trailer mock-up, the nozzles had a K-factor of 80,6 (l/min)/√bar.

The nozzles had an external deflector that discharged a uniformly filled cone of medium-velocity water droplets. The nozzles used in the tests had no nozzle strainer. The recommended discharge pressures range from 1,4 bar to 4,1 bar, which was met in the tests. Discharge pressures in excess of 4,1 bar will result in a decrease in coverage area since the spray pattern tends to draw inwards at higher pressures. The maximum recommended working pressure is 12,1 bar.

As the water spray nozzles were pendent, the system branch lines were rotated, and height adjusted such that the deflector was vertically 150 mm above the underside of the ceiling. The nozzles were installed with their frame arms parallel with branch lines. Figure 35 shows the installation of a water spray nozzle relative to the ceiling and the discharge pattern.



Figure 35. A water spray nozzle as depicted prior Test 1 (left) and the discharge pattern of several nozzles (right).  
Photos: RISE.

## 14.4 The fire test scenarios

### 14.4.1 Passenger car fire test scenario

The passenger car fire test scenario consisted of 36 standard EUR wood pallets arranged in an array that was 2 pallet (wide) × 6 pallets (high) × 3 pallets (long). Each stack was separated 150 mm in the length direction but abutted together in the transversal direction. The wood pallets were placed on a horizontal platform that was sized 4000 mm (L) by 2000 mm (W) and positioned 200 mm above the floor. The platform was covered with one layer of nominally 20 mm thick fire insulation boards.



Part of the array was shielded from direct application of water from overhead sprinklers or nozzles by a horizontal steel sheet plate, simulating the roof of a car. This roof was sized 2075 mm (L) by 1600 mm (W). The width of the roof correlated with the width of the array of wood pallets. Lengthwise, the roof covered half of the length of the array. The top of the roof was 2000 mm above the floor.

Parts of the long sides had vertical sheets made from nominally 20 mm thick fire insulation boards. These sheets simulated the sides of a car, and their overall size was 2400 m (L) by 1200 mm (W). They extended symmetrically along the length of the roof.

Figures 36 through 38 shows the mock-up.



Figure 36. The passenger car mock-up depicted from the front. Photo: RISE.





Figure 37. The passenger car mock-up depicted from the back. Photo: RISE.



Figure 38. The roof over the passenger car mock-up depicted from the back. Photo: RISE.

The fire was initiated using a fire tray sized 1200 mm (L) by 150 mm (W) by 150 mm (H) filled with 20 mm (3,6 litres ) of heptane on a 50 mm water bead (9 litres) that was ignited by a torch.



The fire tray was symmetrically positioned between the first and second rows (from the front) of idle wood pallet stacks, i.e., at the border between the exposed and shielded front part of the array.

#### 14.4.2 Freight truck trailer fire test scenario

The freight truck trailer fire test scenario consisted of 112 standard EUR wood pallets arranged in an array that was 2 pallets (wide)  $\times$  14 pallets (high)  $\times$  4 pallets (long). The wood pallets were placed on a horizontal platform that was sized 3800 mm (L) by 2600 mm (W) and positioned 200 mm above the floor. The platform was covered with one layer of nominally 20 mm thick fire insulation boards.

The back half of the array was shielded from direct application of water from overhead sprinklers or nozzles by a horizontal steel sheet plate, sized 2600 mm (W) by 1900 mm (L). The front half of the array was fully exposed to the water sprays. The edge of the steel plate was along the centerline between two rows of wood pallets. Figures 39 and 40, respectively, shows the mock-up.



Figure 39. The freight truck trailer mock-up depicted from the front. Photo: RISE.



Figure 40. The freight truck trailer mock-up depicted from the back. Photo: RISE.

The fire tray described above was positioned symmetrically between the second and third rows of idle wood pallet stacks, i.e., at the mid-point of the array and thereby at the border between the exposed and shielded part of the array.

## 14.5 Instrumentation and measurements

### 14.5.1 General

All measurements were connected to a data acquisition system and a data logger. The measurements data was recorded at a rate of one scan per second.

### 14.5.2 The measurement of ceiling gas temperatures above the fire

A total of five sheathed thermocouples ( $\varnothing=1$  mm) were used to measure ceiling gas temperatures. One thermocouple (C1) was positioned directly above the point of fire ignition and four additional (C2 through C5) thermocouples were positioned at a 1,5 m radius. The thermocouples were installed 75 mm below the ceiling.

### 14.5.3 The ceiling gas temperatures at the simulated heat detectors

A total of two (C6 and C7) sheathed thermocouples ( $\varnothing=0,5$  mm) were positioned at a radius of 4,5 m from the point of fire ignition to mimic a spot-type fire heat detector. This distance is the maximum horizontal heat detector distance from the fire allowed by the requirements in MSC.1/Circ.1430/Rev.2. The thermocouples were installed 75 mm below the ceiling. These thermocouples were used to determine a realistic activation time of a heat detection system.

### 14.5.4 Surface temperature measurements on steel sheet screens

The surface temperatures at selected locations of the steel sheet screens positioned to the sides of the fire test scenario mock-ups were measured. The steel sheet had a nominal thickness of 1 mm and wire thermocouples ( $\varnothing=0,5$  mm) were spot-welded to the back side of the screens. Each screen had a



600 mm horizontal overhang to be prevent direct wetting of its backside by the sprinklers and nozzles at the ceiling.

For the passenger car fire test scenario, steel sheet screens were positioned at the long sides, respectively, of the mock-up. The horizontal distance to the side of the mock-up was 500 mm. Figure 41 shows the arrangement.



Figure 41. The steel sheet screens along the long sides of the passenger car mock-up. Photo: RISE.

For practical reasons, each long side had three screens abutted together. Each screen was sized 1350 mm (L) by 1800 mm (H) and the bottom part was 200 mm above floor, providing an overall height of 2000 mm. The overall length of 4050 mm covered the entire long side of the mock-up. Each screen had a column of three thermocouples, which were facing the vertical centerline of each of the stacks of idle wood pallets. Table 14 shows the measurement positions and the associated measurement channels.

Table 14. The measurement positions and the associated measurement channels on the steel sheet screens in the passenger car fire scenario. In total, six steel sheet screens were used.

Position	Steel sheet screen	Position of thermocouple	Channel
Right-hand side	1: At the front	Top	C8
		Middle	C9
		Bottom	C10
	2: In the middle	Top	C11
		Middle	C12
		Bottom	C13
	3: At the rear	Top	C14
		Middle	C15
		Bottom	C16
	4: At the front	Top	C17
		Middle	C18

Position	Steel sheet screen	Position of thermocouple	Channel
Left-hand side	5: In the middle	Bottom	C19
		Top	C20
		Middle	C21
		Bottom	C22
	6: At the rear	Top	C23
		Middle	C24
		Bottom	C25

For the freight truck trailer fire test scenario, steel sheet screens were positioned such that they were along the long sides (i.e., right, and left) and at the rear end, respectively, of the mock-up. The horizontal distance to the side of the mock-up was 500 mm. Each long side had two screens abutted together, each sized 1825 mm (L) by 2700 mm (H). The overall length of 3650 mm covered the entire long side of the mock-up. Figure 42 shows the arrangement.



Figure 42. The steel sheet screens facing left hand side of the freight truck trailer mock-up. Similar screens faced the right hand side. Photo: RISE.

Each screen had three columns of thermocouples, which were facing the vertical centerline of each of the stacks of idle wood pallets. Table 15 shows the measurement positions and the associated measurement channels.

Table 15. The measurement positions and the associated measurement channels on the steel sheet screens (long sides) in the freight truck trailer fire scenario. In total, four steel sheet screens were used at the long sides.

Position	Steel sheet screen	Column with thermocouples	Position of thermocouple	Channel
	1: At the front	First column	Top	C8
			Middle	C9
			Bottom	C10
		Second column	Top	C11
			Middle	C12

Position	Steel sheet screen	Column with thermocouples	Position of thermocouple	Channel
Right hand long side		Third column	Bottom	C13
			Top	C14
			Middle	C15
			Bottom	C16
	2: At the rear	First column	Top	C17
			Middle	C18
			Bottom	C19
		Second column	Top	C20
			Middle	C21
			Bottom	C22
		Third column	Top	C23
			Middle	C24
			Bottom	C25
Left hand long side	3: At the front	First column	Top	C26
			Middle	C27
			Bottom	C28
		Second column	Top	C29
			Middle	C30
			Bottom	C31
		Third column	Top	C32
			Middle	C33
			Bottom	C34
	4: At the rear	First column	Top	C35
			Middle	C36
			Bottom	C37
		Second column	Top	C38
			Middle	C39
			Bottom	C40
		Third column	Top	C41
			Middle	C42
			Bottom	C43

The back side had one screen sized 2400 mm (L) by 2700 mm (H) that was positioned 500 mm from the rear end of the mock-up. The overall length covered the entire short side of the mock-up. The screen had three columns of three thermocouples with a symmetrical arrangement of thermocouples over the surface. Figure 43 shows the arrangement.





Figure 43. The steel sheet screen facing the rear end of the freight truck trailer mock-up. Photo: RISE.

Table 16 shows the measurement positions and the associated measurement channels.

Table 16. The measurement positions and the associated measurement channels on the steel sheet screens positioned at the back, short-end of the mock-up in the freight truck trailer fire scenario.

Position	Column with thermocouples	Position of thermocouple	Channel
At the rear end of the mock-up	First column (facing the left-hand side of the array)	Top	C53
		Middle	C54
		Bottom	C55
	Second column	Top	C56
		Middle	C57
		Bottom	C58
	Third column	Top	C59
		Middle	C60
		Bottom	C61

#### 14.5.5 Measurements of system operating pressure and water flow rates

The system operating pressure was measured using a pressure transducer positioned at one of the centermost system branch lines. The pressure transducer was positioned at the end of the pipe, i.e., there was a minimal static pressure difference between the sprinklers or nozzles and the transducer. The water flow rate was measured using a flow meter installed after the water pump unit.

#### 14.6 Fire procedures

The fire test procedures previously discussed in the report was applied.

## 15 Observations during the benchmark fire suppression tests

Main author of the chapter: Magnus Arvidson, RISE.

### 15.1 The fire test program

Table 17 shows the tests in the order that they were conducted and the primary test conditions. The sequence of tests was chosen to limit the amount work needed to prepare a test. Except for changing the ceiling height associated with the fire test scenario, the main task was the rotation of the system branch lines, as the deluge system tests were conducted with pendent water spray nozzles and the dry-pipe system tests with upright automatic sprinklers.

Table 17. The fire test program.

Test	Ceiling height [m]	Type of system	Discharge density [mm/min]	Temperature rating of sprinkler [°C]	RTI-rating of sprinkler	Point of fire ignition
1	2,5	Deluge	5	-	-	Under one nozzle
2						Btw four nozzles
3		Dry-pipe	6,5	68	Standard response	Under one sprinkler
4						Btw four sprinklers
4b						
7	"5"	Dry-pipe	15	141	Standard response	Btw four sprinklers
8						Under one sprinkler
5		Deluge	10	-	-	Under one nozzle
6						Btw four nozzles

The fire test observations are summarized below:

### 15.2 Test 1

The first test was conducted with a deluge system, with the point of fire ignition directly under one open water spray nozzle. The ceiling height was 2,5 m.

The 78 °C temperature threshold was exceeded at channel C6 at 01:02 [min:s] and at channel C7 at 01:26 [min:s]. Water was initiated at 02:20 [min:s], and full system pressure was achieved shortly thereafter, which resulted in a water delivery time of almost 60 s.

Visually, the fire continued to grow after the start of the application of water, as the stacks of idle wood pallets were partly shielded by the roof. However, the fire did not grow very large as the application of water prevented fire spread to the parts outside of the roof. The fact that a line of water spray (on three different branch lines) passed over the longitudinal centerline of the passenger car mock-up improved the application of water over the exposed part of the stacks of idle wood pallets. Water was applied for 30 min. Figures 44 through 47 shows the test.

The test was conducted on May 9, 2022.

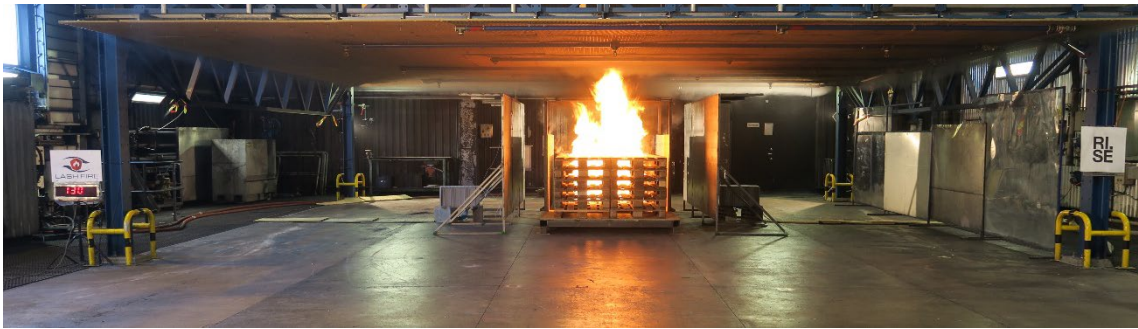


Figure 44. **Test 1:** The fire size at 01:30 [min:s], soon after both thermocouples at a 4,5 m radius from the fire had exceeded the 78 °C temperature threshold. Photo: RISE.



Figure 45. **Test 1:** The fire size at 02:30 [min:s], shortly after the start of the application of water. Photo: RISE.



Figure 46. **Test 1:** The fire size at 08:01 [min:s], at the time the ceiling gas temperatures were the lowest. Photo: RISE.



Figure 47. **Test 1:** The fire size at 14:01 [min:s], after which it started to decline. Photo: RISE.

### 15.3 Test 2

The second test was conducted with a deluge system, with the point of fire ignition between four open water spray nozzles. The ceiling height was 2,5 m. The 78 °C temperature threshold was exceeded at channel C6 at 01:26 [min:s] and at channel C7 at 01:27 [min:s]. Water was initiated at



02:22 [min:s], and full system pressure was achieved shortly thereafter, which resulted in a water delivery time of about 60 s. Water was applied for 30 min. Figures 48 through 51 shows the test.



Figure 48. **Test 2:** The fire size at 01:30 [min:s], soon after both thermocouples at a 4,5 m radius from the fire had exceeded the 78 °C temperature threshold. Photo: RISE.



Figure 49. **Test 2:** The fire size at 02:30 [min:s], shortly after the start of the application of water. Photo: RISE.



Figure 50. **Test 2:** The fire size at 14:00 [min:s], when it reached its peak according to the ceiling gas temperature measurements. Photo: RISE.



Figure 51. **Test 2:** The fire size at 20:01 [min:s], during the stage of decline. Photo: RISE.

The test was conducted on May 9, 2022.

### 15.4 Test 3

This third test was conducted with an automatic sprinkler system, with the point of fire ignition directly under one sprinkler. The ceiling height was 2,5 m.

The first sprinkler activated, as determined by the air pressure loss, at 01:08 [min:s]. Water was initiated at 02:05 [min:s], and full system pressure was achieved shortly thereafter, which resulted in a water delivery time of about 60 s. A second sprinkler activated at 02:45 [min:s] and the last (third) sprinkler at 03:55 [min:s]. In total, three sprinklers activated which provided for a constant water flow rate of 205 l/min, as compared to the nominal water flow rate of 200 l/min. Water was applied for 30 min. Figures 52 through 55 shows the test.

The test was conducted on May 10, 2022.



Figure 52. **Test 3:** The fire at 02:10 [min:s], shortly after water was discharging from the single automatic sprinkler that had activated prior water was allowed to entering the pipe-work. Photo: RISE.



Figure 53. **Test 3:** The fire at 04:00 [min:s], when all three activated sprinklers were flowing. Photo: RISE.



Figure 54. **Test 3:** The fire at 07:00 [min:s], when it started to decline. Photo: RISE.





Figure 55. **Test 3:** The fire size at 20:01 [min:s], during the final stage of decline. Photo: RISE.

## 15.5 Test 4

The fourth test was conducted with an automatic sprinkler system, with the point of fire ignition between four sprinklers. The ceiling height was 2,5 m.

The first sprinkler activated, as determined by the air pressure loss, at 02:18 [min:s]. Water was initiated at 03:20 [min:s], and full system pressure was achieved shortly thereafter, which resulted in a water delivery time of about 60 s. In total, six sprinklers activated, which provided for a constant water flow rate of 398 l/min, as compared to the nominal water flow rate of 400 l/min. Water was applied until about 12:00 [min:s], as the fire was fully extinguished. Figures 56 through 59 shows the test.

The test was conducted on May 10, 2022.



Figure 56. **Test 4:** The fire at 02:20 [min:s], shortly after the air pressure drop of the sprinkler piping indicated that the first sprinkler(s) had activated. Photo: RISE.



Figure 57. **Test 4:** The fire at 03:20 [min:s], when water started to flow from the sprinklers that had activated. Photo: RISE.





Figure 58. **Test 4:** The fire at 05:00 [min:s]. Photo: RISE.



Figure 59. **Test 4:** The fire at 06:30 [min:s]. Only small flames appear at the centre core of the wood pallet array. Photo: RISE.

## 15.6 Test 4b

This test included a slight alteration of the fire test set-up. Two fire trays sized 600 mm by 600 mm by 80 mm (H) were positioned under the passenger car mock-up. Each tray was filled with 14 l of heptane on a small bead of water. The intent was to mimic a fuel spill fire. The fire tray between the stacks of idle wood pallets were ignited first and immediately thereafter the two fire trays below the mock-up.

The fire sprinkler system was similar to that used in Test 4, i.e., an automatic sprinkler system, with the point of fire ignition between four sprinklers.

The first sprinkler activated, as determined by the air pressure loss, at 02:30 [min:s]. Water was initiated at 03:28 [min:s], and full system pressure was achieved shortly thereafter, which resulted in a water delivery time of about 60 s. In total, six sprinklers activated, which provided for a constant water flow rate of 401 l/min, as compared to the nominal water flow rate of 400 l/min.

The fire in the idle wood pallets was extinguished, but the fire in the trays below the mock-up continued to burn. It was observed that the pool fire was not very severe as it was limited by the small free height under the mock-up. In order to modify the fire scenario to include a spill fire underneath the passenger car mock-up, it is concluded that the free height need to be higher. In any case, Test 4b provides a possibility to compare the repeatability of the fire test scenario, comparing Test 4 and Test 4b. Water was applied for 30 min. Figures 60 through 63 shows the test.

The test was conducted on May 11, 2022.



Figure 60. **Test 4b:** The fire at 02:28 [min:s], shortly before the air pressure drop of the sprinkler piping indicated that the first sprinkler(s) had activated. Photo: RISE.



Figure 61. **Test 4b:** The fire at 03:28 [min:s], when water started to flow from the sprinklers that had activated. Photo: RISE.



Figure 62. **Test 4b:** The fire at 04:58 [min:s]. The fire is clearly suppressed. Photo: RISE.



Figure 63. **Test 4b:** The fire at 06:28 [min:s]. Only small flames appear at the centre core of the wood pallet array. Photo: RISE.

## 15.7 Test 7

This test was conducted with an automatic sprinkler system, with the point of fire ignition between four sprinklers, using the freight truck trailer scenario. One of the sprinklers at the front branch line



was plugged, as full system flow rate was not achieved with eight flowing sprinklers. The ceiling height reflected a 5 m actual height.

The first sprinkler activated, as determined by the air pressure loss, at 02:32 [min:s]. Water was initiated at 03:36 [min:s], and full system pressure was achieved shortly thereafter, which resulted in a water delivery time of about 65 s. It seemed that all seven sprinklers had activated at the time water entered the pipe-work. The mean water flow rate during the test was 1 025 l/min, which was slightly lower than the desired 1 075 l/min, and corresponded to a discharge density of 14,3 mm/min.

The test was terminated 25:10 [min:s] using fire hoses and the application of water from the sprinkler system was stopped at 26:25 [min:s]. The reason was the smoke filled the control room and parts of the building. Afterwards, it was determined that the reason was a malfunctioning of an air supply fan. In total, all seven sprinklers activated. Figures 64 through 70 shows the test.

The test was conducted on May 12, 2022.



Figure 64. **Test 7:** The fire at 02:30 [min:s], shortly before the air pressure drop of the sprinkler piping indicated that the first sprinkler(s) had activated. Photo: RISE.



Figure 65. **Test 7:** The fire at 03:40 [min:s], shortly after water started to flow from the sprinklers that had activated. Photo: RISE.



Figure 66. **Test 7:** The fire at 05:00 [min:s]. The fire was initially suppressed. Photo: RISE.



Figure 67. **Test 7:** The fire at 10:00 [min:s]. The fire is gradually growing in size when parts of the array that is shielded from the application of water becomes involved in the fire. Photo: RISE.



Figure 68. **Test 7:** The fire at 18:01 [min:s]. The fire is gradually growing in size when parts of the array that is shielded from the application of water becomes involved in the fire. Photo: RISE.



Figure 69. **Test 7:** The fire at 25:01 [min:s], just prior to the termination of the test. Photo: RISE.



Figure 70. **Test 7:** The fire at 25:41 [min:s], during the termination using fire hoses. Photo: RISE.

## 15.8 Test 8

This test was conducted with an automatic sprinkler system, with the point of fire ignition directly below one sprinkler. One sprinkler at the front and back branch line, respectively, was plugged, as full system flow rate was not achieved with eight flowing sprinklers. The ceiling height reflected a 5 m actual height.

The first sprinkler activated, as determined by the air pressure loss, at 01:44 [min:s]. Water was initiated at 02:51 [min:s], and full system pressure was achieved shortly thereafter, which resulted in a water delivery time of about 65 s. During the delay time, three sprinklers had activated. The fourth sprinkler activated at 05:52 [min:s], the fifth sprinkler at 06:21 [min:s] and the final sixth sprinkler at 08:23 [min:s]. The six flowing sprinklers resulted in a flow rate of about 920 l/min which corresponded well to the desired discharge density of 15 mm/min. Figures 71 through 76 shows the test.

The test was conducted on May 13, 2022.





Figure 71. **Test 8:** The fire at 01:50 [min:s], shortly after the air pressure drop of the sprinkler piping indicated that the first sprinkler(s) had activated. Photo: RISE.



Figure 72. **Test 8:** The fire at 03:00 [min:s], shortly after water was discharging from the initial three automatic sprinklers that had activated. Photo: RISE.



Figure 73. **Test 8:** The fire at 06:00 [min:s], shortly after the activation of the fourth automatic sprinkler. Photo: RISE.





Figure 74. **Test 8:** The fire at 08:30 [min:s], shortly after the activation of the sixth (final) automatic sprinkler. Photo: RISE.



Figure 75. **Test 8:** The fire at 21:01 [min:s], as the fire intensity started to decline. Photo: RISE.



Figure 76. **Test 8:** The fire at 27:01 [min:s]. Photo: RISE.

## 15.9 Test 5

This test was conducted with a deluge system, with the point of fire ignition directly under one open water spray nozzle. The ceiling height reflected a 5 m actual height.

The 78 °C temperature threshold was exceeded at channel C7 at 01:23 [min:s] and at channel C6 at 01:26 [min:s]. Water was initiated at 02:24 [min:s], and full system pressure was achieved shortly thereafter, which resulted in a water delivery time of about 60 s.

During the test, a system valve that was supposed to be fully open was partially closed. This reduced the water flow rate from the desired approximate **900 l/min (10 mm/min)**, starting at 06:10 [min:s] and gradually down to below **500 l/min (5 mm/min)**. The reduced water flow rate resulted in a fire re-growth that required the test to be manually terminated using fire hoses. These efforts were started at about 10:00 [min:s]. Figures 77 through 83 shows the test.

The test was conducted on May 17, 2022.

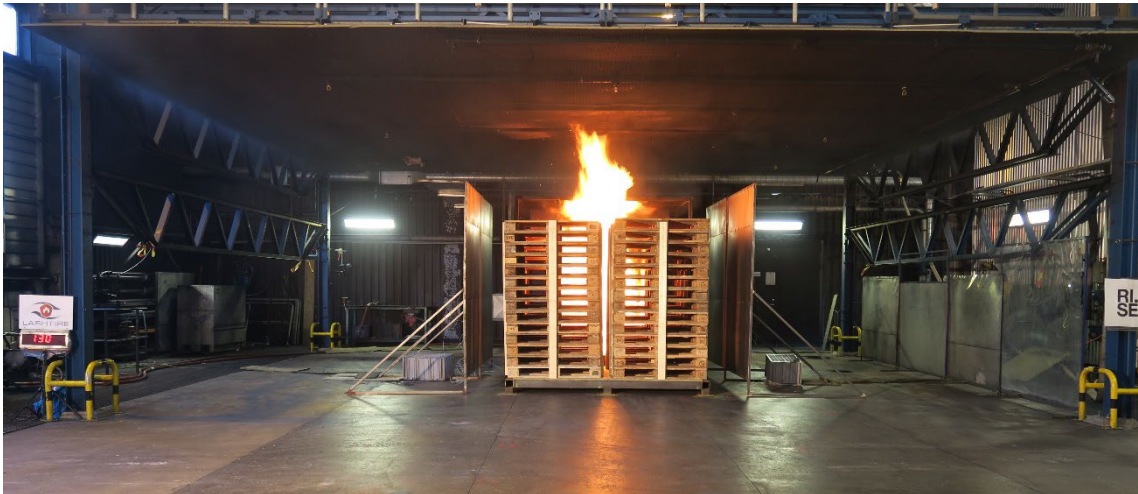


Figure 77. **Test 5:** The fire size at 01:30 [min:s], soon after both thermocouples at a 4,5 m radius from the fire had exceeded the 78 °C temperature threshold. Photo: RISE.



Figure 78. **Test 5:** The fire size at 02:20 [min:s] and 02:30 [min:s], moments before and after the start of the application of water. Photo: RISE.





Figure 79. **Test 5:** The fire size at 06:00 [min:s], when the water flow rate started to become reduced. The measured water flow rate is approximately 920 l/min. Photo: RISE.



Figure 80. **Test 5:** The fire size at 09:00 [min:s]. The measured water flow rate is approximately 490 l/min. Photo: RISE.



Figure 81. **Test 5:** The fire size at 10:40 [min:s], just prior the termination of the test using fire hoses. The measured water flow rate is approximately 480 l/min. Photo: RISE.



Figure 82. **Test 5:** The fire size at 10:50 [min:s], when the test was terminated by applying water from fire hoses. Photo: RISE.



Figure 83. **Test 5:** The fire size documented from a different angle as compared to the photos above but at the same times, 10:40 [min:s] and at 10:40 [min:s], respectively. Photo: RISE.

### 15.10 Test 6

This test was conducted with a deluge system, with the point of fire ignition between four open water spray nozzles. The ceiling height reflected a 5 m actual height.

The 78 °C temperature threshold was exceeded at channel C7 at 01:26 [min:s] and at channel C6 at 01:31 [min:s]. Water was initiated at 02:26 [min:s], and full system pressure was achieved shortly thereafter, which resulted in a water delivery time of about 60 s.

The application of water initially reduced the fire size and the ceiling gas temperatures. But at about 03:10 [min:s] the fire increased in size and the average ceiling gas temperature gradually increased from about 400 °C to about 750 °C at 17:00 [min:s]. Even though it seemed that the ceiling gas temperatures leveled out, the decision was made to terminate the test. At 18:35 [min:s], fire hose streams were applied to the fire to knock it down. Figures 84 through 89 shows the test.

The test was conducted on May 18, 2022.





Figure 84. **Test 6:** The fire size at 01:37 [min:s], soon after both thermocouples at a 4,5 m radius from the fire had exceeded the 78 °C temperature threshold. Photo: RISE.



Figure 85. **Test 6:** The fire size at 02:26 [min:s], shortly after the start of the application of water and a few seconds before full system operating pressure was reached. Photo: RISE.



Figure 86. **Test 6:** The fire size at 03:17 [min:s], at about the time when the fire gradually started to increase in size. Photo: RISE.



Figure 87. **Test 6:** The fire size at 10:07 [min:s], at about the time when the fire gradually started to increase in size. Photo: RISE.



Figure 88. **Test 6:** The fire size at 18:18 [min:s], when the decision was made to terminate the test. Photo: RISE.



Figure 89. **Test 6:** The termination of the test using fire hoses. Photo: RISE.

## 16 Benchmark fire suppression test results

Main author of the chapter: Magnus Arvidson, RISE.

### 16.1 Passenger car scenario

For the deluge system tests using the passenger car mock-up it is observed that the mean ceiling gas temperatures were considerably lower when the point of fire ignition was directly below one nozzle. The same trend is observed for the mean surface temperatures of the target steel sheet plates, although the relative temperature difference was not as large, refer to Figure 90.

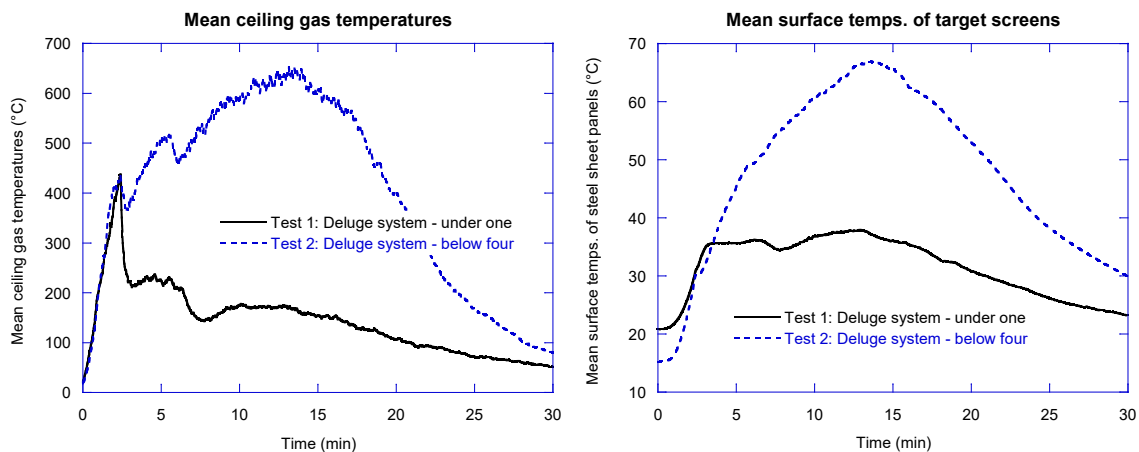


Figure 90. **Tests 1 and 2:** The mean ceiling gas and target steel screen surface temperatures.

For the automatic sprinkler system tests using the passenger car mock-up, the longer delay time (longer distance from the fire plume to the sprinklers) when the point of fire ignition was below four sprinklers as compared to directly under one sprinkler, resulted in higher, initial peak temperatures. However, once the water was flowing, fire suppression performance was better as compared to the scenario when the fire was started directly under one sprinkler. Those trends were captured both with the ceiling gas temperature measurements and the surface temperature measurements on the target steel plates, refer to Figure 91.

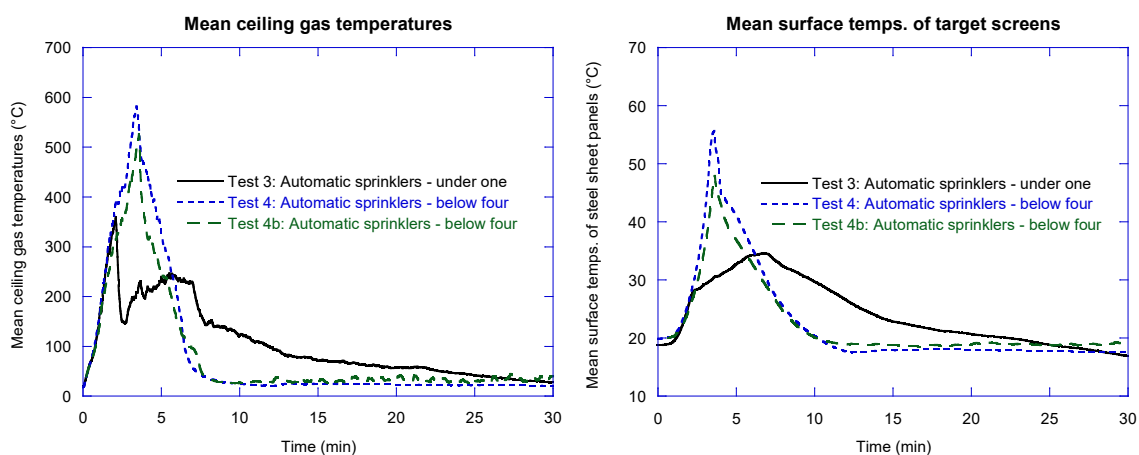


Figure 91. **Tests 3, 4 and 4b:** The mean ceiling gas and target steel screen surface temperatures.

For all five tests discussed above, it is observed that the mean surface temperature of the target steel sheet plates to the right hand side of the mock-up was very similar to those of the target steel sheet plates to the left. This measurement data is not shown here.

## 16.2 Freight truck trailer scenario

For the deluge system tests using the freight truck trailer scenario mock-up, the ceiling gas trends are similar to those of the tests with the passenger car mock-up; the mean ceiling gas temperature was lower when the point of fire ignition was directly below one water spray nozzle. Test 5 had to be terminated as the water flow rate was reduced during the test, so the exact temperature level after the initial fire suppression cannot be determined. The trends of the mean ceiling gas temperatures in the tests are captured by the surface temperature ("grand mean") of all thermocouples on the steel sheet screens. Figure 92 shows the data.

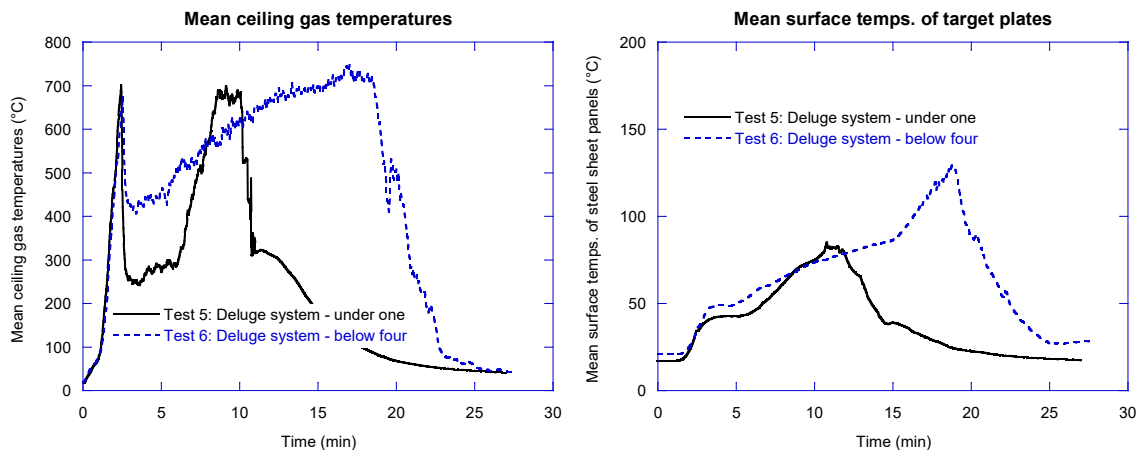


Figure 92. **Tests 5 and 6:** The mean ceiling gas and target steel screen surface temperatures.

Graphs showing the mean surface temperature of the steel sheet screens (right and left hand side, respectively) that were facing the front (exposed) and rear (shielded) parts of the mock-up are shown in Figures 94 and 95, respectively. As expected, the surface temperatures on the screens facing the shielded, rear, part of the mock-up were higher. For both tests, the mean surface temperature was relatively similar on both the right and left hand sides.

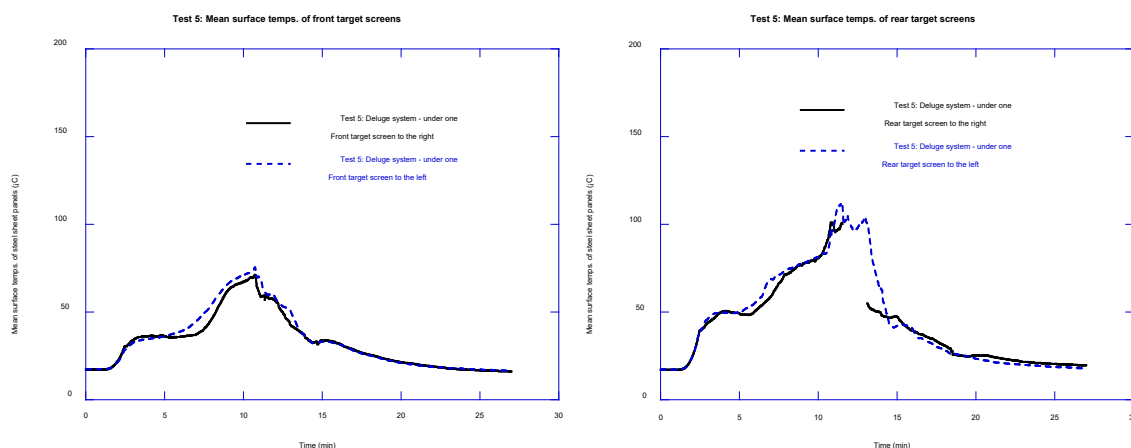


Figure 93. **Tests 5:** The mean target steel screen surface temperatures on the individual target screens.



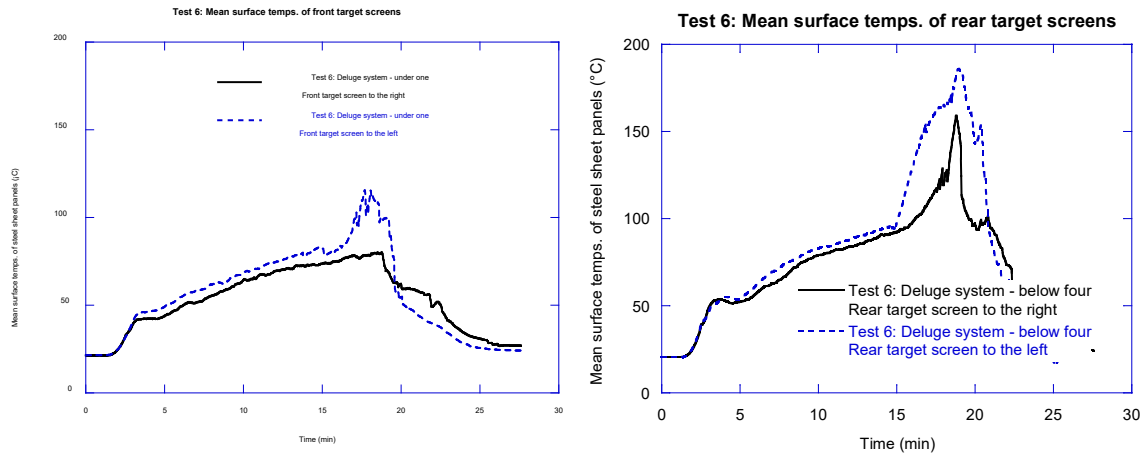


Figure 94. **Tests 6:** The mean target steel screen surface temperatures on the individual target screens.

Figure 95 shows the mean surface temperature on the steel sheet screen directly behind the mock-up for Tests 5 and 6, respectively. The relative temperature difference between the two tests is smaller than indicated by the steel screens facing the long sides of the mock-up.

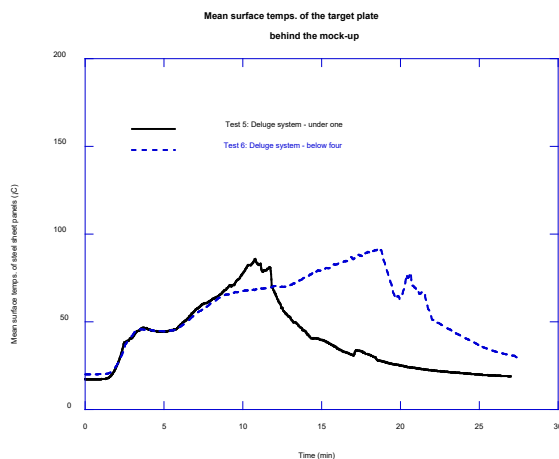


Figure 95. **Tests 5 and 6:** The mean target steel screen surface temperatures on the screen facing the rear end of the mock-up.

For the automatic sprinkler system tests using the freight truck trailer scenario mockup, the longer delay time (longer distance from the fire plume to the sprinklers) when the point of fire ignition was below four sprinklers resulted in higher initial peak temperatures than when the point of fire ignition was directly under one sprinkler. However, once the water was flowing, fire suppression performance was better. This is the same observation as with the tests using the passenger car mockup. The surface temperature (“Grand mean”) of all thermocouples on the steel sheet screens were relatively similar, independent of the position of the point of fire ignition relative to the sprinklers. Figure 96 shows the data.

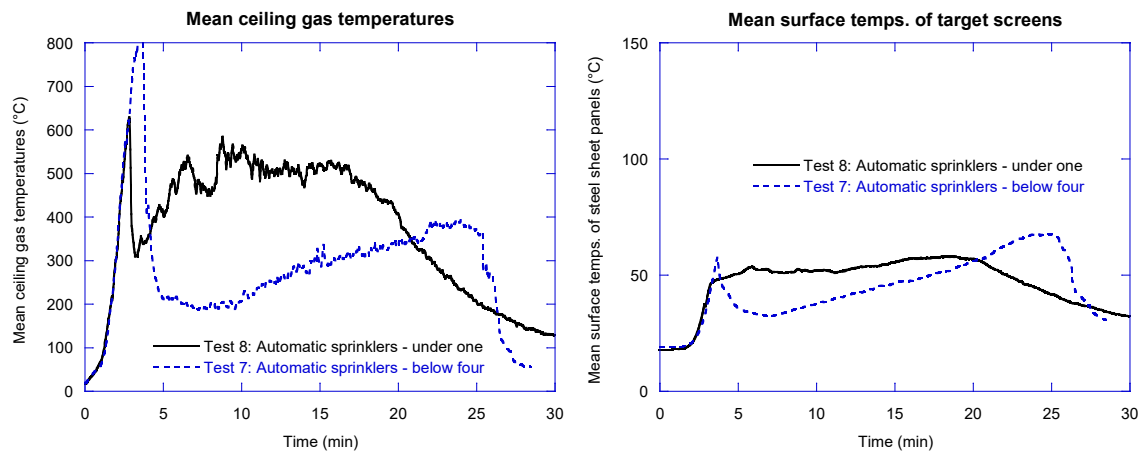


Figure 96. **Tests 7 and 8:** The mean ceiling gas and target steel screen surface temperatures.

Figures 97 and 98, respectively, shows the mean surface temperature of the steel sheet screens (to the right and left hand side, respectively) that were facing the front (exposed) and rear (shielded) parts of the mock-up. As expected, the surface temperatures on the screens facing the shielded part were higher. For both tests, the mean surface temperature is relatively similar on both the right and left hand sides. In Test 7, it is observed that the surface temperatures are gradually increasing during the test, whilst the surface temperatures in Test 8 remains fairly constant.

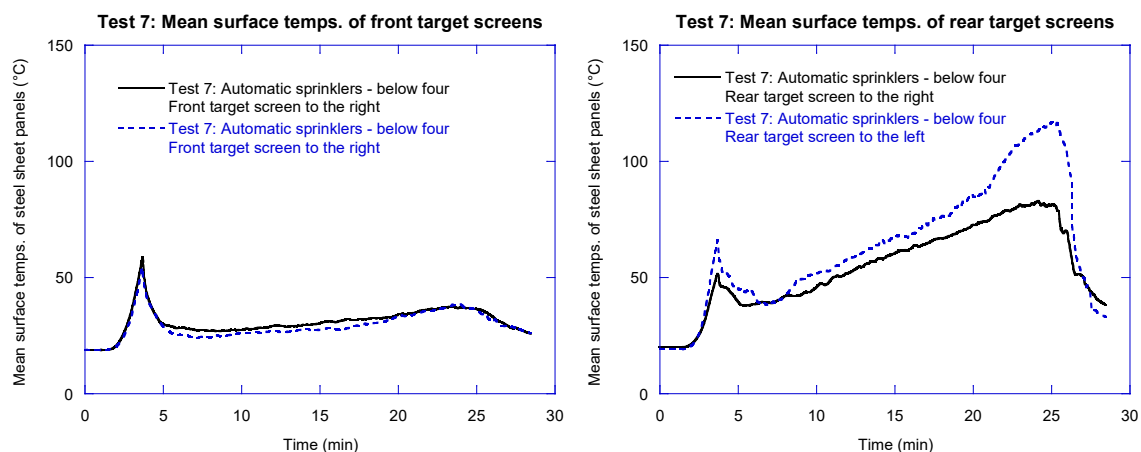


Figure 97. **Tests 7:** The mean target steel screen surface temperatures on the individual target screens.

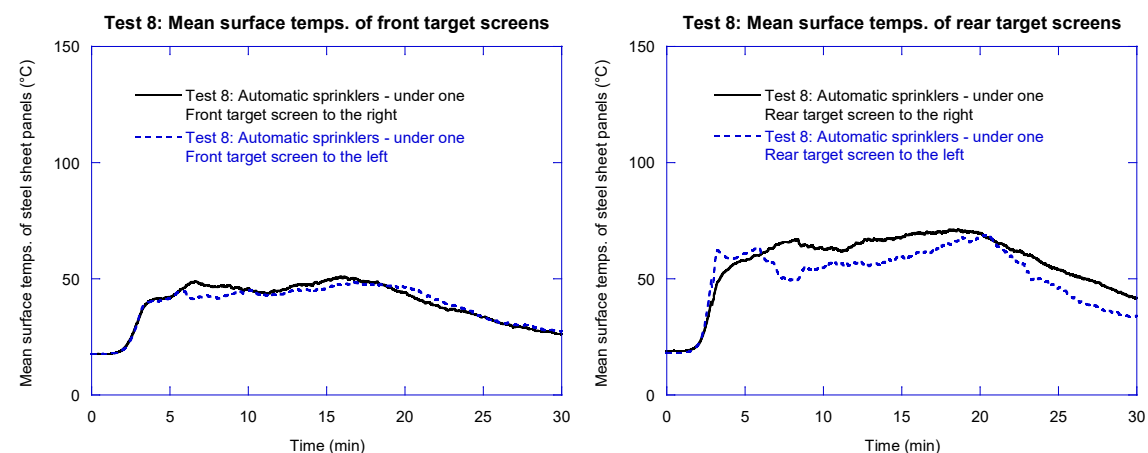


Figure 98. **Tests 8:** The mean target steel screen surface temperatures on the individual target screens.

Figure 99 shows the mean surface temperature on the steel sheet screen directly behind the mock-up for Tests 7 and 8, respectively. The gradual surface temperature increase during Test 7 is observed, however, the temperature difference between Test 7 and Test 8 in absolute terms is relatively small. Based on the peak values, the difference is less than 20 °C.

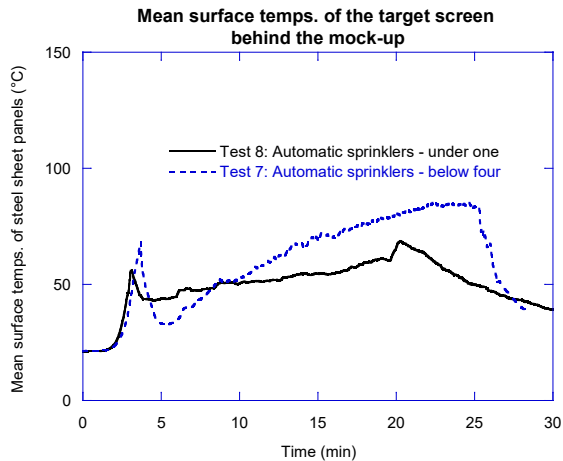


Figure 99. **Tests 7 and 8:** The mean target steel screen surface temperatures on the target screen facing the rear end of the mock-up.

### 16.3 The moisture content of individual wood pallets

Prior to the tests, the moisture content of 10 randomly selected wood pallets was measured with a probe-type moisture meter and documented. Figure 100 shows the measured moisture content of individual pallets prior to each test. The mean value varied from 7,1 % to 14,5 %. The mean value for all wood pallets in the tests was 9,6 %. The pallets had been stored indoors prior the tests, initially in an unheated storage building and thereafter inside the heated fire test hall. It is noted that the mean moisture content in each of the tests is below the 14±2 % required in the current fire test procedures and only a few individual pallets were within this span.

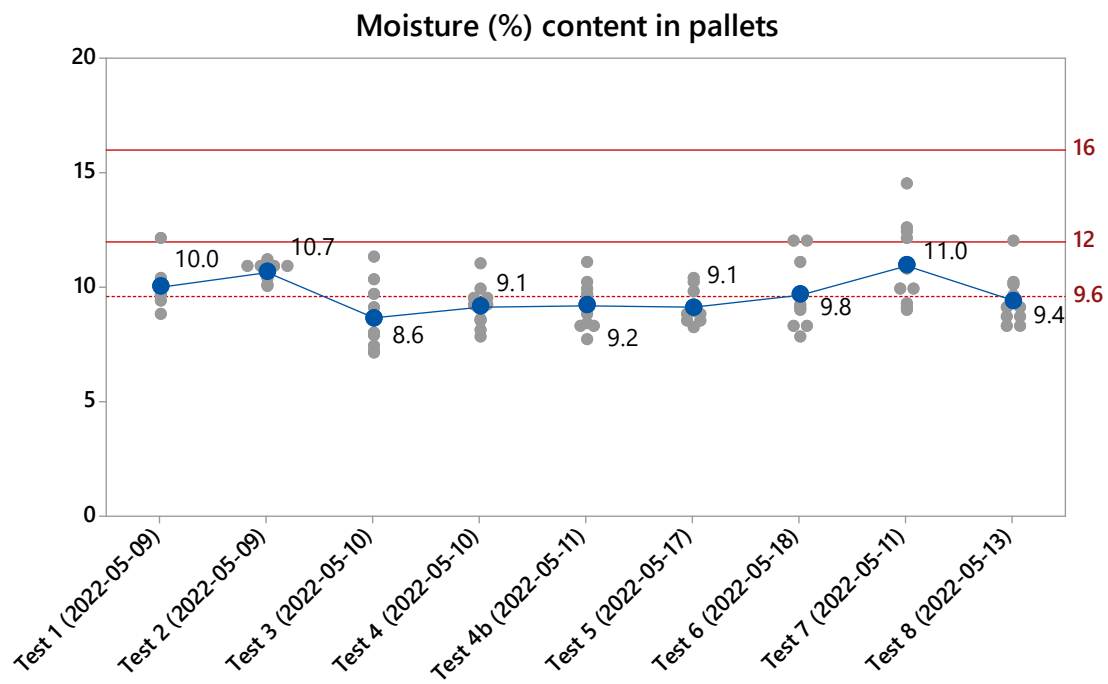


Figure 100. The measured moisture content of randomly selected wood pallets in each of the test.



## 17 Discussion

Main author of the chapter: Magnus Arvidson, RISE.

### 17.1 The objective of the work

MSC.1/Circ.1430 was published on 31 May 2012 and replaced both the prescriptive requirements of Resolution A.123(V) for conventional water spray systems and the performance-based requirements in MSC.1/Circ.1272 for alternative systems. MSC.1/Circ.1430 has undergone two revisions, in 2018 and 2020, but none of the two revisions include any changes to the fire test procedures in the Appendix of MSC.1/Circ.1430. Concerns related to the fire suppression performance of the performance-based option have been raised as the fire test procedures in the Appendix of MSC.1/Circ.1430 set a performance level that is only similar or slightly better than the performance of systems that used to be installed in accordance with Resolution A.123(V).

The overall objective of the work presented here was to establish a harmonized performance level for prescriptive-based and performance-based systems. This was made by re-designing the fire test scenarios such that they reflect the severity in terms of the fire load of modern vehicles and cargo. In a second step, the fire suppression performance of an automatic sprinkler and deluge water spray system was determined in large-scale fire suppression tests.

### 17.2 The conditions in ro-ro spaces, vehicle spaces and special category spaces

These spaces typically extend the full length and width of the ship. Typical structural material used is steel. Further, aluminum alloys can be used as well as alternative materials such as plywood and composite materials. Arrangement of movable (hoistable) car decks is very common on ro-ro passenger ships, usually within one vehicle space above the bulkhead deck. Similar arrangement can also be found on ro-ro cargo ships and vehicle carriers, sometimes with more levels (two or three) of hoistable decks in the same space.

The cargo consists of passenger cars, vans, campers, including APVs, trucks, semi-trailers and trailers, refrigeration/heating units as well as classified goods (IMDG and ADR) and special cargo (non-typical vehicles or units such as roll trailers, excavators, etc.). Vehicles are transported very close to each other, typically at horizontal distance of about 500 mm or less.

### 17.3 Electric vehicle (EV) fire characteristics

This report summarizes small-, intermediate- and large-scale fire tests with lithium-ion batteries and/or electric vehicles and discusses the associated fire characteristics and severity. The literature study of this report indicates that the peak heat release of an electric vehicle fire is comparable to that of a vehicle with an internal combustion engine, given similar sized vehicles.

However, no data in the literature was found relating to the fire suppression performance of automatic sprinkler systems or deluge water spray systems. A series of deluge water spray fire tests were conducted to compare the fire suppression performance of a deluge water spray for fires involving gasoline-powered and battery electric vehicles under as equivalent test conditions as possible. The tests simulated a ro-ro space having a ceiling height of about 5 m and the system design in terms of water discharge densities corresponded to the design recommendations in MSC.1/Circ.1430/Rev.2. The tests indicate that a fire in a battery electric vehicle does not seem to be more challenging than a fire in a gasoline-powered vehicle for the drencher system design given in current international recommendations.

## 17.4 The re-design of the fire test scenarios

The fire test scenarios and the associated fire test mock-ups were re-designed. The designs in the current fire test procedures in the Appendix of MSC.1/Circ.1430/Rev.2 were used as the starting point for the work.

For the passenger car fire test scenario, the intent was to provide a design providing a peak heat release rate in the order of 6 MW. As per the current design, part of the fire was supposed to be shielded from direct application of water from overhead sprinklers or nozzles. The final design consists of an array of 36 pieces of EUR wood pallets, stacked six pallets in height. The low stack height ensures stack stability during a prolonged period of time. This fire load is three times larger than that of the current fire test procedures. The scenario reflects burning of ordinary combustibles and do not include flammable liquid or battery fires. The main differences between vehicles using different energy carriers come from the energy storage (as the battery pack as gas fuel tanks) and delivery system. If the energy storage is not directly involved in the cause of the fire, the early fire growth in cars with different energy carriers will be similar.

For the freight truck trailer fire test scenario, the current number (112 pcs) of pallets were used. However, they were re-arranged in stacks being 14 pallets high instead of the current seven pallet high stacks. Vertical wood supports ensured stack stability. Half of the array is shielded under a roof, similar to the current approach. Even though the total fire load remains unchanged, the re-arrangement of the stacks of pallets will increase the peak heat release rate. Given that all pallets burn simultaneously, the theoretical peak approaches 20 MW.

## 17.5 The re-design of the fire test procedures

The major change relates to the establishment of procedures for testing of dry-pipe and deluge systems, where a delay time is used from the activation of automatic sprinklers in a dry-pipe system. A time delay is also suggested for testing of a deluge system activated by simulated heat detectors prior water discharge. A fixed vertical sprinkler/nozzle-to-ceiling distance is also recommended.

## 17.6 Benchmark fire suppression tests

Regarding the fire test scenarios, the following is concluded:

- The fire growth rate seems very repeatable.
- An attempt was made to use pool fire trays underneath the mock-up, but the vertical distance from the rim of the trays to the underside of the bottom steel plate of the mock-up was too short and the pool fire did not develop. The inclusion of a pool fire scenario underneath the mock-up will require a higher clearance to allow air entering to the pool.
- Based on the ICEV and BEV fire suppression tests (i.e., using actual vehicles), it is suggested that the final design of the passenger car fire test scenario includes one or more fire trays underneath the mock-up. This would add flames projecting from the underneath or from the low sides of the mock-up which will reflect a fire in a flammable liquid fuel spill or a battery pack.
- For some of the freight truck trailer scenario tests, the fire was very severe, which calls for a reduction of the fire load by reducing the idle wood pallet stack heights.

Regarding the measurements, the following is concluded:

- It seems that the use of five (5) ceiling gas thermocouples oriented and positioned as suggested captures system performance well.
- The surface temperature on target steel sheet screens worked well and the measurements captures system performance.

- For the freight truck trailer scenario, it seems sufficient to only measure the surface temperature on target steel sheet screens that are facing the shielded part (with the roof) of long side of the mock-up.
- A steel sheet screen at the back, short side of the mock-up does not seem necessary. The performance of a tested system is captured with target screens at the long sides, as discussed above.

Regarding the performance of the tested systems, the following is concluded:

- For the deluge system tests, the fire suppression performance (as indicated by the ceiling gas temperatures) was better with the point of fire ignition directly under one nozzle as compared to below four nozzles. The cooling of the target steel sheet screens was also better with the point of fire ignition directly under one nozzle.
- The automatic sprinkler activated at a later stage, but the fire suppression performance was better when the point of fire ignition was below four automatic sprinklers as compared to directly under one sprinkler. With upright sprinklers, which is necessitated with a dry-pipe sprinkler system, the discharge density directly below a sprinkler is relatively low which may explain the results. The cooling of the target steel sheet screens was also better with the point of fire ignition below four automatic sprinklers, however, it is likely that the results also are due to the improved fire suppression performance.

Regarding possible acceptance criteria, the following is concluded:

- The performance acceptance criteria need to reflect that the performance of a specific type of sprinkler or nozzle could vary with position of the fire ignition location relative to the sprinklers or nozzles, as observed in these tests. This was specifically noted for the ceiling gas temperatures.
- The relative difference due to the sprinkler/nozzle position based on the mean surface temperatures of the steel sheet target screens was not as large as that based on the ceiling gas temperatures.

### 17.7 The moisture content of the wood pallets

Section 3.2.1 in the Appendix of MSC.1/Circ.1430/Rev.2 says that “The primary fire source for both scenarios consists of EUR standard wood pallets (ISO 6780:2003), stored inside with the moisture content of  $14 \pm 2$  %. Figure 3.2.1 shows details of a EUR pallet.” The requirements do not specify the number of wood pallets included in the measurements, the measurement equipment, if the moisture content limits apply to all tested samples or if it refers to an arithmetic mean value.

The wood pallets used in the benchmark tests had a mean moisture content of 9,6 % (based on all tests), which is significantly lower than these limits. The pallets had been stored indoors prior the tests, initially in an unheated storage building and thereafter inside the heated fire test hall. In other words, the handling of the pallets fulfilled the qualitative requirements but not the quantitative requirements.

Fire test procedures often recommends that the material to be tested or the combustible material that is part of a fire test scenario is conditioned in a controlled environment having a specified temperature and humidity. In this particular case, the magnitude of wood pallets that are required for a series of tests make conditioning under specific environmental conditions unrealistic from a practical perspective.

It is noted that the tests were conducted in May 2022. Wood is a hygroscopic building material, which means that the material can absorb and release water vapor from the surrounding air. The moisture content in wood is constantly adapted to the surrounding climate. When, after a long time, the wood's moisture content has completely adapted to the surrounding climate, it is said to have

reached its equilibrium moisture ratio. The equilibrium humidity ratio is controlled by the relative humidity and the surrounding temperature, with the relative humidity having the greatest influence in the temperature range 0 - 20 °C. As the climate varies throughout the year, the moisture content of wood will also change. Indoors, wood will dry and shrink during the winter months, then absorb moisture and swell again during the summer. The moisture content of wood, both indoors and outdoors, adapts to the relative humidity and temperature of the surroundings. In heated Swedish homes in the central of Sweden, the moisture content in wood throughout the year is on average 7,5 % and it is highest during summer (7 - 12 %) and the lowest during winter (2 - 6 %). On average, it is drier in the north than in the south of Sweden [47].

The concept of target moisture ratio describes the desired average moisture ratio for a lot of wood delivered from a sawmill, refer to EN 14298:2017, Sawn timber – Assessment of drying quality [48]. The sawmills dry the wood to different target moisture ratios depending on what the wood is to be used for. When delivered from the sawmill, the moisture ratio must be adapted either to the further processing or to the environment the product will ultimately be used in. The target moisture ratios of a lot of sawn timber are defined in the standard as well as the permitted variation in moisture ratio between individual pieces of wood in a lot. A lot is defined as a “whole of sawn timber pieces of the same species, same thickness and same specification.”

To comply with a drying specification, measures of the moisture content of a control sample shall satisfy two criteria:

- Criterion 1: The moisture content of each individual piece in a lot shall be between lower and upper limits. In the case of a standard drying, these limits are equal to  $0,7 \times$  target moisture ratio (lower limit) and  $1,3 \times$  target moisture ratio (upper limit). 93,5 % of the pieces of the control sample shall have an individual moisture content between the upper and lower limits.
- Criterion 2: The average moisture content of the controlled pieces taken from the lot shall be within a given range relative to the target moisture content. In the case of a standard drying quality, it is appropriate to refer to Table 1 of the standard.

The number of control samples in a lot that contains between 100 to 150 individual pieces is 20 and the sample size increases with the size of the lot. Some examples of the allowed variation of the average moisture content of a lot and the allowed moisture content of individual pieces within that lot are given in Table 18.

Table 18. Examples of the allowed variation of the average moisture content of a lot and the allowed moisture content of individual pieces within that lot based on the requirements in EN 14298:2017.

Target moisture ratio of a lot (%)	Allowable range of the average moisture content of a lot around the target moisture content (%)			Allowable moisture content of each individual piece (%)	
	Allowed variation (from Table 1 of EN 14298:2017)	Lower limit (%)	Upper limit (%)	Lower limit (%)	Upper limit (%)
8	-1/+1	8,0	9,0	5,6	10,4
10	-1,5/+1,5	8,5	11,5	7,0	13,0
12	-1,5/+1,5	10,5	13,5	8,4	15,6
14	-2,0/+1,5	12,0	15,5	9,8	18,2
16	-2,5/+2,0	13,5	18,0	11,2	20,8

The method for determining the moisture content is crucial. For each of the sampled pieces the moisture content shall be estimated according to EN 13183-2 (Electrical resistance method) or in the case of a dispute, EN 13183-1 (Oven-dry method) shall be used.

EN 13183-2, Moisture content of a piece of sawn timber – Part 2: Estimation by electrical resistance method [49], defines a non-destructive method for estimating the moisture content of a piece of sawn timber using an electrical resistance moisture meter. The standard applies to sawn timber, and



timber which has been planed, or mechanically surfaced by other means. Measurements shall be made with an electrical resistance moisture meter equipped with insulated electrodes, graduated up to 30 % in units of maximum 1 % moisture content. The meter shall be equipped with settings or tables to correct for wood species and temperature. The standard does also specify where and how the measurements shall be undertaken. Because of the strong effects of surface moisture content and possible variations of moisture content in the cross section, insulated electrodes with undamaged insulation should be used.

In conclusion, it is judged that long-term indoor storage of wood pallets would result in a moisture content that is less than the currently required  $14\pm 2$  %, especially when stored in the winter. It is suggested that the requirements related to the moisture content limits of the wood pallets and how the moisture content is determined is evaluated, where reference is given to the standards for sawn timber that was identified.

### 17.8 The next steps

The next step of the process is to formulate revised fire test procedures to replace those in the Appendix of MSC.1/Circ.1430/Rev.2. The design of the fire test scenarios, the fire test procedures and the performance acceptance criteria will be based on the experience and results documented in this report. This is presented in the report D10.5, "Updated test standard for alternative fixed fire-fighting systems".

## 18 References

- 1 "Fire aboard Vehicle Carrier Courage", accident no: DCA15RM024, National Transportation Safety Board Marine Accident Brief, Issued: June 29, 2017
- 2 "Fire on board Vehicle Carrier Honor", accident no: DCA17RM007, National Transportation Safety Board Marine Accident Brief, Issued: March 6, 2017
- 3 "Fire aboard Roll-on/Roll-off Vehicle Carrier Höegh Xiamen, Pier 20, Blount Island Jacksonville, Florida June 4, 2020", National Transportation Safety Board, MAR 21/04, Adopted December 1, 2021
- 4 Marine Investigation Report, "Fire on Vehicle Deck, Roll-On/Roll-Off Passenger Ferry Joseph and Clara Smallwood 8 Nautical Miles South of Port Aux Basques", Newfoundland and Labrador, 12 May 2003, Report Number M03N0050, The Transportation Safety Board of Canada, ISBN 0-662-41768-2, 2005
- 5 "Report on the investigation of the fire on the main vehicle deck of Commodore Clipper while on passage to Portsmouth 16 June 2010", Report No 24/2011, Marine Accident Investigation Branch, November 2011
- 6 "Pearl of Scandinavia Fire 17 November 2010", Marine Accident Report, Division for Investigation of Maritime Accidents, Danish Maritime Accident Investigation Board, Case: 201012794, August 2, 2011
- 7 "Fire on a semi-trailer on board the ferry MECKLENBURG-VORPOMMERN on the Warnow river on 19 November 2010", Summary Investigation Report 515/10, Bundesstelle für Seeunfalluntersuchung – BSU (Federal Bureau of Maritime Casualty Investigation), November 1, 2012
- 8 "Marine Ship Accident Investigation", Final Report, 2/7/2014, No. (E)-Ta-2, Ministry of Transportation of The Republic of Lithuania Marine Ship Accident and Incident Investigation Manager
- 9 URD Fire on 4 March 2014", The Danish Maritime Accident Investigation Board, June 26, 2014
- 10 "Ro-Pax Ferry Stena Spirit truck fire on a car deck at the approach to the port of Gdynia on 31 August 2016", Final Report No. WIM 60/16, State Marine Accident Investigation Commission, August 2017
- 11 "BRITANNIA SEAWAYS, Fire on 16 November 2013", The Danish Maritime Accident Investigation Board, Case number: 2013024446, July 25, 2014
- 12 "Report on the investigation of the fire on the main deck of the ro-ro cargo ferry Corona Seaways in the Kattegat, Scandinavia on 4 December 2013", Casualty Report No 17/2014, Marine Accident Investigation Branch, July 2014
- 13 Resolution A.123(V), "Recommendation on fixed fire extinguishing systems for special category spaces", International Maritime Organization, London, United Kingdom, October 26, 1967
- 14 Friberg, F., Hansen, G., et al, "Extinction of Fire in Ships by Automatic Sprinkler Systems and Fixed Pressure Water-spraying Systems", Denmark, June 1963
- 15 Arvidson, Magnus, Ingason, Haukur and Persson, Henry, "Water Based Fire Protection Systems for Vehicle Decks on Ro-Ro Passenger Ferries, BRANDFORSK Project 421-941", SP Report 1997:03, Swedish National Testing and Research Institute, 1997
- 16 Arvidson, Magnus, "Large Scale Ro-Ro Vehicle Deck Fire Test, NORDTEST Project 1299-96, BRANDFORSK Project 421-941", SP Report 1997:15, Swedish National Testing and Research Institute, 1997

- 17 Video entitled "Large Scale Ro-Ro Vehicle Deck Fire Test, Conducted at SP on the 23rd of May 1997", Swedish National Testing and Research Institute, Borås, 1997
- 18 MSC/Circ. 914, "Guidelines for the approval of alternative fixed water-based fire-fighting systems for special category spaces", June 4, 1999
- 19 Arvidson, Magnus and Torstensson, Håkan, "En förstudie angående vattenbaserade släcksystem för lastutrymmen på fartyg, Brandforsk projekt 511-001", SP Rapport 2002:22 (in Swedish), 2002
- 20 Shipp, M., Annable, K. and Williams, C., "Assessment of the Fire Behaviour of Cargo Loaded on Ro-Ro Vehicle Decks in Relation to the Design Standards for Fire Suppression Systems", BRE Fire and Security, Client report number 227974, November 3, 2006
- 21 FP51/3/2/Rev.1, "Assessment of the fire behaviour of cargo loaded on ro-ro vehicle decks in relation to the design standards for fire extinguishing systems, Submitted by the United Kingdom to IMO Sub-Committee meeting FP51 on Fire Protection, 27 November 2006
- 22 Maccari, Alessandro, "Application of CFD Analysis for Fire Modelling", proceedings from the 2nd international fire on ships conference, London, October 30-31, 2006
- 23 Arvidson, Magnus and Vaari, Jukka (VTT), "A preparatory study of appropriate fire test procedures for sprinkler systems on ro-ro cargo decks", SP Report 2006:02, 2006
- 24 Vaari, Jukka and Ala-Outinen, Tiina, "Performance requirements for fixed water-based fire fighting systems on shipboard vehicle decks", VTT RESEARCH REPORT No. VTT-S-11913-06, 2006
- 25 Annex 6 of FP51/3/1, "The Report of the correspondence group", Submitted by the United States to IMO Sub-Committee meeting FP51 on Fire Protection, 24 October 2006
- 26 MSC.1/Circ. 1272, "Guidelines for the approval of fixed water-based fire-fighting systems for ro-ro spaces and special category spaces equivalent to that referred to in Resolution A.123(V)", June 4, 2008
- 27 Arvidson, Magnus, "Down-scaled fire tests using a trailer mock-up", SP Report 2008:42, ISBN 978-91-85829-58-3, 2008
- 28 Arvidson, Magnus, "Water distribution tests using different water spray nozzles", SP Arbetsrapport 2009:04, 2009
- 29 Arvidson, Magnus, "Large-scale ro-ro deck fire suppression tests", SP Report 2009:29, ISBN 978-91-86319-17-5, 2009
- 30 Arvidson, Magnus, "Sprinkler design guidelines relevant for ro-ro decks", SP Report 2010:33, ISBN 978-91-86319-71-7, 2010
- 31 MSC.1/Circ. 1430, "Revised Guidelines for the Design and Approval of Fixed Water-Based Fire-Fighting Systems for Ro-Ro Spaces and Special Category Spaces", International Maritime Organization, 31 May 2012
- 32 Arvidson, Magnus, "Improved water-based fire suppression systems for ro-ro vehicle decks: The outcome of the IMPRO-project", presentation at Workshop on fires on ro-ro decks, European Maritime Safety Agency, Lisbon, Portugal, 2015
- 33 Larsson Fredrik, "Lithium-ion Battery Safety - Assessment by Abuse Testing, Fluoride Gas Emissions and Fire Propagation", PhD Thesis, ISBN: 978-91-7597-612-9, Chalmers University of Technology, Göteborg, 2017
- 34 Bisschop, Roeland, Willstrand, Ola, Amon, Francine, Rosengren, Max, "Fire Safety of Lithium-Ion Batteries in Road Vehicles", RISE Report 2019:50, RISE Research Institutes of Sweden

- 35 Willstrand, Ola, Bisschop, Roeland and Rosengren, Max, "Fire Suppression Tests for Vehicle Battery Pack", RISE Research Institutes of Sweden, 2019-10-11
- 36 Larsson, Fredrik, Andersson, Petra and Mellander, Bengt-Erik, "Lithium-Ion Battery Aspects on Fires in Electrified Vehicles on the Basis of Experimental Abuse Tests", Batteries 2016, 2, 9
- 37 Austin Ronald Baird, "A Framework for Characterizing the Safety of Li-BESS using Performance Based Code Analysis and Testing", Thesis for the Degree of Master of Science in Engineering, Presented to the Faculty of the Graduate School of The University of Texas, 2019
- 38 Long Jr, R. Thomas, Blum, Andrew F., Bress, Thomas J. and Cotts, Benjamin R.T., "Best Practices for Emergency Response to Incidents Involving Electric Vehicles Battery Hazards: A Report on Full-Scale Testing Results", The Fire Protection Research Foundation, One Batterymarch Park, Quincy, Massachusetts, U.S.A., June 2013
- 39 Lecocq, Amandine, Bertana, Marie, Truchot, Benjamin and Marlair, Guy, "Comparison of the Fire Consequences of an Electric Vehicle and an Internal Combustion Engine Vehicle", International Conference on Fires in Vehicles - FIVE 2012, September 2012, Chicago, United States, pp. 183-194
- 40 Watanabe, N., Sugaw, O., Suwa, T., Ogawa, Y., Hiramatsu, M., Tomonori, H., et al, "Comparison of fire behaviours of an electric-battery-powered vehicle and gasoline-powered vehicle in a real-scale fire test", Second International Conference on Fires in Vehicles, Chicago, 2012
- 41 Lam, C., MacNeil, D., Kroeker, R., Loughheed, G., Lalime, G., "Full-Scale Fire Testing of Electric and Internal Combustion Engine Vehicles", Fourth International Conference on Fire in Vehicle, Baltimore, 2016
- 42 "Single Cell Thermal Runaway Initiation (SCTRI) – Test – (Propagation)", Excerpt from the draft test procedures developed by NHTSA to be shared with GTR, pp. 168-289, National Highway Traffic Safety Administration, year of publication unknown
- 43 Willstrand, Ola, Bisschop, Roeland, Blomqvist, Per, Temple, Alastair and Anderson, Johan, "Toxic Gases from Fire in Electric Vehicles", RISE Report 2020:90
- 44 Arvidson, Magnus, "Down-scaled fire tests using a trailer mock-up", SP Report 2008:42, ISBN 978-91-85829-58-3, ISSN 0284-5172, SP Technical Research Institute of Sweden, Borås 2008
- 45 EN 1991-1-2, "Eurocode 1: Actions on structures - Part 1-2: General actions - Actions on structures exposed to fire", November 2002
- 46 FM Global Property Loss Prevention Data Sheets 2-0, "Installation Guidelines for Automatic Sprinklers", January 2014, Interim Revision January 2018
- 47 "Fuktkvot (Moisture ratio)", <https://www.svenskttra.se/trafakta/allmant-om-tra/tra-och-fukt/> (accessed 2023-01-12)
- 48 EN 14298:2017, "Sawn timber – Assessment of drying quality", Approved: 2017-11-17, Published: 2017-11-17, Edition: 2
- 49 EN 13183-2, "Moisture content of a piece of sawn timber – Part 2: Estimation by electrical resistance method", Approved 2003-04-11, edition 1



## 19 Indexes

### 19.1 Index of tables

Table 1.	Structural heights of beams at Stena Flavia.....	18
Table 2.	Structural heights of beams at Magnolia seaways.....	18
Table 3	Summary of the test conditions and results associated with the heat release results from the references discussed above.....	50
Table 4.	The design and installation criteria of three certified deluge systems for ro-ro spaces having a ceiling height up to and including 2,5 m. ....	65
Table 5.	The design and installation criteria of two certified systems using automatic nozzles for ro-ro spaces having a ceiling height up to and including 2,5 m.....	65
Table 6.	The design and installation criteria of three certified deluge systems for ro-ro spaces having a ceiling height up to and including 5 m. ....	66
Table 7.	The design and installation criteria of three certified systems using automatic nozzles for ro-ro spaces having a ceiling height up to and including 5 m.....	66
Table 8.	The approximate delay time from the start of a fire until water is discharged. ....	73
Table 9.	The principal fire test approach in the revised fire test procedures.....	74
Table 10.	The suggested fire test approach in the revised fire test procedures. ....	75
Table 11.	The maximum spacing of fire detectors given in the FSS Code. ....	77
Table 12.	The water discharge densities provided in tables 4-1 to 4-3 in section 4 of MSC.1/Circ.1430. ....	80
Table 13.	The suggested choice of automatic sprinklers and nozzles for the benchmark fire suppression tests. ....	81
Table 14.	The measurement positions and the associated measurement channels on the steel sheet screens in the passenger car fire scenario. In total, six steel sheet screens were used.....	90
Table 15.	The measurement positions and the associated measurement channels on the steel sheet screens (long sides) in the freight truck trailer fire scenario. In total, four steel sheet screens were used at the long sides. ....	91
Table 16.	The measurement positions and the associated measurement channels on the steel sheet screens positioned at the back, short-end of the mock-up in the freight truck trailer fire scenario.....	93
Table 17.	The fire test program.....	94
Table 18.	Examples of the allowed variation of the average moisture content of a lot and the allowed moisture content of individual pieces within that lot based on the requirements in EN 14298:2017.....	120

### 19.2 Index of figures

Figure 1.	Typical cargo stowage on ro-ro passenger and ro-ro ships. Photo: FLOW. ....	17
Figure 2.	Typical vehicle space on a ro-ro passenger ship (photo from Stena Flavia). Photo: FLOW. ....	18
Figure 3.	Typical vehicle space deck structure arrangement with insulation of the steel deck. Photo: FLOW.....	19
Figure 4.	Typical vehicle space on a ro-ro cargo ship, with the arrangement of a movable deck. Photo: FLOW.....	19
Figure 5.	Typical vehicle space on a ro-ro passenger and ro-ro cargo ship with movable deck arrangement. Photo: FLOW.....	20
Figure 6.	The fire damage to the vehicle carrier Courage [1]. ....	21
Figure 7.	The fire damage to the vehicle carrier Honor [2].....	22

Figure 8.	Exterior boundary-cooling during the fire in the vehicle carrier Höegh Xiamen, a defensive strategy following an explosion that injured nine firefighters, five of them seriously [3].	23
Figure 9.	The fire damage to the freight ('tractor') truck and the attached trailer on board Joseph and Clara Smallwood. It was concluded that fire likely started in the freight truck. Note: From these photos it appears that fire have spread from the cabin of the freight truck and towards the back, thereby involving the attached trailer. The exterior of the trailer exhibit (at least the side shown in the photo) very little fire damage [4].	25
Figure 10.	The fire damage to the moving and storage trailer and drop trailer (containing building supplies) in the fire on board Joseph and Clara Smallwood. Note: From these photos it seems that the fire never involved the content of the moving storage trailer, that looks like a metal structure. The photo indicate that a tarpaulin has been fitted over its top, which could be an indication of efforts to protect its content after the fire. The drop trailer has been involved but to a small extent. The photos do not tell if the fire spread through the roof of the trailer [4].	25
Figure 11.	The damage to one of the refrigerated trailers in the fire on board Commodore Clipper [5].	26
Figure 12.	The damage to the electric car in the fire on board Pearl of Scandinavia [6].	27
Figure 13.	The damage to the VW Transporter in the fire on board Mecklenburg-Vorpommern [7].	29
Figure 14.	The fire damage to the semi-trailer and the VW Transporter in the fire on board Mecklenburg-Vorpommern.	29
Figure 15.	The fire damage to the cars on the trailer after the fire on Victoria Seaways [8].	30
Figure 16.	The main car deck on board URD, that was fully stowed on the day of fire [9].	32
Figure 17.	The fire damage to the lorry on board URD [9].	32
Figure 18.	The fire damage to roof of the refrigerator truck on board Stena Spirit [10].	34
Figure 19.	The fire damage to the freight parked next to the refrigerator truck on board Stena Spirit [10].	34
Figure 20.	The fire damaged vehicles and trailers on the main deck on board Corona Seaways [12].	36
Figure 21.	The jet flame from a cable feedthrough in a battery back []. Photo: RISE.	42
Figure 22.	Jet flames from 21700 cylindrical cells. Photo: RISE. Note that the image is distorted as it is proprietary. The flame length is approximately 1.5 m. The system shown had several hundreds of 21700 cells.	43
Figure 23.	The measured heat release rate from a stand-alone battery pack used for an electric vehicle. The gas burners used to initiate the fire provided a constant heat release rate of 400 kW (turned off at about 20 minutes) that is included in the graph [38].	44
Figure 24.	The heat release rate histories for an EV and an analogous ICE vehicle from car manufacturer 1 in the tests at INERIS reported by Lecocq et al. [39].	45
Figure 25.	The heat release rate histories for an EV and an analogous ICE vehicle from car manufacturer 2 in the tests at INERIS reported by Lecocq et al. [39].	46
Figure 26.	The heat release rate histories in the ETOX-project that involved an ICE and two BEVs. The ICEV A and BEV A vehicles were similar except for the powertrain [34].	49
Figure 27.	The freight truck trailer mock-up. A total of 112 wood pallets are arranged in two parallel stacks, each containing seven wood pallets. The overall length is eight stacks. Half of the array is shielded from direct application of water from overhead nozzles by a horizontal steel sheet plate. The other half is fully exposed to the water spray. Fire trays with	

	commercial heptane are positioned underneath the stacks for fire ignition. Photos: RISE Fire Research AS. ....	61
Figure 28.	The two fire trays centrally located under the wood pallets that is used to initiate the fire. Photos: RISE Fire Research AS. ....	61
Figure 29.	The passenger car mock-up. It includes a total of 12 EUR wood pallets arranged in two stacks, each containing six pallets. Photos: RISE Fire Research AS. ....	62
Figure 30.	A photo sequence showing the fire development with eight rows of stacks of idle wooden pallet stacks during 1:4 model-scale tests. Photos: RISE. ....	71
Figure 31.	The suspended ceiling during the preparation work for the tests using the passenger car mock-up. The ceiling height was 2,5 m. The pipe-work has been prepared for the deluge system tests (pendent nozzles). Photo: RISE. ....	82
Figure 32.	The suspended ceiling when installed for the tests using the freight truck trailer mock-up. The ceiling height was 3,7 m. With the reduced height of the mock-up, this resulted in a realistic clearance corresponding to a full-height freight truck trailer and a ceiling height of 5 m. The pipe-work has been prepared for the automatic sprinkler system tests (upright sprinklers). Photo: RISE. ....	83
Figure 33.	The automatic sprinklers used in the tests: Upright, standard coverage, standard response sprinklers with a nominal operating temperature of 68 °C and a K-factor of 80,6 (l/min)/√bar (left) and a nominal operating temperature of 141 °C and a K-factor of 161,4 (l/min)/√bar (right). The sprinklers had 5 mm diameter glass bulbs. Photos: RISE. ....	84
Figure 34.	An automatic sprinklers as depicted prior Test 5 (left) and a close-up of its discharge pattern (right). Photos: RISE. ....	85
Figure 35.	A water spray nozzle as depicted prior Test 1 (left) and the discharge pattern of several nozzles (right). Photos: RISE. ....	85
Figure 36.	The passenger car mock-up depicted from the front. Photo: RISE. ....	86
Figure 37.	The passenger car mock-up depicted from the back. Photo: RISE. ....	87
Figure 38.	The roof over the passenger car mock-up depicted from the back. Photo: RISE. ....	87
Figure 39.	The freight truck trailer mock-up depicted from the front. Photo: RISE. ....	88
Figure 40.	The freight truck trailer mock-up depicted from the back. Photo: RISE. ....	89
Figure 41.	The steel sheet screens along the long sides of the passenger car mock-up. Photo: RISE. ....	90
Figure 42.	The steel sheet screens facing left hand side of the freight truck trailer mock-up. Similar screens faced the right hand side. Photo: RISE. ....	91
Figure 43.	The steel sheet screen facing the rear end of the freight truck trailer mock-up. Photo: RISE. ....	93
Figure 44.	Test 1: The fire size at 01:30 [min:s], soon after both thermocouples at a 4,5 m radius from the fire had exceeded the 78 °C temperature threshold. Photo: RISE. ....	95
Figure 45.	Test 1: The fire size at 02:30 [min:s], shortly after the start of the application of water. Photo: RISE. ....	95
Figure 46.	Test 1: The fire size at 08:01 [min:s], at the time the ceiling gas temperatures were the lowest. Photo: RISE. ....	95
Figure 47.	Test 1: The fire size at 14:01 [min:s], after which it started to decline. Photo: RISE. ....	95
Figure 48.	Test 2: The fire size at 01:30 [min:s], soon after both thermocouples at a 4,5 m radius from the fire had exceeded the 78 °C temperature threshold. Photo: RISE. ....	96
Figure 49.	Test 2: The fire size at 02:30 [min:s], shortly after the start of the application of water. Photo: RISE. ....	96
Figure 50.	Test 2: The fire size at 14:00 [min:s], when it reached its peak according to the ceiling gas temperature measurements. Photo: RISE. ....	96

Figure 51.	Test 2: The fire size at 20:01 [min:s], during the stage of decline. Photo: RISE. ....	96
Figure 52.	Test 3: The fire at 02:10 [min:s], shortly after water was discharging from the single automatic sprinkler that had activated prior water was allowed to entering the pipe-work. Photo: RISE. ....	97
Figure 53.	Test 3: The fire at 04:00 [min:s], when all three activated sprinklers were flowing. Photo: RISE. ....	97
Figure 54.	Test 3: The fire at 07:00 [min:s], when it started to decline. Photo: RISE. ....	97
Figure 55.	Test 3: The fire size at 20:01 [min:s], during the final stage of decline. Photo: RISE. ....	98
Figure 56.	Test 4: The fire at 02:20 [min:s], shortly after the air pressure drop of the sprinkler piping indicated that the first sprinkler(s) had activated. Photo: RISE. ....	98
Figure 57.	Test 4: The fire at 03:20 [min:s], when water started to flow from the sprinklers that had activated. Photo: RISE. ....	98
Figure 58.	Test 4: The fire at 05:00 [min:s]. Photo: RISE. ....	99
Figure 59.	Test 4: The fire at 06:30 [min:s]. Only small flames appear at the centre core of the wood pallet array. Photo: RISE. ....	99
Figure 60.	Test 4b: The fire at 02:28 [min:s], shortly before the air pressure drop of the sprinkler piping indicated that the first sprinkler(s) had activated. Photo: RISE. ....	100
Figure 61.	Test 4b: The fire at 03:28 [min:s], when water started to flow from the sprinklers that had activated. Photo: RISE. ....	100
Figure 62.	Test 4b: The fire at 04:58 [min:s]. The fire is clearly suppressed. Photo: RISE. ....	100
Figure 63.	Test 4b: The fire at 06:28 [min:s]. Only small flames appear at the centre core of the wood pallet array. Photo: RISE. ....	100
Figure 64.	Test 7: The fire at 02:30 [min:s], shortly before the air pressure drop of the sprinkler piping indicated that the first sprinkler(s) had activated. Photo: RISE. ....	101
Figure 65.	Test 7: The fire at 03:40 [min:s], shortly after water started to flow from the sprinklers that had activated. Photo: RISE. ....	101
Figure 66.	Test 7: The fire at 05:00 [min:s]. The fire was initially suppressed. Photo: RISE. ....	102
Figure 67.	Test 7: The fire at 10:00 [min:s]. The fire is gradually growing in size when parts of the array that is shielded from the application of water becomes involved in the fire. Photo: RISE. ....	102
Figure 68.	Test 7: The fire at 18:01 [min:s]. The fire is gradually growing in size when parts of the array that is shielded from the application of water becomes involved in the fire. Photo: RISE. ....	102
Figure 69.	Test 7: The fire at 25:01 [min:s], just prior to the termination of the test. Photo: RISE. ....	103
Figure 70.	Test 7: The fire at 25:41 [min:s], during the termination using fire hoses. Photo: RISE. ....	103
Figure 71.	Test 8: The fire at 01:50 [min:s], shortly after the air pressure drop of the sprinkler piping indicated that the first sprinkler(s) had activated. Photo: RISE. ....	104
Figure 72.	Test 8: The fire at 03:00 [min:s], shortly after water was discharging from the initial three automatic sprinklers that had activated. Photo: RISE. ....	104
Figure 73.	Test 8: The fire at 06:00 [min:s], shortly after the activation of the fourth automatic sprinkler. Photo: RISE. ....	104
Figure 74.	Test 8: The fire at 08:30 [min:s], shortly after the activation of the sixth (final) automatic sprinkler. Photo: RISE. ....	105
Figure 75.	Test 8: The fire at 21:01 [min:s], as the fire intensity started to decline. Photo: RISE....	105
Figure 76.	Test 8: The fire at 27:01 [min:s]. Photo: RISE. ....	105
Figure 77.	Test 5: The fire size at 01:30 [min:s], soon after both thermocouples at a 4,5 m radius from the fire had exceeded the 78 °C temperature threshold. Photo: RISE. ....	106



Figure 78.	Test 5: The fire size at 02:20 [min:s] and 02:30 [min:s], moments before and after the start of the application of water. Photo: RISE.....	106
Figure 79.	Test 5: The fire size at 06:00 [min:s], when the water flow rate started to become reduced. The measured water flow rate is approximately 920 l/min. Photo: RISE. ....	107
Figure 80.	Test 5: The fire size at 09:00 [min:s]. The measured water flow rate is approximately 490 l/min. Photo: RISE.....	107
Figure 81.	Test 5: The fire size at 10:40 [min:s], just prior the termination of the test using fire hoses. The measured water flow rate is approximately 480 l/min. Photo: RISE. ....	107
Figure 82.	Test 5: The fire size at 10:50 [min:s], when the test was terminated by applying water from fire hoses. Photo: RISE. ....	108
Figure 83.	Test 5: The fire size documented from a different angle as compared to the photos above but at the same times, 10:40 [min:s] and at 10:40 [min:s], respectively. Photo: RISE. ..	108
Figure 84.	Test 6: The fire size at 01:37 [min:s], soon after both thermocouples at a 4,5 m radius from the fire had exceeded the 78 °C temperature threshold. Photo: RISE.....	109
Figure 85.	Test 6: The fire size at 02:26 [min:s], shortly after the start of the application of water and a few seconds before full system operating pressure was reached. Photo: RISE....	109
Figure 86.	Test 6: The fire size at 03:17 [min:s], at about the time when the fire gradually started to increase in size. Photo: RISE. ....	109
Figure 87.	Test 6: The fire size at 10:07 [min:s], at about the time when the fire gradually started to increase in size. Photo: RISE. ....	110
Figure 88.	Test 6: The fire size at 18:18 [min:s], when the decision was made to terminate the test. Photo: RISE. ....	110
Figure 89.	Test 6: The termination of the test using fire hoses. Photo: RISE.....	110
Figure 90.	Tests 1 and 2: The mean ceiling gas and target steel screen surface temperatures. ....	111
Figure 91.	Tests 3, 4 and 4b: The mean ceiling gas and target steel screen surface temperatures. ....	111
Figure 92.	Tests 5 and 6: The mean ceiling gas and target steel screen surface temperatures. ....	112
Figure 93.	Tests 5: The mean target steel screen surface temperatures on the individual target screens.....	112
Figure 94.	Tests 6: The mean target steel screen surface temperatures on the individual target screens.....	113
Figure 95.	Tests 5 and 6: The mean target steel screen surface temperatures on the screen facing the rear end of the mock-up. ....	113
Figure 96.	Tests 7 and 8: The mean ceiling gas and target steel screen surface temperatures. ....	114
Figure 97.	Tests 7: The mean target steel screen surface temperatures on the individual target screens.....	114
Figure 98.	Tests 8: The mean target steel screen surface temperatures on the individual target screens.....	114
Figure 99.	Tests 7 and 8: The mean target steel screen surface temperatures on the target screen facing the rear end of the mock-up.....	115
Figure 100.	The measured moisture content of randomly selected wood pallets in each of the test.	116

## 20 ANNEX A

Free-burn fire tests of stacks of idle wood pallets were conducted at RISE in two different test series. The intent was to provide input for the development of a passenger car mock-up.

### 20.1 The first test series

In the first test series, one test was conducted with an array that was 1 pallet (wide) by 10 pallets (high) by 4 pallets (long), i.e., a total of 40 wood pallets. The array is shown in Figure A-1.



Figure A-1 The fire test set-up with 40 idle wood pallets in four stacks with 10 pallets each.

The overall height was about 1,45 m and part of the top surface was covered by two layers of nominally 10 mm thick non-combustible cement fibre boards to simulate the roof of a car. These boards were laid directly on the top of the pallet stacks and secured using wood screws.

To improve stability of the pallet stacks, 45 mm by 90 mm vertical wood studs were secured to the short side of each stack using wood screws. The fire was initiated using a fire tray sized 600 mm (L) by 200 mm (W) by 50 mm (H) filled with 3,6 litres (30 mm) of heptane on a 10 mm water bead. The tray was positioned at the floor, close to the mid-point of the array.

The average measured moisture content, based on the measurement of ten pallets, was 10,4 % with a Standard Deviation of 0,6 %. The average weight of the pallets was 21,0 kg. All pallets were recycled pallets.

The heat release rate was measured using a large-scale calorimeter. The heat flux was measured with a heat flux meter centred in front of each long side, respectively. The devices were positioned 1,15 m above floor at a horizontal distance of 1,0 m from the face of the stack. In addition, Plate Thermometers were positioned close to the heat flux meters.

Figures A-2 through A-4 shows selected photos from the test.

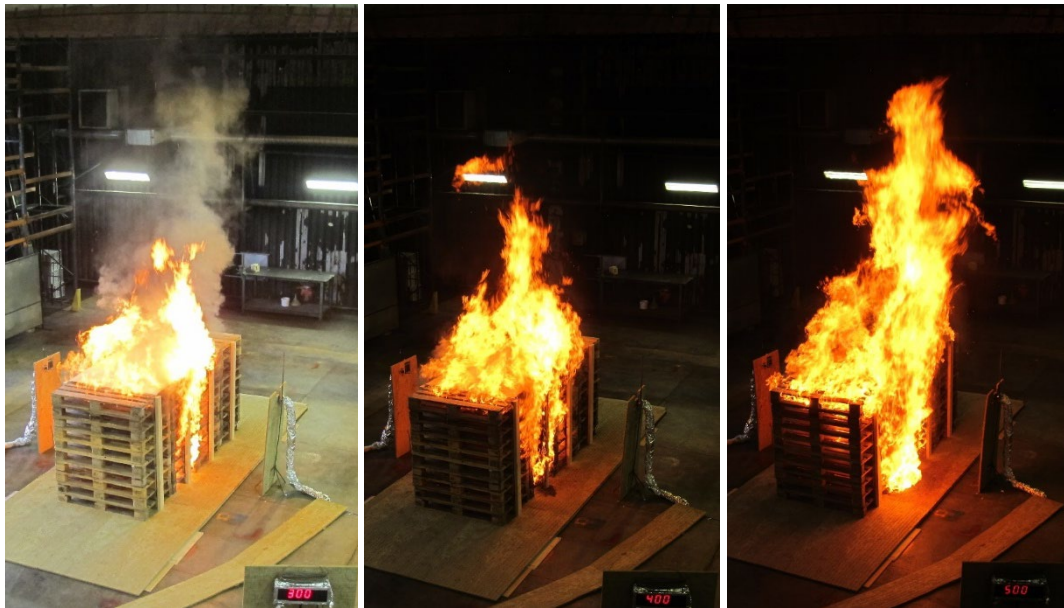


Figure A-2 The fire size at 03:00 [min:s], 04:00 [min:s] and 05:00 [min:s], respectively.

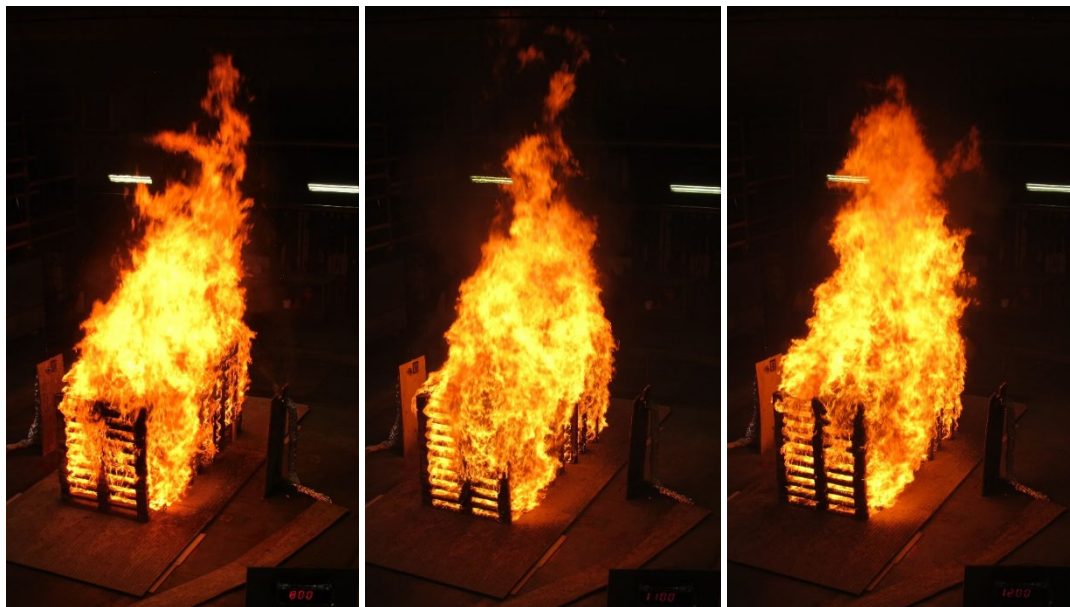


Figure A-3 The fire size at 08:00 [min:s], 11:00 [min:s] and 12:00 [min:s], respectively. The peak heat release rate was reached at approximately 12:12 [min:s].





Figure A-4 The fire size at 15:00 [min:s], when the fire intensity had started to decline, at 15:50 [min:s], moments after the partial collapse of the stacks and at about 18:00 [min:s], moments after the collapse of remaining stacks.

Figure A-6 shows the measured total and convective heat release rates for basically the full duration (the test was terminated after 160 minutes) and for the first 20 minutes.

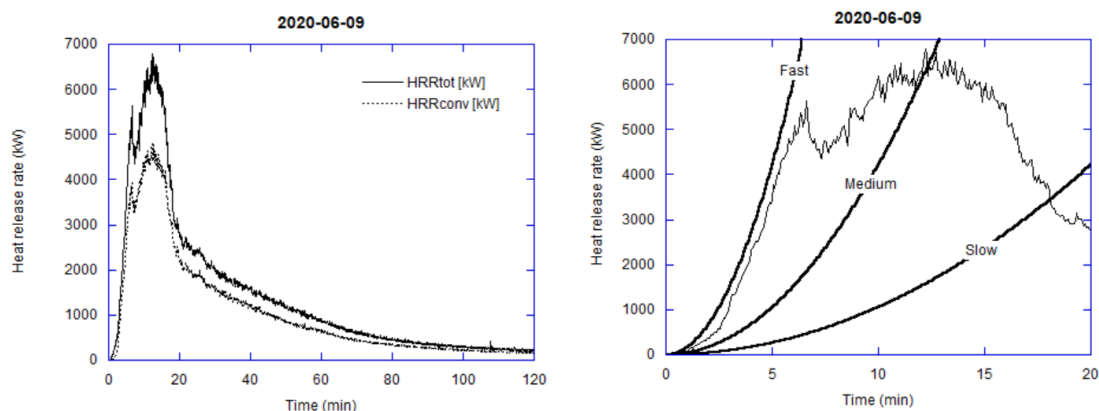


Figure A-5 The total and convective heat release histories (left) and the fire growth rate (right) compared to standard fire growth rate curves.

The fire peaked at 6,8 MW after 12:12 [min:s] and the total heat release approached 10,7 GJ. The peak heat release rate was close to that estimated prior the test, based on previous fire test data. Furthermore, assuming a burning efficiency of 0,8, the total fire load of 13,4 GJ correlates well with the theoretical approximation. The maximum total convective heat release rate was 4,8 MW.

The fire growth rate up to about 06:30 [min:s] resembles a “fast” fire growth rate in accordance with the exponential t-squared ( $t^2$ ) fire growth rate curves, which are commonly used for fire protection design purposes. This initial part of the fire involved fire spread across the top half of the array, likely due to the partial coverage of the top by the non-combustible boards. The fire then peaked once the entire top surface area of the array was burning. Thereafter, the fire was reduced for almost a minute before the flames continued to involve all surfaces of the pallets. This phase of the fire growth was slower and not as steady as the first part but did result in the maximum peak at 12:12 [min:s]. Following this, a gradual reduction in intensity was observed as combustibles were consumed. This also resulted in a partial (three of four stacks) collapse at 15:50 [min:s] and a more

rapid reduction in fire intensity. At about 18:00 [min:s], the remaining stack collapsed, which resulted in a fire that consistently decayed until virtually all combustible material was consumed.

Figure A-6 shows the measured heat fluxes and the surface temperatures of the Plate Thermometers. It is observed that both peak levels and the shape of the curves indicate that the fire spread was very symmetrical. The heat flux peaked at  $78 \text{ kW/m}^2$  and  $72 \text{ kW/m}^2$ , respectively. The surface temperatures of the Plate Thermometers peaked at  $756^\circ\text{C}$  and  $729^\circ\text{C}$ , respectively.

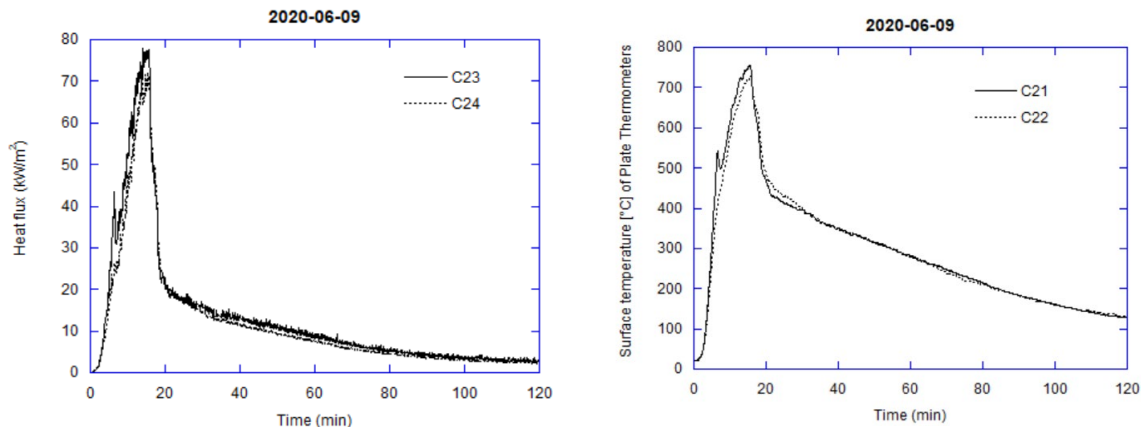


Figure A-6 The heat fluxes (left) and the surface temperatures of the Plate Thermometers (right).

The test results can be compared to the large-scale vehicle fire tests that are discussed in this report and summarized in Table 1. It is observed that the peak heat release rate of  $6,8 \text{ MW}$  is comparable with those reported, although some tests do indicate the possibilities for a more intense fire. The total heat release approached  $10,7 \text{ GJ}$ . Although this was higher than those reported in large-scale vehicle fire tests, it should not be judged as an extreme value as the intent is to simulate the fire load of a large sized car.

The initial fire growth rate of the fire is reasonably realistic. Reported values to reach the peak heat release range from 6 minutes to 30 minutes, as compared to about 12 minutes recorded in the test. It should, however, be emphasized that the fire growth rate is dependent on where a fire is initiated (external or internal and the specific position) and the size of the igniter.

The measured average peak heat flux of around  $75 \text{ kW/m}^2$  is also higher than reported values of actual car fires. Peaks in the order of  $50 \text{ kW/m}^2$  to  $60 \text{ kW/m}^2$  have been reported. The higher values obtained in this test can be explained by the fact that no 'side plates' or similar were used to simulate the body of a vehicle. The whole area of the flames was visible to the heat flux meters.

The repeatability of the fire scenario cannot be determined based on one test. However, it is likely that initial fire growth rate would be repeatable with the size of the fire ignition source that was used. Collapse of the stacks may influence the repeatability at a later stage of the fire duration. For this test, a partial collapse occurred after at 15:50 [min:s]. A full collapse as the one observed may be prevented or at least delayed if the stacks are positioned inside a steel sheet body and/or with cross-supports on each short side of the stacks. A vertical collapse due to the consumption of combustibles is harder to prevent but would likely occur at a later stage.

## 20.2 The second test series

For the second series of tests, a mock-up made from steel sheet had been constructed. Figure A-7 shows the arrangement.





Figure A-7 The passenger car mock-up.

Fire ignition was achieved with an 800 mm (L) by 150 mm (W) fire tray filled with 2 l of heptane on a 2 l layer of water. The fire tray was inserted between the last block of the second stack of the main stacks, i.e., almost at the mid-point of the main stack.

Each stack of pallets was secured, to prevent it from early collapse, using cross bars on the side faces of the stacks. The supports were made from 45 mm by 90 mm wood studs. Wood screws were used on the top and bottom, respectively, pallets.

A Plate Thermometer and a heat flux meter was positioned at each side, respectively, of the set-up. The vertical height was adjusted to be at mid-height of the virtual side windows of the car. The horizontal distance was at 500 mm from the side plates of the mock-up.

#### 20.2.1 Test 1

Date: March 16, 2021.

The four main stacks contained 10 pallets each. Therefore, the total amount of pallets was  $4 \times 10 + 1 \times 5 = 45$  pallets. The roof over the main stack consisted of a 20 mm Rockwool sheet with a steel sheet plate positioned above.

It was observed that the roof over the main part of the mock-up collapsed relatively early in the test, probably after around 5 minutes after ignition. In other words, the roof construction was too weak.

The fire peaked at 7,9 MW after around 12 minutes. The total heat release rate measurement malfunctioned (due to a leak in the gas sampling line) after around 21 minutes, but at this stage the fire was gradually declining. The test was terminated 47 minutes after ignition. The convective heat release rate measurement was fully functioning during the entire test.

The front (low) stack of pallets collapsed after around 21 minutes, with additional collapse of the other pallets following. The collapse can be observed in the heat release data as prompt reduction of the heat release rate. The Plate Thermometers peaked in excess of 700 °C. The heat flux meters peaked at 59 kW/m<sup>2</sup> and 90 kW/m<sup>2</sup>, respectively. Figure A-8 shows the measurement results.

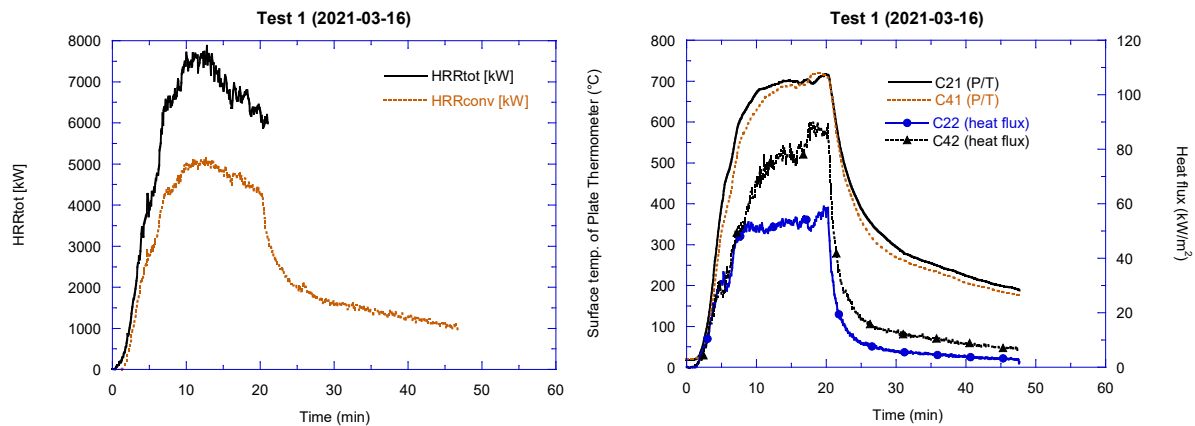


Figure A-8 Test 1: The total and convective heat release rate histories (left) as well as the surface temperature of the Plate Thermometers and the heat flux (right).

### 20.2.2 Test 2

Date: March 17, 2021.

For this test, the stack height of the four main stacks was reduced to 8 pallets. In other words, the full test set-up contained  $4 \times 8 + 1 \times 5 = 37$  pallets, almost 20 % less pallets than in Test 1. The roof was re-constructed and consisted of a sandwich construction with an outer layer (on both sides) of 2 mm steel sheet plates and a core of 20 mm Rockwool. The construction was bolted together.

The fire peaked at 7,1 MW after around 12 minutes. The total heat release rate measurement malfunctioned (due to a leak in the gas sampling line) after around 32 minutes, but at this stage the fire was declining. The test was terminated 60 minutes after ignition. The convective heat release rate measurement was fully functioning during the entire test.

As in Test 1, collapse occurred after around 21 minutes, although this collapse is less visible in the heat release data. Visually, it appeared that a large portion of the core of the wood pallets were consumed at the collapse. The rapid consumption of the wood correlates with the fact that the fire size dropped rapidly after about 15 minutes.

The Plate Thermometers peaked at around 750 °C. The heat flux meters peaked at 74 kW/m<sup>2</sup> and 102 kW/m<sup>2</sup>, respectively. Figure A-9 shows the measurement results.

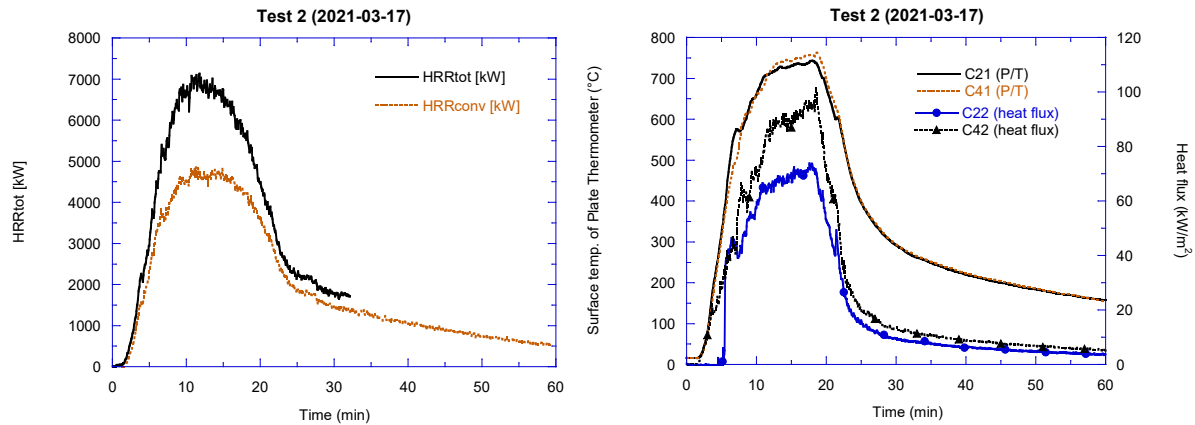


Figure A-9 Test 2: The total and convective heat release rate histories (left) as well as the surface temperature of the Plate Thermometers and the heat flux (right).

### 20.2.3 Test 3

Date: March 18, 2021.

The amount and arrangement of the idle wood pallets were identical; however, the point of fire ignition was moved to the front (5 pallet high) stack of wood pallets. The fire tray was inserted between the second (last) block of the bottommost pallet. The tray was raised from the floor by using concrete blocks.

A third roof design was tested, that consisted of a frame made from 20 mm by 20 mm square iron. A 2 mm steel sheet was put on top and Rockwool insulation underneath this plate. The roof lasted the full duration of the test but was warped by the heat.

As expected, the fire growth rate was slower in this test as the fire primarily spread in one direction. The fire peaked at 6,3 MW after around 16 minutes. The total heat release rate measurement malfunctioned (due to a leak in the gas sampling line) after around 38 minutes, but at this stage the heat release rate was less than 2 MW. The test was terminated almost 120 minutes after ignition. The convective heat release rate measurement was fully functioning during the entire test.

The Plate Thermometers peaked at slightly over 700 °C. The heat flux meters peaked at 82 kW/m<sup>2</sup> and 69 kW/m<sup>2</sup>, respectively. Figure A-10 shows the measurement results.

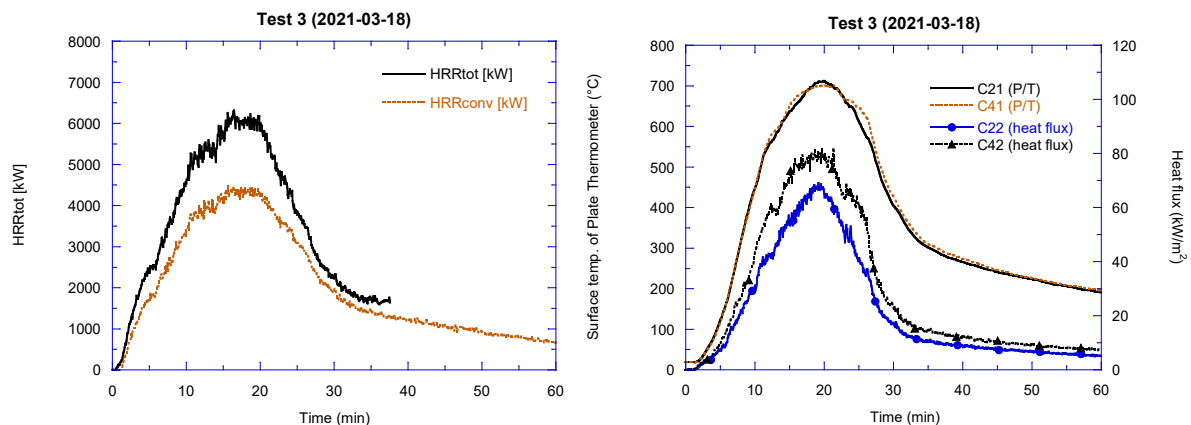


Figure A-10 Test 3: The total and convective heat release rate histories (left) as well as the surface temperature of the Plate Thermometers and the heat flux (right).

Figure A-11 shows the total heat release rates from all three tests.

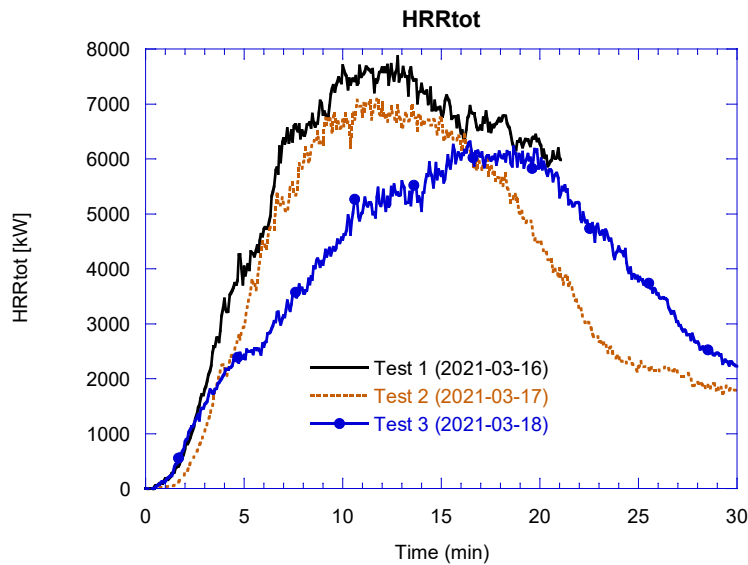


Figure A-11 The total heat release rate histories from all three tests. **Test 1:**  $4 \times 10 + 1 \times 5 = 45$  pallets. **Test 2 and Test 3:**  $4 \times 8 + 1 \times 5 = 37$  pallets. Fire ignition at the front stack in Test 3.

The peak values of the measurements are summarized in the Table A-1.

Table A-1 The peak values obtained in the second series of free-burn fire tests.

Test	Peak HRRtot [MW]	Peak HRRconv [MW]	Peak Plate Thermometer temperature [°C]		Peak heat flux [kW/m <sup>2</sup> ]	
			C21	C41	C22	C42
1	7,9	5,1	718	722	59	90
2	7,1	4,9	746	764	74	102
3	6,3	4,5	713	702	69	82

Higher Plate Thermometer temperatures and heat flux values were recorded in Test 2 than in Test 1. This is likely because the strength of the roof was better in Test 2, which directed the flames towards the measurement equipment.

The following observations was made related to the design of the mock-up.

- The stability of the stacks of wood pallets was good due to the use of the cross supports on each stack. Collapse was delayed and occurred when a large portion of the core of the wood pallets had been consumed. Improved stability would require unreasonable measures.
- The roof over the main stack needs to be re-designed to withstand the heat of a free-burn fire. As testing using sprinklers will cool the ceiling and limit the heat release rate, a sandwich design (sheet meatal - Rockwool - sheet meatal) with square iron at the perimeters is likely sufficient. Alternatively, the vertical and horizontal supports of the roof may be cooled by water circulating through the square iron.
- The other parts of the mock-up withstood the heat well.
- The fire size in Test 2 exceeded 7 MW. A reduction of the height of the main stacks from eight pallets (in total 37 pallets) to seven pallets (in total 33 pallets) will reduce the fire size with about 10 %, which still can be considered a realistic scenario.

Figures A-11 to A-15 shows selected photos from the Test 2.





Figure A-12 **Test 2:** The fire size at 03:10 [min:s], reaching 1,0 MW and at 05:00 [min:s], reaching 3,0 MW.



Figure A-13 **Test 2:** The fire size at 07:00 [min:s], being about 5,0 MW and at 09:00 [min:s], reaching 6,3 MW.

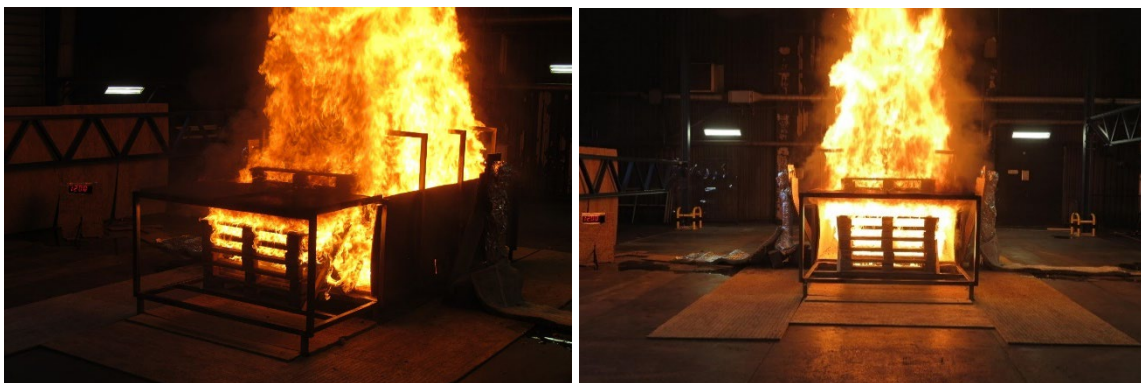


Figure A-14 **Test 2:** The fire size at 12:00 [min:s], approaching about 6,9 MW (the peak).



Figure A-15 **Test 2:** The fire size at 21:10 [min:s], being 3,1 MW (left). The photo is taken moments before the collapse of the idle wood pallets and at 23:10 [min:s] being 2,7 MW (right). The photo is taken two minutes after the collapse of the idle wood pallets.

## 21 ANNEX B

### 21.1 Introduction

Electric vehicle (EV) deployment has been growing rapidly over the past ten years and will likely continue to grow. Basically, all car manufacturers in the world are introducing new fully electric or hybrid vehicles, partially in response to increasing efficiency and emissions standards. Large-scale free-burn fire tests [1, 2, 3] indicate that the peak heat release of a battery electric vehicle (BEV) fire is comparable to that of a vehicle with an internal combustion engine (ICEV), given similar sized vehicles. From these tests it is noted that the involvement and the time to involvement of the fuel tank and the battery pack of the vehicles have an influence on the fire growth rate and the severity of the fire.

However, there is limited information available about the fire suppression performance of sprinkler systems. Water spray systems (often denoted “drencher systems”) are typically installed on ro-ro cargo and ro-ro passenger ships. Roll-on/roll-off (ro-ro) ships are designed to carry wheeled cargo such as passenger cars, freight trucks, buses, and motorcycles, which are driven on and off the ship on their own wheels. The ships are large, with ro-ro spaces that extend the full length and width of the ship. The drencher systems consist of deluge sections with open water spray nozzles. The sections are manually operated in case of fire. Concerns have arisen about whether these systems are able to control a fire in an electric vehicle and if the design of the system in terms of water flow rates needs to be increased.

The objective of the tests was to compare the fire suppression performance of a deluge water spray system for fires involving ICEVs and BEVs in test conditions that are as equivalent as possible. The tests simulated a ro-ro space having a ceiling height of about 5 m and the system design in terms of water discharge densities corresponds to the design recommendations in MSC.1/Circ.1430/Rev.2 [4].

### 21.2 The vehicles used in the tests

Two pairs of vehicles, i.e., a total of four vehicles, were used in the tests. Each pair of vehicles was chosen to be as similar as possible, except for the powertrain, refer to Table B-1. All vehicles were sport utility vehicles (SUVs). The make and model of the vehicles are not provided, but all vehicles are considered representative of modern vehicles in the marketplace.

---

<sup>1</sup> Lam, C., MacNeil, D., Kroeker, R., Loughheed, G., Lalime, G., “Full-Scale Fire Testing of Electric and Internal Combustion Engine Vehicles”, Fourth International Conference on Fire in Vehicle, Baltimore, 2016

<sup>2</sup> Watanabe, N., Sugaw, O., Suwa, T., Ogawa, Y., Hiramatsu, M., Tomonori, H., et al, “Comparison of fire behaviours of an electric-battery-powered vehicle and gasoline-powered vehicle in a real-scale fire test”, Second International Conference on Fires in Vehicles, Chicago, 2012

<sup>3</sup> Willstrand, Ola, Bisschop, Roeland, Blomqvist, Per, Temple, Alastair and Anderson, Johan, “Toxic Gases from Fire in Electric Vehicles”, RISE Report 2020:90

<sup>4</sup> MSC.1/Circ. 1430/Rev.2, “Revised Guidelines for the Design and Approval of Fixed Water-Based Fire-Fighting Systems for Ro-Ro Spaces and Special Category Spaces”, International Maritime Organization, 8 December 2020

Table B-1 The vehicles used in the tests.

	ICEV1	BEV1	ICEV2	BEV2
Model year	2022	2022	2021	2021
Type of vehicle	Compact SUV	Compact SUV	Subcompact crossover SUV	Subcompact crossover SUV
Length [mm]	4 728	4 584	4 151	4 151
Width [mm]	1 839	1 852	1 791	1 791
Height [mm]	1 687	1 640	1 532	1 534
Wheelbase [mm]	2 789	2 771	2 561	2 557
Curb weight, inclusive of driver [kg]	1 614	2 120	1 295	1 598
Drive	Front wheel drive	Rear wheel drive	Front wheel drive	Front wheel drive
Transmission	Manual (6-speed)	Automatic (single-speed)	Manual (6-speed)	Automatic (single-speed)
Fuel or type of battery	Gasoline	Lithium-Ion pouch cells	Gasoline	Lithium-ion prismatic cells
Battery cell chemistry	Not applicable	Li-NMC	Not applicable	Li-NMC
Fuel tank or battery capacity	58 l	82 kWh (total) 77 kWh (usable)	44 l	50 kWh (total) 45 kWh (usable)
Amount of fuel and charge level used in the test	52,2 l (90 %)	69,3 kWh (90 %)	39,6 l (90 %)	40,5 kWh (90 %)

ICEV1 and BEV1 were similar except for the powertrain. BEV1 was geometrically slightly smaller but was about 30 % heavier than the ICEV1, mainly due to the weight of the battery pack. It is also noted that BEV1 was built on a dedicated BEV platform with a simple flat rectangular battery pack design, with several battery modules positioned side by side between the wheel axles. The vehicle had Lithium Nickel Manganese Cobalt oxides (Li-NMC) pouch cells. BEV1 had a huge glass panel that stretches almost over the entire width of the roof.

ICEV2 and BEV2 were basically identical except for the powertrain as the vehicles are designed using a modular platform that allows different powertrains. The electric version is about 20 % heavier, mainly due to the weight of the battery pack. The vehicle had Li-NMC prismatic cells, with the battery modules primarily arranged in one pack beneath the area of the back seat and in one pack beneath the area of the front seats.

### 21.3 The positioning of the vehicles

Six steel sheet trays were positioned at the floor of the fire test hall, symmetrically under the four water spray nozzles described below. Each tray measured 2500 mm (W) by 1000 mm (L) by 150 mm (H). The long sides of the trays were joined using bolts, long side-to-long side, to provide a total area of 2500 mm (W) by 6000 mm (L), equalling 15 m<sup>2</sup>. The outer rim height of the trays was 150 mm, but the inner tray rims were designed with a lower height of 75 mm at the long sides that faced each other.

Prior the tests, the trays were filled with 75 mm of water to achieve an unbroken water surface. Four goose-necks at the short sides ensured a constant level of water despite water being discharged into the trays by the over-head deluge water spray system.



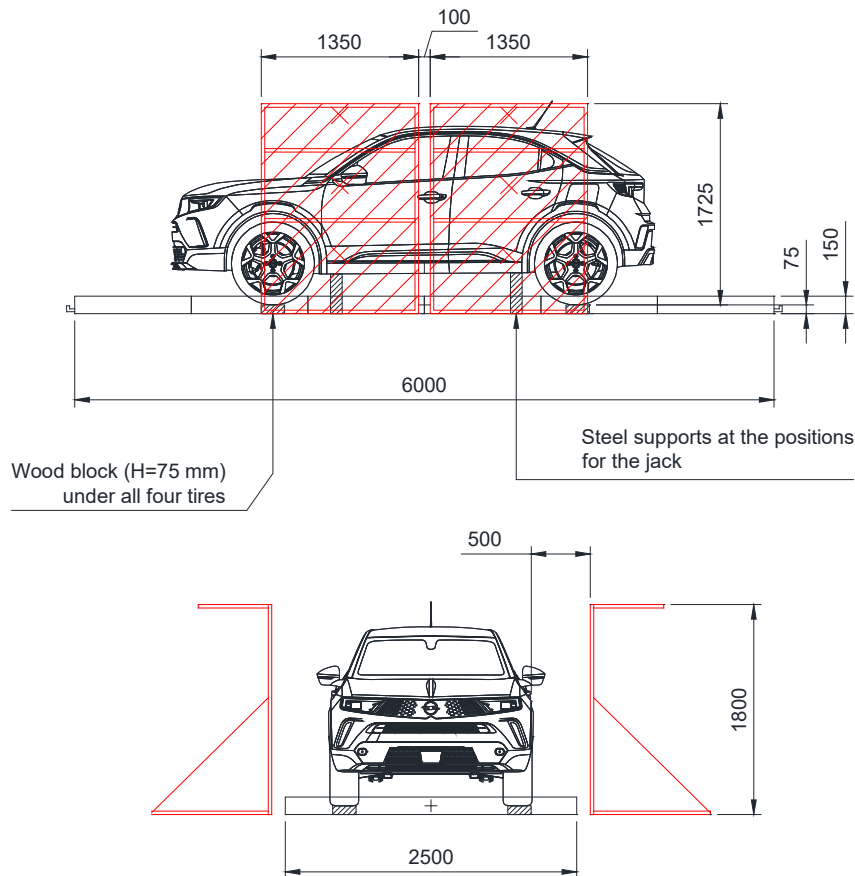


*Figure B-1 The arrangement of the vehicle in the tray filled with water, with the steel sheet screens to the sides. All measures in mm.*

The vehicle under test was positioned symmetrically in the tray. Each of the tires was positioned on a small wood block that was 75 mm in height, making the vertical distance from underside of the vehicle to the water surface equal to the actual distance measured to a road surface. In addition, supports were placed at the jack brackets to prevent the vehicle from tilting or collapsing during a test. The intention was to improve the test-to-test repeatability by improving the stability of the vehicles. Figure B-1 shows the arrangement.

#### 21.4 The preparation of the vehicles

Vehicle components with the potential to explode when heated and become projectiles were either removed or punctured. All airbags were removed, and shock absorbers and hydraulic dampers were punctured. The air pressure in all tires was released. The 12 V battery of all vehicles was removed to avoid any unnecessary contamination by lead in the run-off water.

The fuel tank was filled with unleaded 95-E10 to 90 % of the nominal tank capacity. This gasoline quality is a fuel which contains up to 10 % of ethanol, in accordance with the latest (from 2021) European specifications. A small (15 mm) circular hole was drilled at the bottom of the fuel tank, close to the longitudinal centreline of the vehicle. The hole was fitted with a rubber plug, which was disconnected at the start of the test to allow an outflow of fuel over the water surface of the fire tray. The outflow was immediately ignited with a torch.

The propulsion battery pack was charged to 90 % of its useable capacity. A small circular (22 mm diameter for BEV1) and square (30 mm × 30 mm for BEV2) hole was drilled through the protective

plate under the battery pack. This allowed the penetration of one of the battery modules at the rear, left-hand side of the vehicle by a nail. The nail was pointed, had a diameter of 20 mm and was driven by a pneumatic cylinder placed inside the tray underneath the vehicle. The penetration depth was about 70 mm. If the combustion gases did not self-ignite, electric igniters positioned close to the nail and marshals that were placed at the top edge of the rim of the fire tray were supposed to ignite the gases.

### 21.5 The deluge water spray system

Four water spray nozzles were installed in a hydraulically balanced pipe-work, having a nozzle spacing of 3,05 m by 3,05 m. Each of the nozzles covered an area of 9,3 m<sup>2</sup>. The pipe-work was constructed from DN50 (2") steel pipe. A pressure transducer was installed at the end of one of the branch lines. The distribution line of the pipe-work had a solenoid valve that was remotely operated. The flow rate of water was controlled via a diaphragm control valve connected to a compressed air supply. The control valve provided a constant pressure downstream of the valve, irrespective of the inlet pressure. However, the desired water flow rate of 372 l/min to obtain a 10 mm/min discharge density was fine-tuned by an operator if required. The nominal water pressure at each nozzle was 1,3 bar. Potable water was supplied from the public main without the need for a pump.

The nozzles used in the tests were open (non-automatic), pendent directional discharge water spray nozzles for fire protection purposes with a nominal K-factor of 80,6 (l/min)/√bar). The nozzles had an external deflector that discharged a uniformly filled cone of medium-velocity water droplets at a 180° spray angle. The nozzles used in the tests had no nozzle strainer.



Figure B-2 The spray pattern of the four water spray nozzles used in the tests

The nozzles were installed with their frame arms parallel with the system branch lines, and thereby perpendicular to the long sides of the vehicle. The nozzles were positioned approximately 5,0 m

above the water surface in the tray, as measured to the deflectors. This reflects a similar clear height in a ro-ro space on a ship. Figure B-2 shows the spray pattern of the four nozzles.

## 21.6 Fire test procedures

The intent was to initiate fire in such a way that the liquid fuel or the battery pack was involved at the initial stage of the fire. This was done by making a mechanical penetration of the fuel tank and the battery, combined with small fire ignition sources that ensured that fire ignition occurred. Although it can be argued that this type of fire ignition scenario is extremely rare, the approach was required to obtain a straightforward comparison of the two distinct types of vehicles.

The application of water was manually initiated at a convective heat release rate of 1 MW, which corresponded to a total heat release rate of about 1.5 MW. This threshold was chosen to ensure that the fire had indeed involved the vehicle and at a time when continued fire growth was to be expected.

Water was discharged for 30 min. Thereafter, the fire re-growth was documented by allowing the vehicle to be completely consumed in the fire. The approach facilitated the handling (scrapping) of the vehicles after the tests and provided an indication of the degree to which the fire was controlled by the application of water.

## 21.7 Instrumentation and measurements

The following measurements were undertaken during each test:

### 21.7.1 Heat release rate measurements

The tests were conducted under a large-scale calorimeter having a hood connected to an evacuation system capable of collecting all the combustion gases produced by the fire. The hood is 6 m in diameter with its lower rim 8 m above the floor. Gas temperature, velocity, the generation of gaseous species such as CO<sub>2</sub> and CO, and the depletion of O<sub>2</sub> were measured in the evacuation system duct.

Based on the heat release rate measurements, certain key parameters were calculated:

**The maximum one-minute average total heat release rate:** The total heat release rate includes the energy released by both convection and radiation, as well as the heat being conducted away and absorbed within the test set-up. The heat radiation component of the total heat release rate accounts for approximately one-third of the energy generated by a fire. Heat radiation is the primary mechanism by which the fire spreads to adjacent vehicles. The maximum total heat release rate is, therefore, a measure of the potential for fire spread, as well as an overall fundamental measure of fire severity.

**The maximum one-minute average convective heat release rate.** About two-thirds of the energy generated by a fire is released through convection. Convection determines the velocities and temperatures in the fire plume. Moreover, the proportion of water droplets that penetrate the fire plume from a sprinkler or nozzle depends on the velocities and temperatures. Therefore, the maximum convective heat release rate is an important measurement in these tests.

**The maximum five-minute average convective heat release rate.** The energy convected upwards is largely responsible for the heating of exposed steel at the ceiling and could impact the operation of automatic sprinklers (if used). The maximum value of the convective heat release rate helps to characterize the severity of the fire. However, regarding heat transfer, the duration time is as important as magnitude.

**The total energy generated from fire ignition until the end of water discharge:** This parameter provides a possibility to compare how much energy is released during the entire test and is less influenced by abnormal or random events that occur during a test.

#### 21.7.2 The gas temperature inside the vehicle

The gas temperature (C21) was measured inside the vehicle with a sheathed ( $\varnothing=1$  mm) thermocouple. The thermocouple was positioned between the headrests of the front seats.

#### 21.7.3 The gas temperature above the vehicle

The gas temperature (C22) above the vehicle was measured with a sheathed ( $\varnothing=1$  mm) thermocouple. The thermocouple was positioned 100 mm below the system pipe-work, at the connection point between the distribution pipe and the branch lines, i.e., above the mid-point of the vehicle. The vertical distance from the water surface in the tray to the thermocouple was approximately 5 m.

#### 21.7.4 The surface temperature on steel sheet screens to the sides of the vehicle

Two steel sheet screens were positioned at each long side of the tested vehicle. Each screen was sized 1350 mm (L) by 1800 mm (H) and had a nominal thickness of 1 mm. The screens were positioned symmetrically with respect to the wheel axles and 100 mm apart. The horizontal distance to the side of the vehicle was 500 mm. Each steel screen had a horizontal 600 mm wide overhang that prevented water from wetting its back side.

The surface temperatures at selected locations of the steel sheet screens were measured using wire thermocouples ( $\varnothing=0,5$  mm) that were spot-welded to the back side of the screens (C23 to C34). Each screen had a column of three thermocouples positioned along its vertical centerline. Table B-2 shows the measurement locations and the associated measurement channels.

*Table B-2 The measurement positions and the associated measurement channels on the steel sheet screens. In total, four steel sheet screens, two on each side of the vehicle, were used.*

Position	Steel sheet screen	Position of thermocouple	Vertical distance from the top of the steel sheet screen (mm)	Channel
Right-hand side	1: At the front	Top	100	C23
		Middle	700	C24
		Bottom	1300	C25
	2: At the rear	Top	100	C26
		Middle	700	C27
		Bottom	1300	C28
Left-hand side	3: At the front	Top	100	C29
		Middle	700	C30
		Bottom	1300	C31
	4: At the rear	Top	100	C32
		Middle	700	C33
		Bottom	1300	C34

#### 21.7.5 Heat radiation measurements

The heat radiation was measured with heat flux meters facing the long side of the vehicle. The devices were positioned 1125 mm above the water surface in the tray and at a horizontal distance of 500 mm from the right (C35) and left (C36) side of the vehicle. The position was between the steel



sheet screens described above, at the 100 mm gap. The height of the devices above the floor corresponded to the approximate midline of the side windows of the vehicle.

#### 21.7.6 Plate Thermometer measurements

One Plate Thermometer was positioned along the longitudinal centerline of the vehicle, at a horizontal distance of 1500 mm from the front (C37) and rear (C38) of the vehicle, respectively. The vertical distance measured to the center point of the water surface in the tray was 750 mm.

The Plate Thermometer consists of a 0,7 mm thick Inconel 600 steel plate with a front face measuring 100 mm by 100 mm. A sheathed thermocouple is spot-welded to the plate that is insulated on the backside. The device is sensitive to heat convection, but compared to a conventional thermocouple, significantly more sensitive to heat radiation [5, 6].

#### 21.7.7 Measurements of the system operating pressure and water flow rate

The system operating pressure (C39) was measured using a pressure transducer positioned at one of the system branches. The pressure transducer was positioned at the end of the pipe, i.e., there was a minimal static pressure difference between the nozzles and the transducer. The water flow (C40) rate was measured using a flow meter installed after the flow control device.

#### 21.7.8 Still photographs and video recordings

The tests were documented using still photos and video recordings with cameras from several distinct positions and a thermal image camera at one position.

### 21.8 Fire test observations

The following observations were made during the tests:

**ICEV1:** The initial fire development was fast as the gasoline fuel spread across the water surface. The application of water that started at 01:12 [min:s] temporarily limited the fire growth rate, refer to Figure B-3, but at about 02:30 [min:s] the fire re-developed rapidly as the spill area increased in size. This is likely due to a larger burn-through of the fuel tank. A peak heat release rate of almost 8 MW was recorded at about 03:30 [min:s], refer to Figure B-4. At that time, the fuel spill area extended almost to the front end of the tray. Visually, about 90 % of the 15 m<sup>2</sup> surface area of the tray was burning. This stage was followed by a gradual decline of the fire size as the gasoline fuel was steadily consumed. At 06:00 [min:s] the gasoline fuel was completely consumed, and the fire was located at the rear of the vehicle, including the rear tires. About 30 s earlier, flames were also observed through the front side window at the left-hand side (driver's side) of the vehicle, indicating that the interior of the passenger compartment was burning.

Following the burn out of the fuel spill, the fire size never exceeded 2 MW and the fire size was gradually reduced until the application of water was terminated.

---

<sup>5</sup> Wickström, Ulf, "The plate thermometer - A simple instrument for reaching harmonized fire resistance tests", SP-REPORT 1989:03, Swedish National Testing and Research Institute, Borås, 1989

<sup>6</sup> Wickström, Ulf, "The plate thermometer - A simple instrument for reaching harmonized fire resistance tests", Fire Technology, Volume 30, No. 2, 1994



Figure B-3 **ICEV1:** The fire size at 01:12 [min:s], at the start of the application of water from the overhead water spray nozzles, viewed from a position in front of (left) and behind (right) the vehicle.



Figure B-4 **ICEV1:** The fire size at the most intense stage at about 03:30 [min:s], viewed from a position in front of (left) and behind (right) the vehicle.

At the time the water flow was stopped, the fire visually involved the engine compartment and the passenger compartment, with observed burn-through of the windscreen and the front side window at the left-hand side. Once the water flow was stopped, the fire re-developed and burned at a level of around 2,2 MW for about seven minutes before it slowly decreased in size. The increase in fire size was visually associated with an initial increase of the fire inside the passenger compartment, with flames projecting through the windscreen and the side windows. It was also observed that the side windows at the right-hand side had partly burnt through. During this stage, the paint on the hood started to blacken and the paint of the roof ignited and burned. It is noticeable that the paint on the hood and on the roof of the vehicle was virtually undamaged because of the application of water. The gap in the windscreen increased in size which allowed the fire in the passenger compartment to increase. The fire reached its peak during the stage when all windows had been completely

damaged. To some extent, the fire in the engine compartment contributed, as flames were observed in a gap that opened between the hood and fenders. These flames eventually involved the front tires, and it is clear that this sequence of events extended the post-application peak heat release rate.

**BEV1:** Fire ignition was immediate when the nail penetrated the battery module, with flames projecting from the left-hand side of the vehicle and generation of visible smoke. At 00:20 [min:s], smoke plumes at both sides of the vehicle appeared, originating from the rear wheelhouses, followed by short duration jet flames at 01:00 [min:s]. At 02:00 [min:s], plenty of burning melted plastic pieces from the low-side panels were observed. At about 04:45 [min:s] it was observed that all four tires and the wheelhouse liners start to become involved in the fire. At about 05:30 [min:s], the smoke plumes originating from the area above the rear tires turned into durable jet flames, which gradually increased the fire involvement of the rear tires. At 07:00 [min:s] flames were observed at the areas of the water drainage hole in front of the windscreen at the left-hand side of the vehicle. These flames grew in size and extended above the roof at 09:50 [min:s]. At about 10:00 [min:s] the fire started to involve the plastic parts at the rear (left) end of the vehicle, which resulted in an increase in the fire growth rate. The rear was fully involved in the fire at 12:10 [min:s]. At 12:40 [min:s] the application of water was initiated, refer to Figure B-5. This resulted in a prompt reduction of the heat release rate. However, from the measurements it is noticed that the fire gradually re-developed starting at about 14:45 [min:s]. Visibility was obscured by the water spray and smoke, but at 16:00 [min:s], durable jet flames extending from the area above the rear tires were observed. At about 18:00 [min:s] a more rapid fire re-growth is noticed and the second heat release rate peak at 19:00 [min:s] is associated with the fire involvement of the battery pack, the rear tires, and the interior of the passenger compartment, with flames through the side windows. Figure B-6 shows the fire size when it was the most intense. After this stage, the fire size declined but re-developed again at 21:45 [min:s], as the fire inside the passenger compartment increased. Visually, it seemed that the contribution to the fire from the rear of the battery pack was small. The fire re-growth may be due in part to the involvement of the mid- and front battery modules. At 25:00 [min:s], it is observed that area under the front hood and front tires are severely involved in the fire. The progressing fire spread towards the front of the vehicle lasted for about 11 minutes, from 18:00 [min:s] to 29:00 [min:s], where the fire size fluctuated between about 1 MW and 3 MW. The fire size steadily decreased until the water flow was terminated at 42:40 [min:s]. At that time, only small flames were visible at the underside of the vehicle, with smoke gradually increasing.



Figure B-5 **BEV1:** The fire size a few seconds prior the start of the application of water from the overhead water spray nozzles at 12:40 [min:s], viewed from a position in front of (left) and behind (right) the vehicle.



Figure B-6 **BEV1:** The fire size at the most intense stage at about 19:00 [min:s], viewed from a position in front of (left) and behind (right) the vehicle.

Once the water flow rate was terminated, the fire did not re-develop until about 61:00 [min:s], i.e., after about 18 minutes. It was observed that the glass sunroof remained intact due to the application of water, but the rear window and most of the windscreen had broken. Visually, the fire re-developed in an area close to the driver's seat. At about 68:00 [min:s], the glass sunroof above the driver's seat started to gradually break down and the fire size increased as it involved the unwetted interior. The fire was spreading towards the right-hand side of the vehicle and peaked at almost 3 MW at 73:00 [min:s], before it started to decrease. The fire spread inside the passenger compartment continued, which led to a second peak of about 2 MW at 79:00 [min:s], when the area of the luggage compartment was involved in the fire. After this stage, the fire size gradually declined as the combustibles burnt out.



**ICEV2:** The fire ignited immediately, and the initial fire development was fast as the gasoline fuel spread across the water surface, with higher flames initially observed at the left-hand side of the vehicle. The application of water started at 00:58 [min:s], refer to Figure B-7. To some extent this temporarily reduced the spill fire size at the right-hand side of the vehicle. During this stage, the fire size varied between 2 MW and 3 MW. At about 03:00 [min:s], the fire size increased rapidly as the spill area increased in size, with higher flames appearing at the right-hand side again. This increase is likely due to a larger burn-through of the fuel tank. A peak heat release rate of approximately 5,3 MW was recorded at about 04:00 [min:s], refer to Figure B-8. Visually, the spill fire was located at the rear of the fire tray and at the right-hand side of the vehicle. The spill area visually extended at most up to the front tires. The peak lasted for about 30 s, thereafter the fire gradually declined as the gasoline fuel was steadily consumed. At 05:10 [min:s] it seemed that most of the gasoline fuel had been consumed and the fire was located at the rear, including involvement of the rear tires. At this time, burn-through of the rear side window on the left-hand side was observed.

This intense stage was followed by a steadily decreasing fire size as the plastic parts at the rear of the vehicle and the rear tires were consumed. At 23:00 [min:s] the fire basically involved only the rear tires and the engine compartment, where the fire was completely shielded from the application of water. At about 24:00 [min:s], flames were observed from the front side window at the right-hand side of the vehicle. These flames gradually increased in size, likely as the damaged area of the window increased. At 26:00 [min:s], these flames intermittently extended between 0,5 m and 1 m above the roof of the vehicle and occasionally became so large that they touched the steel sheet screen to the right. At 31:10 [min:s], flames were also observed from a damaged area at the front side window on the left-hand side. These flames were growing larger and when the application of water was stopped at 30:58 [min:s] it was observed that the fire size immediately increased inside the passenger compartment of the vehicle, with flames extending through the side windows and shortly thereafter through the windscreen that rapidly burnt through to its full extent. When visibility improved, it was also observed that the rear window had broken. The most intense stage of the fire inside the passenger compartment lasted for about 7 minutes and peaked at around 2,3 MW before it slowly declined.



Figure B-7 **ICEV2:** The fire size shortly after the start of the application of water from the overhead water spray nozzles at 00:58 [min:s], viewed from a position in front of (left) and behind (right) the vehicle.





Figure B-8 **ICEV2:** The fire size at the most intense stage at about 04:00 [min:s], viewed from a position in front of (left) and behind (right) the vehicle.

At about 42:00 [min:s] the fire started to spread towards the front of the vehicle, with flames moving underneath the right-hand side of the hood and in the front right wheelhouse. At about 46:30 [min:s], almost all of the plastic parts of the front were involved in the fire, whilst part of the passenger compartment was still burning. This resulted in a short, second peak of about 1,5 MW and a slow decay in the fire size as the combustibles at the front and inside the passenger compartment were consumed. The trend of steady decay was broken at about 73:00 [min:s] when the fire in the front tires and inside the front part of the compartment intensified, leading to a peak of almost 900 kW at about 78:00 [min:s]. Thereafter, all combustibles were progressively consumed.

**BEV2:** The first flare-up occurred at 00:57 [min:s] but no sustained burning was observed. At 02:12 [min:s], burning drops of melted plastic appeared at irregular intervals from the underside of the vehicle. These droplets fell into the layer of water, which prevented a pile of melted plastic to form. The number of droplets gradually increased with time and at 03:00 [min:s] several droplets per second was observed. At 05:30 [min:s], burning plastic was flowing through the hole where the nail penetrated the battery pack. At this time visible smoke was also observed. The melted plastic formed a burning pile at the top of the pneumatic jack that extended through the layer of water. At 03:47 [min:s], the flammable gases ignited, with flames going from the underside and up the right-hand side of the vehicle. Moments later, these flames disappeared. At 04:30, flames were observed again. These flames extended from the underside of the vehicle and stretched up the side of the back door and extended from the area above the rear tire at the left-hand side. Once again, the flames disappeared after a few seconds, followed by a flare-up underneath the vehicle. It was also observed that the amount of smoke increased.

The major contribution to the fire after this stage came from burning parts of the undercarriage plastic cover panels that fell down from the underside of the vehicle. At 07:15 [min:s] a jet flame appeared from the left-hand underside of the vehicle and a few seconds later a similar jet flame appeared from a more central part of the battery pack. These jet flames were intense for about ten seconds before they vanished, but other (less intense flames) were observed shortly thereafter. Once these flames faded away the fire growth rate slowed down, with occasional jet flames being observed. The fire started to increase in size at about 11:00 [min:s], once it involved the plastic panels at the sides and started to spread to the front tires and plastic panels surrounding the front

wheelhouses. At this stage, durable jet flames appeared from the rear wheelhouses, indicating a larger involvement of the rear battery pack. These jet flames involved the rear tires in the fire. At about 12:00 [min:s] flames were observed at the areas of drainage holes in front of the windscreen. These flames grew and the smoke observed through the grill indicates that the electric motor and the associated equipment became involved in the fire. The rear plastic panel fell down gradually at about 15:30 [min:s], increasing the size of the fire. The application of water started at 16:45 [min:s], refer to Figure B-9. This resulted in a prompt reduction of the heat release rate. Shortly after the application of water, the rear window burnt through, which may have exposed part of the interior to the water spray. But the opening also allowed air to enter, which increased the fire. At about 22:00 [min:s] the fires in the rear part of the battery pack and the rear tires were reduced, observed as less intense jet flames. At 24:00 [min:s], large flames at the front edge of the hood were observed, indicating fire spread that was shielded from the application of water. The fire was the most intense at about 24:40 [min:s], refer to Figure B-10, when it visually involved the passenger and engine compartments. Flames from the rear wheelhouses do also suggest that the battery pack was involved in the fire.



Figure B-9 **BEV2:** The fire size a few seconds prior and after the start of the application of water from the overhead water spray nozzles at 16:45 [min:s], viewed from a position in front of (left) and behind (right) the vehicle.



Figure B-10 **BEV2:** The fire size at the most intense stage at about 24:40 [min:s], viewed from a position in front of (left) and behind (right) the vehicle.

Once the water flow was stopped at 46:45 [min:s], only small flames were observed at the underside of the vehicle in an area in front of and behind the rear left-hand tire, at the front wheelhouse to the left and inside the passenger compartment. It was observed that all windows had broken, which probably allowed access of water to the inside of the vehicle. Fire re-growth was observed shortly after the end of water application and initially involved fire spreading to unburnt combustibles (plastic) at the front of the vehicle. But the fire also progressed inside the vehicle and towards the rear. About a minute after the end of water application, short fire flare-ups were observed which may be due to the fire in combustible gases expelling from individual cells of the battery pack at the rear. These flare-ups continued at intervals between 30 s and 60 s as the fire inside the passenger compartment progressed towards the rear of the vehicle.

When all unburnt combustibles were involved the fire burnt intensely at a level of between 2 MW and 3 MW for around eight minutes. At this stage, large flames were observed through all window openings, and at the front and the rear of the vehicle. During the final five minutes of this eight-minute stage, intermittent flames were observed at the rear end and from the rear wheelhouses. These flames are probably associated with the burn-out of the rear battery pack. The intermittent fire was captured by the measurements and the overall heat release rate contribution is in the order of 500 kW. After this stage, starting at 64:30 [min:s], the fire declined as the remaining combustibles burnt out.

## 21.9 Test results

Table B-3 shows the heat release rate results, as recorded prior to or after the start of the application of water, with the key parameters discussed above in bold.

Table B-3 Heat release rate results, as recorded prior to or after the start of the application of water, with the key parameters discussed above in bold.

	ICEV1	BEV1	ICEV2	BEV2
Date of test	Sept. 23, 2022	Sept. 21, 2022	Sept. 27, 2022	Sept. 29, 2022
Time to discharge of water [min:s]	01:12 (72 s)	12:40 (760 s)	00:58 (58 s)	16:45 (1 005 s)
Time to end of discharge of water [min:s]	31:12 (1 872 s)	42:40 (2 560 s)	30:57 (1 857 s)	46:45 (2 805 s)
Peak total heat release rate [kW]	7 978	2 944	5 324	1 975
Maximum one-minute average total heat release rate [kW]	<b>7 198</b>	<b>2 525</b>	<b>4 765</b>	<b>1 625</b>
Peak convective heat release rate [kW]	3 594	1 195	2 323	1 138
Maximum one-minute average convective heat release rate [kW]	<b>3 080</b>	<b>904</b>	<b>1 890</b>	<b>947</b>
Maximum five-minute average convective heat release rate [MJ]	<b>1 467</b>	<b>633</b>	<b>1 006</b>	<b>639</b>
Total heat release [MJ] from fire ignition to end of water discharge	<b>2 637</b>	<b>2 189</b>	<b>1 784</b>	<b>1 370</b>
Total heat release [MJ] from fire ignition to the end of test	5 241	4 510	4 765	4 474

Figures B-11 and B-12 show the heat release rate histories for each pair of vehicles.

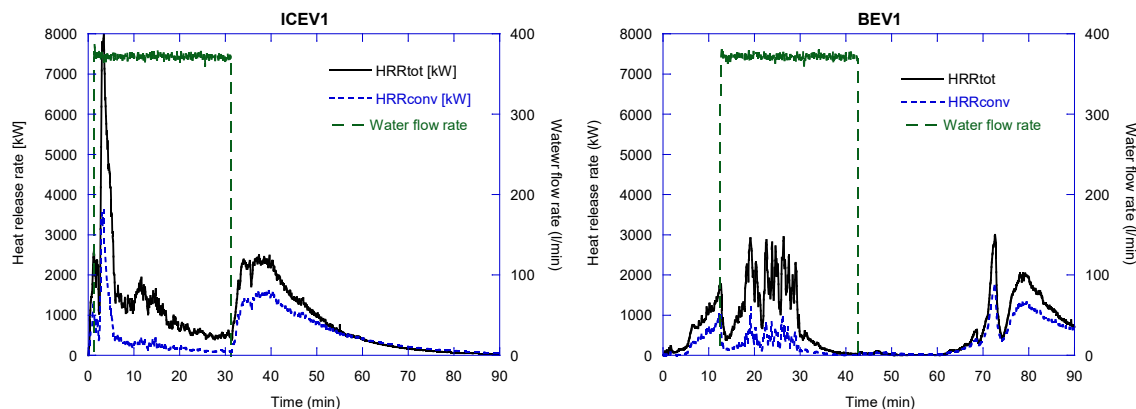


Figure B-11 The total and convective heat release rate histories for ICEV1 and BEV1.

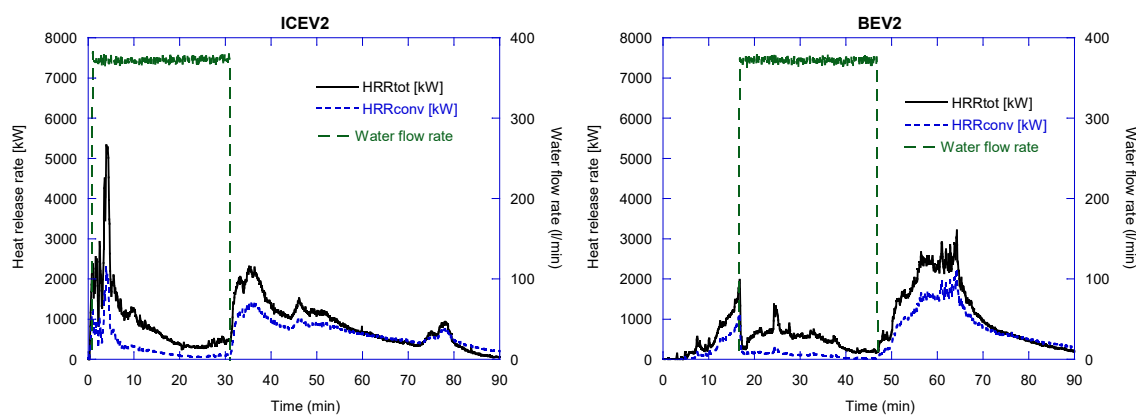


Figure B-12 The total and convective heat release rate histories for ICEV2 and BEV2.



Table B-4 shows the temperature and heat flux measurement results as recorded prior to or after the start of the application of water.

Table B-4 Temperature and heat flux measurement results as recorded prior to or after the start of the application of water.

	ICEV1	BEV1	ICEV2	BEV2
Date of test	Sept. 21, 2022	Sept. 23, 2022	Sept. 27, 2022	Sept. 29, 2022
Mean water flow rate [l/min]	372	373	371	374
Peak gas temp. above the vehicle [°C]	340	56	135	166
Maximum average surface temp. on right-hand side steel sheet screen [°C]	407	149	277	165
Maximum average surface temp. on left-hand side steel sheet screen [°C]	339	139	251	163
Peak heat flux to the right of the vehicle [kW/m <sup>2</sup> ]	98	7	44	5
Peak heat flux to the left of the vehicle [kW/m <sup>2</sup> ]	138	6	59	6
Peak surface temp. on Plate Thermometer in front of the vehicle [°C]	70	43	33	36
Peak surface temp. on Plate Thermometer behind the vehicle [°C]	88	87	78	76

Figures B-13 and B-14 show the gas temperature above the vehicle and the surface temperatures of the Plate Thermometers (P/T) in front of and behind the vehicle. Note that the time scale extends to 60 min and not to 90 min as in the previous figures, to better capture the sequence of events when the water spray system was operating.

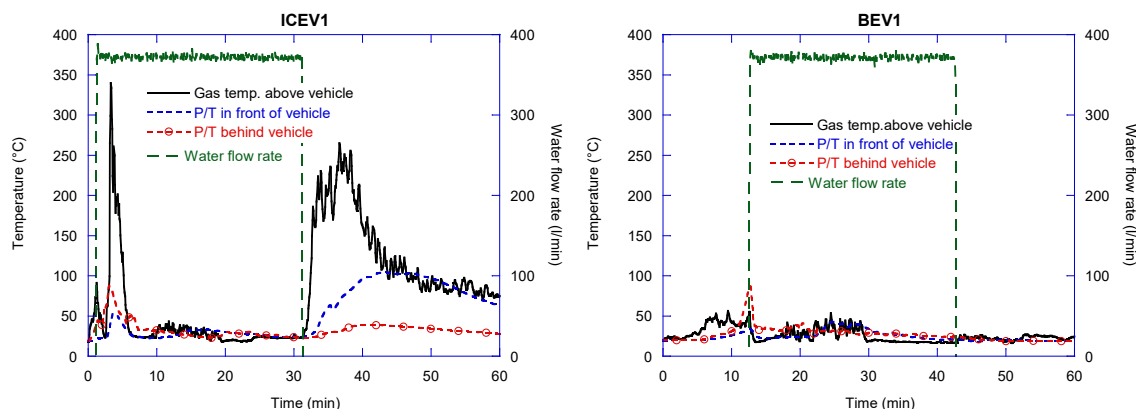


Figure B-13 The gas temperature above the vehicle and the surface temperatures of the Plate Thermometers (P/T) in front of and behind the vehicle for ICEV1 and BEV1.

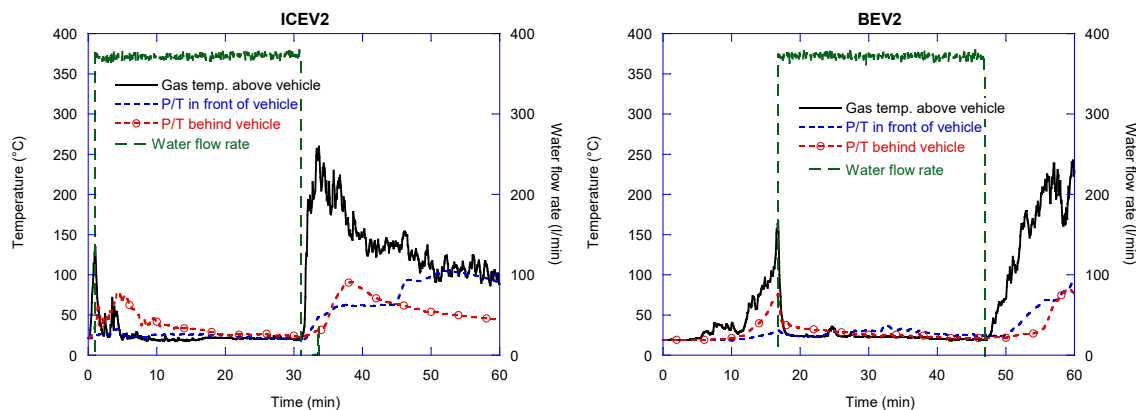


Figure B-14 The gas temperature above the vehicle and the surface temperatures of the Plate Thermometers (P/T) in front of and behind the vehicle for ICEV2 and BEV2.

Figures B-15 and B-16 show the mean surface temperature of the steel sheet screens to the sides of the vehicle.

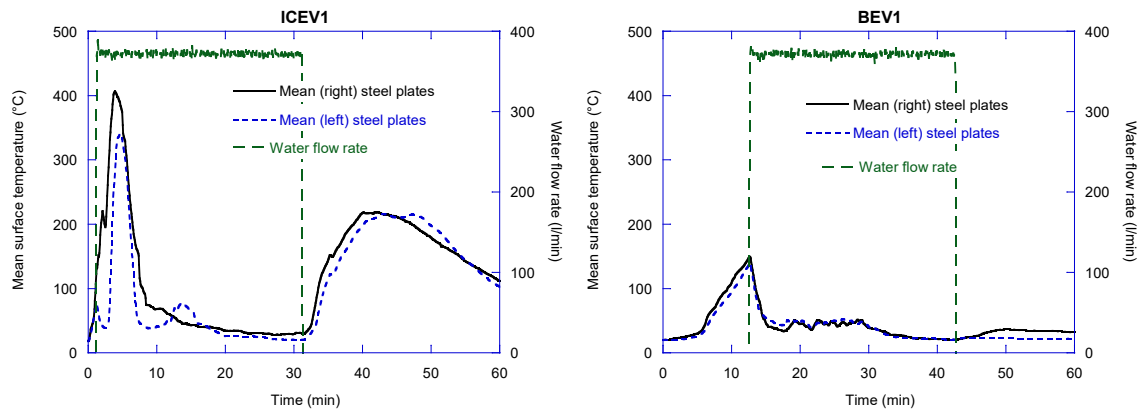


Figure B-15 The mean surface temperature on the steel sheet screens to the right and left of the vehicle for ICEV1 and BEV1.

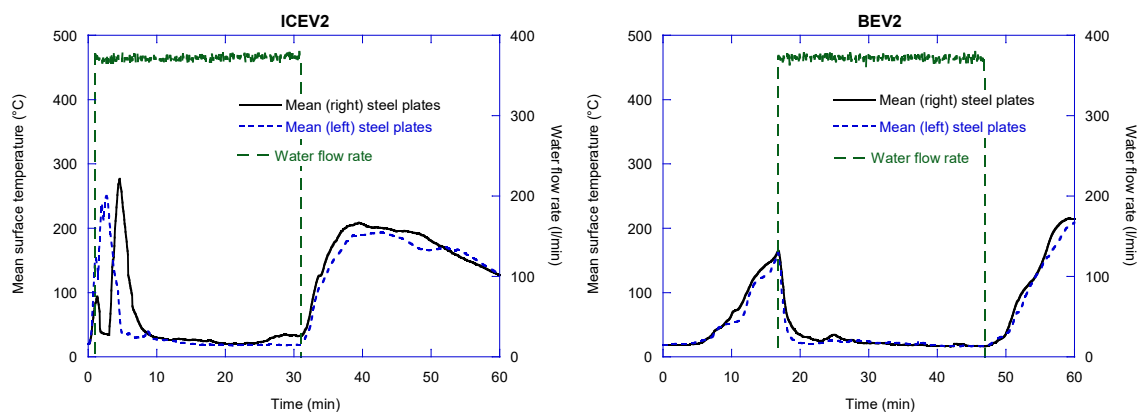


Figure B-16 The mean surface temperature on the steel sheet screens to the right and left of the vehicle for ICEV2 and BEV2.

## 21.10 Discussion

### 21.10.1 The fire scenarios

The fire ignition scenarios are considered unlikely but were necessitated by the desire to initiate the fire either in the gasoline fuel or in the battery pack and thereafter allow the fire to spread to other combustible parts of the vehicle. Both fire ignition scenarios proved to work from the aspect that fire ignition was immediate in the flammable gases of the fuel spill fire as well as in the flammable gases escaping the battery pack, except for BEV2 where fire ignition occurred immediately but the presence of stable flames was a little delayed.

Thereafter, the fire scenarios of the two types of vehicles were quite different. The gasoline fuel spill fire in the ICEV tests developed rapidly and the application of water was initiated after about a minute. The fire in the battery pack of the BEVs developed slower, involved other combustibles gradually and the application of water was initiated after more than twelve minutes and sixteen minutes, respectively.

The fires in the ICEVs were initially suppressed, but the flowing gasoline fuel spill fire caused more damage to the fuel tank that resulted in an increase of the spill area and peak heat release rate.

Plastic fuel tanks in passenger vehicles are designed to meet international fire test requirements [7] and should withstand a spill fire test scenario for two minutes, which correlates well with the observations of their integrity in these tests. The peak heat release rate occurred during a period from between three and four minutes (ICEV1) and four and four and a half minutes (ICEV2). The peak heat release rate of ICEV1 was higher than that of ICEV2, which correlates with the larger quantity of gasoline used in ICEV1. After the burn-out of the spill fire at about six minutes (ICEV1) and five minutes (ICEV2), fire continued in combustibles such as the tires, the plastic liners in the wheelhouses, undercarriage plastic cover panels, inside the passenger compartment and inside the engine compartment. These combustibles are completely or partly shielded from the application of water from the overhead water spray nozzles. During this stage of the continued 30-min application of water, the heat release rate gradually decreased as these combustibles were consumed. Once the application of water was terminated, fire re-developed inside the passenger compartment, partly as the extent of damage to windows increased. Additionally, the paint and external front parts of the vehicle that were not involved in the fire due to the application of water started to burn. The post-application peak heat release rates were significant for both vehicles.

The fire in the BEVs had involved other combustibles to a larger extent when the application of water was initiated. Even though these combustibles were completely or partly shielded from the application of water, the fire was promptly suppressed. The fire re-growth experienced for BEV1 is primarily associated with the battery packs where the fire progressed from the rear part (where fire ignition took place) towards the front part. However, contributions from the passenger compartment were also observed. The progress of the fire from battery module to battery module is captured by regular peaks in the heat release measurement. For BEV2, the fire re-growth was not as significant and involved the passenger and engine compartments. Flames from the rear wheelhouses do also suggest that the battery pack was involved in the fire. Once the application of water was terminated, fire re-development was significantly slower in BEV1 (after about 18 min) than in BEV2 (basically immediately). The post-application fire re-growth involved unburnt combustibles such as the paint and front plastic panels as well as unburnt parts of the interior. The post-application peak heat release rates were significant for both vehicles. For BEV1, it seems that the battery pack burnt out during the 30-minute application of water. For BEV2, water entering through the window openings may have prevented the battery modules from being fully consumed. During the burn-out of the vehicle after the end of water application, it visually seems that a fire in the battery pack to some extent contributed to the overall fire severity.

It is concluded that the peak heat release rate was significantly higher for ICEV1 than for BEV1, as well as for ICEV2 compared to BEV2, which is associated with the short, but intense, gasoline fuel spill fire. The maximum five-minute average convective heat release rate captures the severity of the fire over a longer period. The parameter value was the highest for ICEV1; more than twice as high as for BEV1 and BEV2. The value for ICEV2 was lower than that of ICEV1, as the vehicle was smaller with a smaller amount of liquid fuel.

The total heat release rate from fire ignition and to the end of water application was slightly higher for ICEV1 as compared to BEV1 and higher for ICEV2 as compared to BEV2. The same trend is observed for the total heat release rate for the entire test, which included the burn-out of the vehicles.

---

<sup>7</sup> Addendum 33: Regulation No. 34, Revision 3, "Uniform provisions concerning the approval of vehicles with regard to the prevention of fire risks", United Nations, 12 November 2015

### 21.10.2 The performance of the water spray system

The performance of the water spray system was adequate for both types of vehicles. One concern can be raised - a flammable liquid spill fire could involve adjacent vehicles; a large fuel spill burns very intensely, and the liquid could spread under adjacent vehicles. The degree of fire control was established by terminating the water flow and observing the time to fire re-growth and the magnitude of the fire. For both types of vehicles, the fire re-peaked at between 2 MW and 3 MW after the application of water was terminated. This is an indication that the heat release rate of the fires was indeed reduced by the water spray, despite the fact that the fire was, to a large degree, shielded. Once the wetting and cooling of the body of a vehicle stopped, it was observed that damage to windows will occur or increase, paint will start to burn, and unburnt combustibles will ignite that contribute to fire re-growth.

The gas temperature above the vehicle was promptly reduced in the BEV tests to a level of 50 °C or less during water discharge. For the ICEV tests, a short peak reaching 340 °C (ICEV1) and 135 °C (ICEV2) was observed after the application of water was initiated, which relates to the increase of the gasoline fuel spill fire. After this stage, the gas temperature was reduced to less than 50 °C.

None of the Plate Thermometer surface temperatures peaked at any significant levels in any of the tests. It is observed that the peak temperature of the device facing the rear of the vehicles was consistently higher than the device facing the front. This observation seems logical as the fire was started at the rear part of the vehicles. The heat fluxes measured during the tests with the BEVs were lower than in the tests with the ICEVs. The two devices were positioned at a height corresponding to the midline of the side windows.

Manual fire-fighting efforts were not part of the study but based on the tests it can be argued that an intentional premature termination of a drencher system should be avoided. When the water spray system is turned-off, resources should be readily available to manage a re-developing fire.

### 21.11 Conclusion

Concerns about the performance of drencher systems in ro-ro cargo spaces on board ships have been raised regarding the increased number of battery electric vehicles being transported. The objective of these tests was to compare the fire suppression performance of a deluge water spray system for fires involving ICEVs and BEVs in test conditions as equivalent as possible. The tests simulated a ro-ro space having a ceiling height of about 5 m with a system design in line with the recommendations in MSC.1/Circ.1430/Rev.2.

It is concluded that a fire in the two types of vehicles is different but have similarities. A fuel spill fire associated with an ICEV develops very rapidly, peaks high but burns out fast, whilst a fire starting in the battery pack of a BEV develops slower, is not as large but burns longer. The scenario of the fire in other combustibles, such as the tires, exterior and undercarriage plastic parts and inside the passenger compartment is similar.

The deluge water spray controlled the fire, irrespective of the type of vehicle, measured as a reduction of gas temperatures above the vehicle, the surface temperatures of adjacent steel sheet screens, the surface temperature of Plate Thermometers, and reduced heat radiation. Fire control was also documented by a reduction of the heat release during water application and clear fire re-growth with significant fire sizes once the application was terminated. The overall conclusion from the tests is that a fire in a BEV does not seem to be more challenging for the drencher system design given in MSC.1/Circ.1430/Rev.2 than a fire in an ICEV of comparable size. One concern is raised - a



flammable liquid spill fire could involve adjacent vehicles due to its intensity and as the liquid spill could spread under adjacent vehicles.

#### 21.12 Acknowledgement

The tests were conducted in the LASH FIRE project. The LASH FIRE project ([www.lashfire.eu](http://www.lashfire.eu)) is an international research project aiming to significantly reduce the risk of fires on board ro-ro ships by developing and validating effective operative and design solutions. LASH FIRE is addressing a total of twenty challenges covering the entire “fire protection chain”; it comprises both preventive and mitigating risk control measures in all stages of fires originating in ro-ro spaces. The project is running from September 2019 to August 2023. The project has received funding from the European Union’s Horizon 2020 research and innovation programme under grant agreement No 814975. The information in this paper reflects only the author’s view and the Agency is not responsible for any use that may be made of the information it contains.

The vehicle manufacturers that sponsored the tests with vehicles are acknowledged. Martin Carlsson at Stena Rederi AB is also acknowledged for raising the demand and assisting in realizing the tests.